Steel TIPS
STRUCTURAL STEEL EDUCATIONAL COUNCIL
TECHNICAL INFORMATION & PRODUCT SERVICE

May 2007

Progressive Collapse Prevention of Steel Frames with Shear Connections

By

Abolhassan Astaneh-Asl, Ph.D., P.E.
Professor
Department of Civil and Environmental Engineering
And
Center for Catastrophic Risk Management
(www.ccrm.berkeley.edu)
University of California, Berkeley

Progressive Collapse Prevention of Steel Frames with Shear Connections

By Abolhassan Astaneh-Asl

Abstract

This Steel Technical Information and Product Services (Steel TIPS) report provides information and technologies that can be used to protect steel building structures against progressive collapse in the event of removal of a column. Chapter 1 provides general information on progressive collapse of steel building structures. Chapter 2 provides information on progressive collapse behavior of steel frames with shear connections. Design guidelines are provided, and a numerical example demonstrates application of the guideline. Chapter 3 discusses the tests performed on the exterior frame of a full-size test structure where the beam-to-column connections were bolted seat angles with an additional bolted single angle connecting the web of the girders to the columns. The tests consisted of removing the middle column of the exterior frame and pushing the joint at the top of the removed column down 19, 24, and 35 inches to measure the strength, stiffness, and ductility of the structure as well as the connections. The steel frame with shear connections showed considerable resistance to progressive collapse after removal of a column. This was primarily due to the development of catenary force in the beams that were connected to the top of the removed column and to a lesser extent to membrane (catenary) action of the steel deck of the floors adjacent to the area of collapse. Chapter 4 discusses the research project conducted to investigate the use of steel cables to prevent progressive collapse of new steel building structures and develop design recommendations. The tests showed that the use of cables would increase progressive collapse resistance of the steel structures significantly. Chapter 5 focuses on the results of progressive collapse tests done on the exterior frame of the test structure where the beam-to-column connections were typical shear tab (single plate) shear connections. The tests were repeated adding steel cables to the structure to investigate the feasibility of using steel cables as a retrofit measure to prevent progressive collapse of the existing steel building structures with only shear connections. These tests found that the specimen with shear- tab connections alone (without the cables) had considerable strength after removal of the column and was able to resist design gravity loads primarily because of the catenary tension force developed in the girders that were connected to the removed column as well as due to the additional catenary (membrane) force developed in the steel deck of the floor. The addition of the cable, as a retrofit measure, was also very efficient in adding strength to the progressive collapse resistance of the existing structure.

First Printing, May 2007 (Posted on http://www.steeltips.org)

Abolhassan Astaneh-Asl, Ph.D., P.E., Professor of Structural Engineering, University of California, Berkeley
Phone: (925) 946-0903, E-mail: Hassan@Astaneh.net, Web: http://www.astaneh.net
University Web Site: http://www.ce.berkeley.edu/~astaneh

Acknowledgments

Funding for this publication was provided in part by the California Iron Workers Administrative Trust. The publication of this report was made possible through the support of the Structural Steel Educational Council (SSEC). The author wishes to thank all SSEC members, particularly Fred Boettler, SSEC Administrator, James J. Putkey, and Patrick M. Hassett for their technical input and review comments.

The research projects reported in Chapters 3, 4 and 5, were conducted by the author and his graduate and undergraduate research students at the University of California at Berkeley. In particular, the excellent work of former research collaborators and students Ricky Hwa, Brant Jones, Roger Jung, Erik Madsen, Samuel Tan, Sunil Tellis, Wendy Wang, Albert Wong, Qiuhong Zhao, and Yongkuan Zhao on these projects is acknowledged and appreciated. The test specimen used in these studies was fabricated by the Herrick Corporation ,and the tests were conducted in the Structural Laboratories of the Department of Civil and Environmental Engineering of the University of California at Berkeley. The efforts of Jamie Winans, formerly of Herrick Corporation, Jeff Higginbotham, William Mac Cracken, Chris Moy, Richard Parsons, Dr. Lev Stepanov, Mark Troxler, and Douglas Zulaica, all laboratory staff at UC Berkeley, are sincerely appreciated. The research projects were supported, in part, by the General Services Administration (GSA);Magnusson, Klemencic Associates (MKA); the American Institute of Steel Construction (AISC); the National Science Foundation (NSF); the University of California, Berkeley (UCB); and the Herrick Corporation. The support and input received from program mangers and technical officers of the supporting agencies, specially from Dr. Nestor Iwankiw, Thomas Schlafly, and Sergio Zoruba, all of the AISC; Dr. S.C. Liu of the NSF; Willie Hirano of the GSA; and Jon Magnusson, Brian Dickson, and Ignasius Seilie, all of the MKA; were very essential to the projects summarized here and sincerely appreciated. John Crawford of Karagozian & Case mentioned the idea of placing cables at the corners of a wide flange shape beam to the author at a meeting of the AISC Committee for Blast and Impact Resistant Design of Buildings in 2001. We implemented the idea in retrofit of existing steel buildings and conducted the tests summarized in Chapter 5 on this concept. The author expresses his appreciation and would like to credit John Crawford with the idea.

The opinions expressed in this document are solely those of the author and do not necessarily reflect the views of the University of California, Berkeley where he is a professor of structural engineering, or the Structural Steel Educational Council and other agencies and individuals whose names appear in this report.

Progressive-Collapse-Prevention of Steel Frames with Shear Connections

By **Dr. ABOLHASSAN ASTANEH-ASL, P.E.**
Professor
Department of Civil and Environmental Engineering,
University of California, Berkeley

TABLE OF CONTENTS

Notations

A = cross sectional area of the member
A_e =effective net area in tension
A_n = net area in tension
A_g = cross sectional area of the member
a = distance from weld line to bolt line in shear tab connections
DCR = demand-to-capacity ratio
E = modulus of elasticity
F_y = yield stress of steel
k_c = axial stiffness of connection
k_s = stiffness that structure provides to a connection against its horizontal movement
L = length of each beam segment in the three-hinge beam (see Figure 2.2)
P = applied vertical load
P_y = applied vertical load at the time of yielding of the beam segments
P_u = maximum value of applied load
R_n = nominal strength
T = axial tensile (catenary) force in the beam see Figure 2.2
T_y = axial tension yield capacity of the beam segments in three hinge beam= $A\ F_y$
T_{ui} = capacity for the failure mode number i
U = shear lag factor in tension members
U_e = elastic strain energy
Δ = axial elongation of each beam segment, (see Figure 2.2).
θ = rigid body rotation of the beam segments, same as rotation of the end connections (see Figure 2.2).
ε = axial tensile strain in the beam
δ = vertical displacement under the applied load P
$d\delta$ = incremental vertical displacement under the applied load P
ε_y = yield strain
θ_y = rigid body rotation of the beam segments when the member reaches the axial yield point
δ_y = vertical displacement under the applied load P at the time of yielding of the beam segments
Δ_u = maximum value of member elongation
θ_u = rigid body rotation of the beam segments when member reaches ultimate capacity
$\Delta_{u\text{-}conn}$= ultimate elongation of hinges (i.e. shear connections)
δ_u = vertical displacement under the applied load P when the load reaches ultimate value
A_{gv} = gross area in shear
F_{bv} = strength of bolt in shear
A_b =area of bolt
F_w =strength of weld electrode
A_w = area of weld
P_d = design capacity reduced for dynamic effects $P_u/2.0$
P_{LRFD} = factored load combination for progressive collapse considerations= $2(DL+0.25LL)$

1. INTRODUCTION

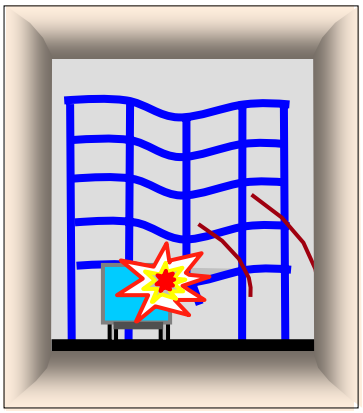

1.1. Introduction to Protection of Structures against Blast

Due to increased threat of terrorist attacks on buildings, the issue of protecting occupants in the event of such criminal acts has become exceedingly important. Although terrorists used airplanes to attack the World Trade Center on September 11, 2001, the use of car bombs to attack buildings remains a more likely scenario. Buildings located on public streets can be especially vulnerable to car- bomb attacks. There are three main preventive steps to either block those attacks or minimize their effect on people and buildings. Figure 1.1 shows those steps. The first and most important is to prevent the attacks *before* they occur by detecting the terrorist plans and intercepting them. In fact, intelligence and law-enforcement agencies state that they have detected a number of those plots and saved countless lives and huge economic damages. However, due to secret nature of terror plots, as the past tragic car bomb attacks have shown, there is always a possibility that some of those might go undetected. To protect buildings against those incidents, one course of action could be preventing car bombs from getting too close to buildings. Such measures would include erecting barriers outside buildings or setting buildings back from public street access, Step 2 in Figure 1.1.

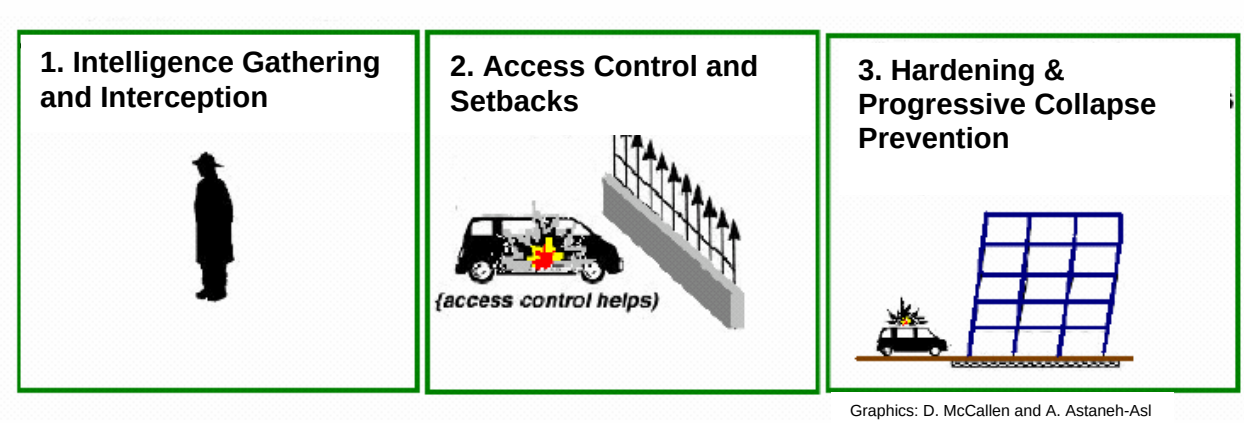

Figure 1.1. Three Main Steps in Protecting Buildings against Car Bomb Attacks

If the steps of "using interception and access control or setbacks do not succeed in preventing a car-bomb from reaching the building and exploding, the event may result in fatalities, injuries, and property damage and even partial or complete collapse of the structure.

Therefore, the third step focuses on measures to strengthen the capability of the structure itself to defuse or minimize the catastrophic effects of the attack. In the following, we will focus primarily on economic and feasible technical measures to take in design and construction process that would ideally prevent or significantly reduce the effect of the explosions on buildings and save lives and properties without creating an appearance of the building turned into a bomb shelter.

Particularly for steel structures, clever use of steel's similar properties in tension and compression as well as its ability to deform significantly prior to fracture (ductility), can result in very efficient, economical and non-intrusive solutions that can reduce the damage to local and limited area during the blast and prevent catastrophic progressive collapse immediately after the blast.

1.2. Casualties and Damage due to an Explosion

Casualties and damage from an explosion near a building occurs in two phases: (a) at the instant when the explosion occurs(during a fraction of second) and during the time immediately after the explosion when the damaged structure under gravity load may collapse in a progressive manner before the occupants can escape or be evacuated. The following discusses these two distinct phases of structural behavior. The scope of this report is to provide information on technologies that can be utilized to prevent progressive collapse during the second phase and after the explosion. The emphasis will be on steel structures with shear connections such as those with braced frames or shear walls.

1.2.a. Casualties and Damage Caused by the Explosion during the Blast

During an explosion, which takes a fraction of a second, the high velocity and high pressure of the air along with the shock waves generated by the explosion carry debris and shrapnel and hit the people and building causing injuries, even fatalities, and considerable damage. The relatively brittle building elements, such as glass, bricks, concrete, tile, and façade stone that are broken loose due to the blast become more shrapnel and high-speed flying debris to cause further casualties and damage inside the building. Tragically, preventing casualties and injury to those who are very close to the explosion is very difficult and costly if not impossible. However, measures can be taken in design and construction to cause the building itself and its components to act as protection for the occupants in the event of an attack without turning the building into a bunker. The study of past car-bomb attacks has shown that glass shards and high-speed flying debris were a major cause of casualties and injuries during explosions. Although there are technologies and products available that can resist the pressure of a blast without breaking and becoming high-speed flying debris, their discussion and the related issues are outside the scope of our studies here.

Competent design professionals with knowledge and experience of modeling the blast and the dynamic characteristics of the material and building components under high-strain rate loading can study the response of structures to blast effects and using powerful software to conduct nonlinear dynamic analysis of the structures subjected to blast loads. Such software should be capable of simulating the explosion itself and transferring the air pressure and shock

waves of the explosion from the source to the building components. Two powerful software applications commercially available and used by the author and his research associates, are Dytran and Nastran developed and marketed by the MSC Software Corporation (www.mscsoftware.com). The pre and post processor Patran used with these software packages makes the powerful tool very easy to use..

Short of those types of high-powered analyses, there are technical documents, information, and guidelines, such as TM5-1300 (GSA 2003), and DoD-UFC-4-020-3 (DoD 2005b) that can be used by design professionals to establish the performance of buildings during explosion. The documents that deal with the force of explosives and the kind of damage caused by a certain amount of explosive, prudently, are not in the public domain nor posted on the Internet. In the post 9/11 era, design professionals dealing with protection of buildings against terrorist attacks are confronting the dilemma of how much information to put in the public domain regarding blast-resistance and protection of structures against terrorist attacks Still, for the best guidance one may refer to the U.S. Department of Defense (DOD), the source of most of the information in this field, on how to deal with those questions. Deducting from the information posted on the web sites of DOD, it may be correct to state that the only information DOD does not want to make available to the general public is the information revealing *how much damage certain amounts of certain explosive types can cause* Other information that does not divulge the relationship between explosion and the resulting damage, yet may be used to protect people and buildings from injuries and damage, is widely and publicly distributed by the Department of Defense.

Of special interest to design professionals is the information that DoD has posted on its web site, http://www.hnd.usace.army.mil/techinfo/engpubs.htm, for public use without any restriction, especially DoD's Internet posting of unrestricted information, guidelines, and technical reports on the following items:

1. The levels of protection against blasts and establishing the level of protection that a building might need

2. Preventing car bombs from getting too close to a building

3. Preventing creation of glass shards and loose debris that can be carried by air pressure and shock waves during an explosion and that can cause injuries and property damage

4. Investigating the possibility of progressive collapse after the blast has occurred and has caused local damage and preventing the progressive collapse

As mentioned earlier in this report, I will focus on the item 4. An attempt has been made to ensure that the information in this report cannot be used to increase the knowledge of harmful actions that hurt people or damage buildings I believes that the information provided here can enhance measures to protect lives and property in an efficient and feasible way and without much noticeable change in the functionality, architectural appearance, or living spaces of civilian buildings.

1.2.b. Casualties and Damage after an Explosion Due to Progressive Collapse

During an explosion, depending on the size and type of the explosive device and the type and response characteristics of the building, some local damage is expected to occur. After an explosion, the damaged building is subjected to its service load (gravity and wind) and possibly fire. The issue of post-explosion fires, although very important, is outside the area of expertise of the author and is not discussed here. During the post-explosion phase, depending on the extent of damage to the structure of the building and the damage tolerance of the building, one of two outcomes is possible. Either the damaged building is able to continue to support the applied loads without partially or fully collapsing, or the inflicted damage or the ensuing fire are sufficient to result in progressive collapse of a significant portion or of the entire structure.

If the structure is capable of surviving an explosion and remains standing with only relatively insignificant localized damage and no progressive collapse, the injuries and damage are limited to those that occurred during the explosion, and the occupants can be evacuated to safety with the injured ones taken care of by first responders and health care professionals. A good example of this outcome is the performance of the north tower of the World Trade Center when in 1993 terrorists exploded a car bomb in the basement parking structure near the south-side exterior columns of the tower. Although the explosion resulted in loss of portions of basement floors, the columns were able to carry the gravity load from above even after loosing the bracing provided by the girders of the lost floors. Despite the tragic losses of the lives of six people and injury of more than 1000, there was no progressive collapse.

If a blast causes partial or full collapse of the structure in a domino effect, such progressive collapse can result in a large number of casualties and injuries, the result of the falling debris of the progressively collapsing structure. A tragic example of this case is the 1995 car-bomb attack on the reinforced concrete Murrah Federal Office Building in Oklahoma City where 168 people lost their lives, many of them as a result of progressive collapse of more than 70% of the structure (ASCE 2005), Figure 1.2. Table 1.1 shows a summary of major terrorist car-bomb attacks on U.S. facilities resulting in hundreds of lives lost and thousands of people injured.

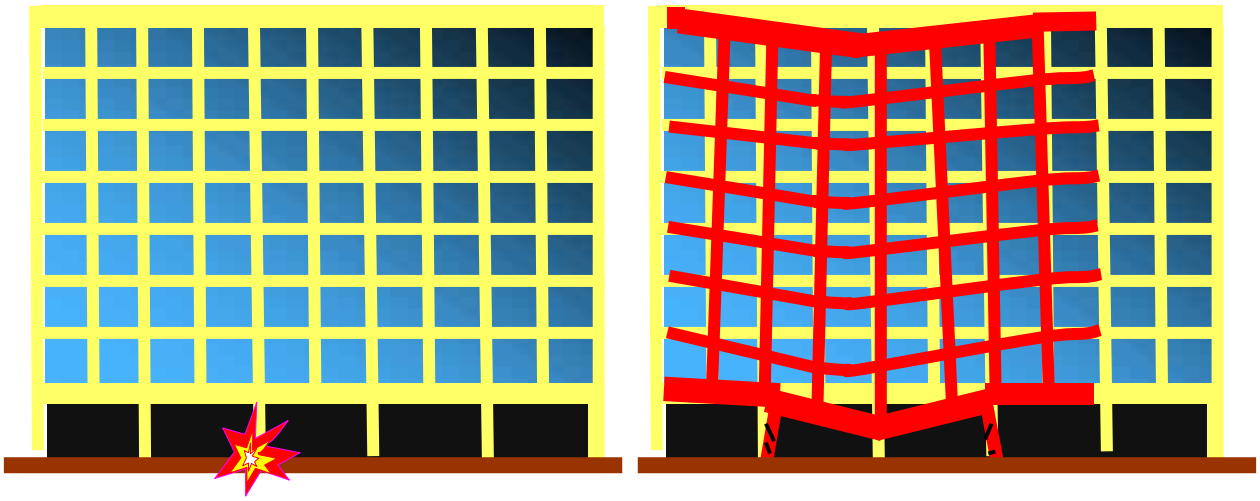

Figure 1.2. Sketch of Murrah Federal Building in Oklahoma City with Location of Blast and Progressively Collapsed Portion

1.3. Definition of Progressive Collapse

The ASCE-7 Standard: Minimum Design Loads for Buildings and Other Structures (ASCE 2005), defines progressive collapse in its commentary as:

> *"Progressive collapse is defined as the spread of initial local failure from element to element, eventually resulting in the collapse of an entire structure or a disproportionately large part of it.*
> *Some authors have defined resistance to progressive collapse to be the ability of a structure to accommodate, with only local failure, the notional removal of any single structural member." (ASCE 2005, Section C1.4).*

This definition, which is gaining acceptance in the profession, will be used in this document.

Table 1.1. Major Car Bomb Terrorist Attacks on Buildings*

Year	Location	Facility	Number of People Perished*
1983	Beirut, Lebanon	U.S. Embassy	63
1983	Kuwait City, Kuwait	U.S. Embassy Annex	4
1983	Beirut, Lebanon	U.S Marine Corp Barracks	242
1984	Beirut, Lebanon	U.S Embassy Annex	13
1993	New York, USA	World Trade Center	6
1995	Oklahoma City, USA	Murrah Federal Building	168
1995	Saudi Arabia	U.S Military Office Building	6
1996	Saudi Arabia	U.S. Military Housing Building	19
1998	Dar Es Salaam, Tanzania	U.S. Embassy	10
1998	Nairobi, Kenya	U.S. Embassy	291
2002	Bali, Indonesia	Sari Club	202
2003	Riyadh and Dhahran, Saudi Arabia	3 housing Complexes	20
2003	Casablanca, Morocco	5 different buildings	41
2003	Jakarta, Indonesia	Hotel Building	11
2003	Baghdad, Iraq	U.N. Headquarters	20

* Note: The information in the last column regarding the number of casualties is based on official statements and reports by reliable press agencies. However, in many cases, the exact numbers of casualties have not been established or conflicting numbers are reported in the press.

1.4. Code Requirements on Progressive Collapse Prevention

Prior to the tragic 1993 car-bomb attack on the World Trade Center, almost all terrorist attacks on U.S. citizens and interests were abroad and directed towards military personnel and installations, see Table 1.1. The Department of Defense, using its expertise and vast knowledge and experience in dealing with protection of military facilities against explosives, developed guidelines and technical information on blast-resistant design of structures and prevention of progressive collapse. One of the documents, TM5-1300 (2003), is used extensively by design professionals in protective design of building structures against car-bomb attacks. Other

documents, such as those published by Unified Force Command of the Department of Defense (DOD, 2003, 2005a, and 2005b), are also used as quasi-codes for protective design.

Another important document on progressive collapse prevention is Progressive Collapse Analysis and Design Guidelines for New Federal Office Buildings and Major Modernization Projects (GSA, 2003), published by the General Services Administration. Outside the United .States, in the United Kingdom, where civilian buildings were subjected to terrorist bomb attacks, as early as 1970s, guidelines and code provisions regarding blast-protection of buildings and prevention of progressive collapse were incorporated into national codes. In the United States, after the 1993 World trade center attack and especially after the 1995 catastrophic attack on the Murrah Building in Oklahoma City, the first generation of code provisions and commentary geared towards application to civilian facilities were introduced and incorporated into national codes and standards. For example, the ASCE-7 Standard (ASCE 2005) in its Section 1.4 General Structural Integrity, has the following provision:

> *Buildings and other structures shall be designed to sustain local damage with the structural system as a whole remaining stable and not being damaged to an extent disproportionate to the original local damage. (ASCE, 2005, Section C1.)*

In more recent years, the U.S. federal government has increasingly focused on protecting buildings against terrorist attacks by funding research and development projects to address the problem. The efforts were to develop mitigation and protective measures to reduce the damage and prevent casualties and major injuries of the occupants in the event of a terrorist attack, in particular terrorist car bombs. One such effort was the project undertaken by the author and his research associates to investigate the effects of car bombs on low-rise buildings and develop innovative technologies to protect buildings and their occupants from car-bomb attacks. The project funded by the Army and Advanced Technology Institute is summarized in Astaneh-Asl, Heydari, and Zhao 2003.

2. PROGRESSIVE COLLAPSE OF FRAMES WITH SIMPLE (SHEAR) CONNECTIONS

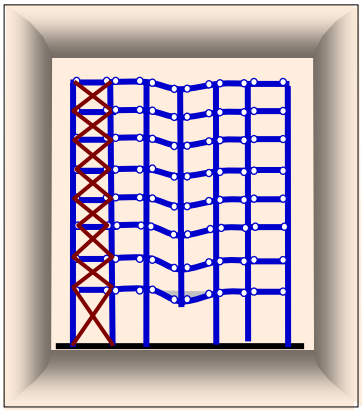

2.1. INTRODUCTION

The beam-to-column connections of a typical braced frame are shear connections with relatively small moment capacity. Frames with shear connections can also be found in structures where moment frames or shear walls (steel or concrete) are used as the lateral load resisting systems. In these structures, beams and columns outside the moment frame or shear wall system typically are connected to each other using shear connections. This chapter focuses on the issues related to progressive collapse resistance of steel frames with shear connections when a column is suddenly removed. I discuss the progressive collapse behavior of a two-span girder with pin-pin end connections after the middle support is suddenly removed. First, I present a summary of the elastic behavior of classic a three-hinge beam as derived by Timoshenko (1955) then extend it to inelastic behavior of an actual three-hinge beam with typical steel shear connections. The actual behavior of steel frames with shear connections, based on test results, are discussed in Chapters 3 and 5 with a summary of the full scale tests conducted at the University of California, Berkeley (Astaneh-Asl, et al, 2001a, 2001b and 2001c) and Tan and Astaneh-Asl 2003a.

2.2. BEHAVIOR OF SIMPLE FRAMES AFTER REMOVAL OF A COLUMN

To understand better the behavior of a simple frame, that is. a frame with simple beam-to-column connections, after removal of a column, shown in Figure 2.1(a), I consider the behavior of the simply supported girder connected to the removed column. Figure 2.1(b) shows the two-span girder. Assuming that the two spans are equal and the rest of the structure can provide axial rigidity to the supports, the two-span girder is idealized as a pin-pin girder shown in Figure 2.1(c). In the following section, behavior of the three-hinge girder shown in Figure 2.1(c) is investigated.

2.2.a Behavior of 3-Hinge Beams Subjected to Concentrated Load at Mid-span

The three-hinge span shown in Figure 2.2 represents a two span segment of a simply supported frame where a column has been suddenly removed. The elastic behavior of 3-hinge beam subjected to mid-span concentrated load has been addressed in classical textbooks such as Timoshenko (1955) as an example of the exception to applicability of the Catigliano's Method often used to establish elastic load-displacement relationship. In this case the stiffness of the

system against vertical displacement of the applied load is solely provided by the catenary force T developed in the two beam segments. The following derivation of load-displacement relationship during the elastic phase of behavior is from Timoshenko(1955).

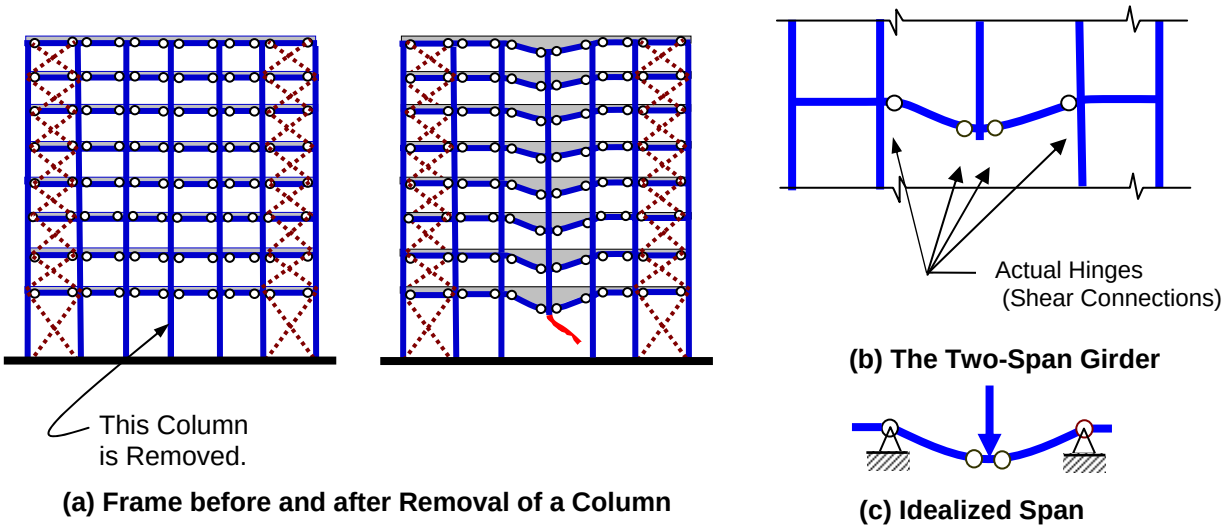

Figure 2.1. Braced Frame before and after Removal of a Column and the Two-Span Girder

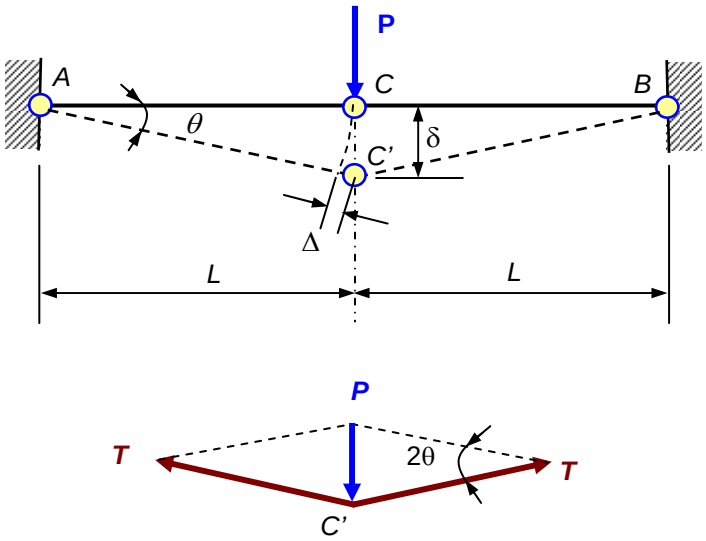

Figure 2.2. The Three-Hinge Beam Treated by Timoshenko (1955)

2.2.c Relationship between Applied Load and Deformation in Three-hinge Beams

To establish a relationship between the applied load *P* and the resulting displacement, I use *equilibrium* of forces and *compatibility* of displacements. Consider *AC'B* in Figure 2.2 to be the

deflected shape of the three-hinge beam ACB. The unit elongation (that is the axial tensile strain) of either beam in its deformed condition from compatibility of displacements in Figure 2.2 is:

$$\varepsilon = \Delta / L = \left(\frac{L}{\cos\theta} - L \right) / L = \frac{1}{\cos\ \theta} - 1 \tag{2.1}$$

Where,

ε = axial tensile strain in the beam

Δ = axial elongation of each beam segment (see Figure 2.2)

θ = rigid body rotation of the beam segments, same as rotation of the end connections (see Figure 2.2)

L = length of each beam segment in three-hinge beam (see Figure 2.2)

During the initial elastic phase of behavior, displacements and angle θ are small and the term $1/\cos\ \theta$ in equation 2.1 can be replaced with $1+\theta^2/2$ approximately. Then, replacing $1/\cos\ \theta$ with this approximate value we obtain:

$$\varepsilon = \frac{\theta^2}{2} \tag{2.2}$$

The corresponding tensile force, t, in the beams is:

$$T = AE\varepsilon = \frac{AE\theta^2}{2} \tag{2.3}$$

Where,

T = axial tensile (catenary) force in the beam (see Figure 2.2)

A = cross sectional area of the member

E = modulus of elasticity

From the condition of equilibrium of point C' in Figure 2.2,

$$P\ =\ 2\theta T \tag{2.4}$$

Eliminating T between Equation 2.4 and Equation 2.3 results in:

$$P = AE\,\theta^3 \tag{2.5}$$

Replacing θ with L/δ, its approximate value for small displacements yields

$$\delta = L\ \sqrt[3]{\frac{P}{AE}} \tag{2.6}$$

Where,

P = applied vertical load

δ = vertical displacement under the applied load P

Equation 2.6 indicates that, unlike in the most typical cases in structural engineering, for this case the displacement is not proportional to the applied load although the material is still elastic and follows Hooke's law. The reason for the elastic, nonlinear behavior exhibited here is the development of catenary axial force T in the beam. The value of catenary force is obtained by eliminating θ between Equations 2.4 and 2.5:

$$T = \sqrt[3]{\frac{P^2 AE}{8}} \tag{2.7}$$

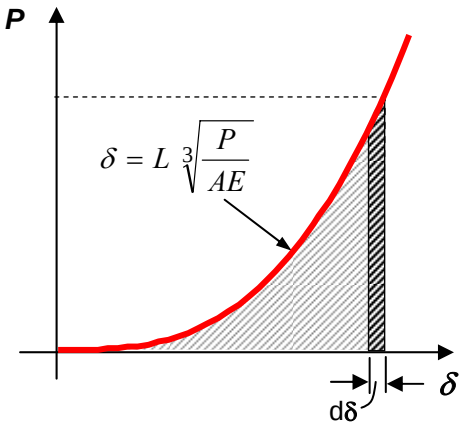

Figure 2.3. Force- Displacement Relationship for a Three-Hinge

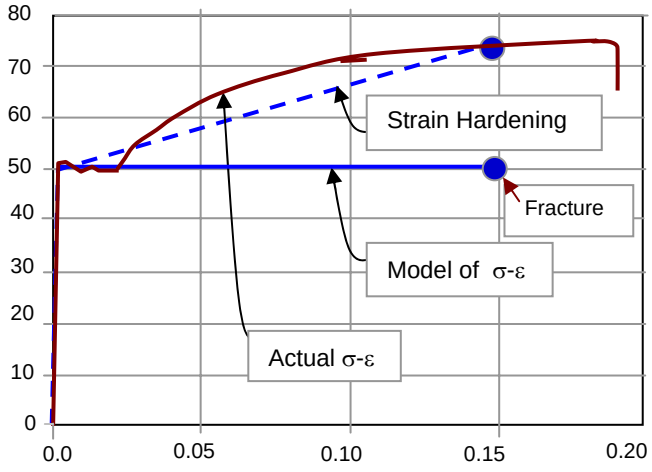

Figure 2.4. Actual and Simplified Stress-Strain Relationship for Steel

Figure 2.3 shows a graphic representation of Equation 2.6 with the variation of δ in terms of applied P. The area under the curve is the elastic strain energy stored in the beams, which are given by:

.

$$U_e = \int_0^{\delta} P d\,\delta \tag{2.8}$$

Substituting P from Equation 2.6 in the above Equation 2.8 results in:

$$U_e = \frac{AE}{L^3}\int_0^{\delta} \delta^3 d\delta = \frac{AE\,\delta^4}{4L^3} = \frac{P\delta}{4} = \frac{PL}{4}\sqrt[3]{\frac{P}{AE}} \tag{2.9}$$

Where,
U = elastic strain energy
$d\delta$ = incremental vertical displacement under the applied load P

When the axial catenary force reaches the yield capacity of the cross-section of the beam, the yield strength of the system is reached. The values of θ_y, P_y, and δ_y corresponding to the yield point are:

$$\varepsilon_y = \frac{F_y}{E} \tag{2.10}$$

$$\theta_y = \sqrt{2\varepsilon_y} = \sqrt{\frac{2F_y}{E}} \tag{2.11}$$

$$T_y = AE\varepsilon_y = AF_y \tag{2.12}$$

$$P_y = 2\theta_y T_y = (AF_y)\sqrt{\frac{8F_y}{E}} \tag{2.13}$$

$$\delta_y = (L)\left(\sqrt[3]{\frac{P_y}{AE}}\right) = L\sqrt{\frac{2F_y}{E}} \tag{2.14}$$

Where,

ε_y = yield strain
θ_y = rigid body rotation of the beam segments when the member reaches the axial yield point
T_y = axial tension yield capacity of the beam segments in three-hinge beam
P_y = applied vertical load at the time of yielding of the beam segments
δ_y = vertical displacement under the applied load P at the time of yielding of the beam segments

Figure 2.5 shows a variation of P, the applied load, compared to δ, the vertical displacement. Notice that the yield point is reached when the axial load in the member reaches AF_y. After yielding of the member, the axial force in the member remains at the constant level of P_y since no strain hardening is assumed. However, the applied load P continues to increase as shown in Figure 2.3. This increase in P is due to increase in the angle θ, which results in an increase in $P=2T\theta$ even when T is constant and at the T_y level. Point U in Figure 2.3 is the point of ultimate capacity and is reached when the axial strain in the member reaches ε_u the ultimate strain of the material Considering the ultimate strain of steel to be 0.15, then the angle θ, when the axial strain in the member reaches this ultimate value, is $cos^{-1}(1/1.15)$ equal to about 30 degrees.

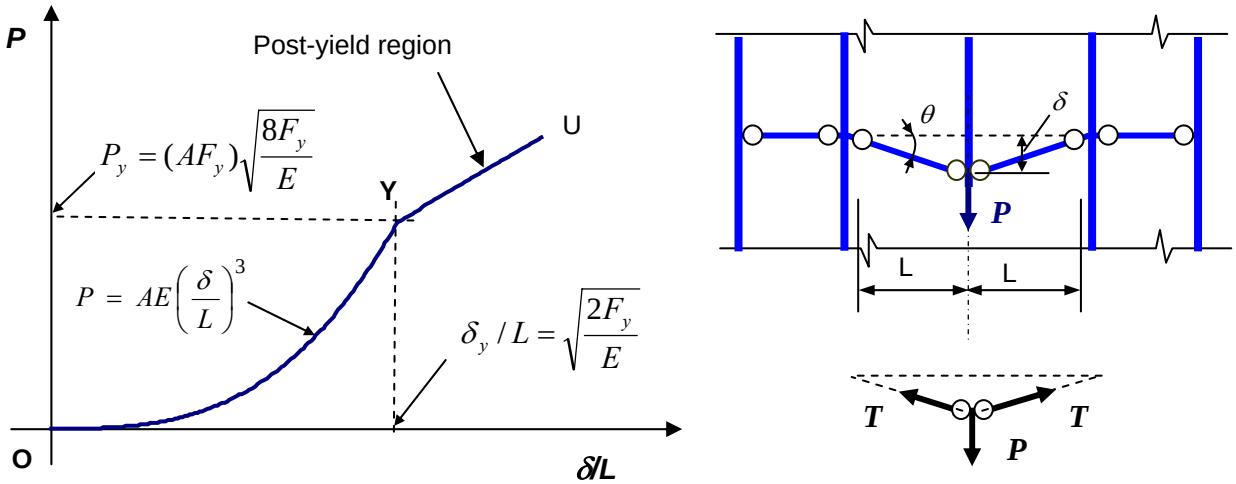

Figure 2.5. Force -Displacement Relationship for a three-Hinge Beam

Equations 2.10 through 2.14 can be applied to actual beams by taking into account the fact that the ends of the beams in actual structures are not totally restrained against horizontal movement as the pin connections of Figure 2.3 would imply. Figure 2.6 shows more realistic end- support conditions for a catenary beam with shear connections represented by springs k_c and the stiffness of supporting structure in horizontal direction represented by springs k_s.

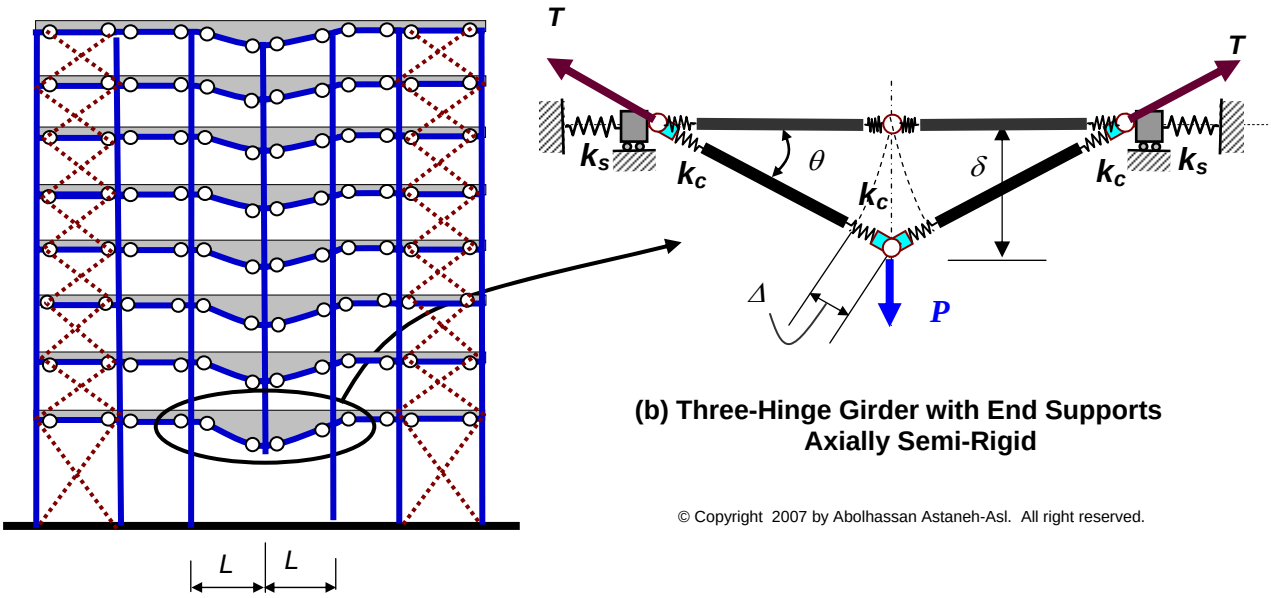

Figure 2.6. Beam Collapse Mechanism and Development of Axial Catenary Force, *T,* in Frames with Shear Connections

The ultimate stage of behavior is reached if either the hinges (shear connections) fail in rotation combined with axial tension or the member segments fracture under the catenary tension force. Therefore, to establish the ultimate capacity P_u of the span, first need to establish the ultimate value of the angle θ, denoted as θ_u, that the joints (shear connections) can tolerate without fracture. Also to establish the ultimate value of elongation, Δ, denoted as Δ_u, that the beam and connection assembly can tolerate before fracture.

In frames with shear connections, as the load P is applied to the beam, due to development of catenary action the end connections are pulled in. The horizontal movement of the end of the beam will add to the elongation ,Δ, of the beam; see Figure 2.6. Any increase in the value of Δ will increase deflection δ as well as angle θ, resulting in an increase in the value of force P for a given tension T as indicated by Equation 2.4 The amount of horizontal movement of the end of the beam depends on the stiffness of the end connections in the horizontal direction, k_c, as well as the stiffness of the supporting structure, k_s. In steel structures, if the floors are in place and not destroyed by blast, stiffness k_s can be quite large compared to stiffness k_c of the shear connections, especially in frames with bolted shear connections where, due to slippage and bolt-hole elongation, stiffness k_c can be relatively small compared to stiffness k_s.

Assuming stiffness of the support, k_s , to be much larger than the stiffness of the connection, k_c, and using elongation of the connection as the only source of elongation for the member while ignoring elastic elongation of the beam, the angle θ in Figure 2.6 is:

$$\theta_u = \tan^{-1}(\delta_u / L) \cong \delta_u / L = \frac{\sqrt{(L + 2\Delta_{u-conn})^2 - L^2}}{L} \tag{2.15}$$

$$\theta_u = \sqrt{\left(1 + \frac{2\Delta_{u-conn}}{L}\right)^2 - 1} \tag{2.16}$$

Where,

θ_u = rigid body rotation of the beam segments when the member reaches its ultimate capacity

$\Delta_{u\text{-}conn}$= ultimate elongation of the hinges (that is shear connections)

δ_u = vertical displacement under the applied load P when the load reaches the ultimate value

Information on the axial stiffness of steel shear connections is limited. The full-scale tests of catenary action of girders in frames with shear connections conducted by the author's research team shed some light on this issue. These tests (Astaneh-Asl et al. 2001a and 2001b,Tan and Astaneh-Asl 2003a, 2003b), which were bolted seat angles and shear tabs, summarized later in Chapters 3 and 5 respectively, indicated that the tested shear connections could elongate at least ¾ inch in the axial direction prior to reaching a fracture failure mode. Tests of bolted double-angle shear connections under shear and axial load (Ho and Astaneh-Asl.l993 and De Stefano and Astaneh-Asl 1991) also indicated that the ultimate axial elongation of these connections easily exceeds ¾ inch. Until more research results on axial ductility of shear connections become available, I suggest the use of a conservative value for axial elongation of steel shear connection equal to 5/8 inch. In bolted shear connections, this axial elongation is primarily due to slippage, bearing deformation in the hole, and bending of the edge distance in the horizontal direction. In welded shear connections, the axial elongation is primarily due to yielding of the steel in tension. In both connections, the elongation occurs only if the connection is designed to have yielding of the gross area of steel in tension govern over other more brittle failure modes such as fracture of the net area, block shear failure, and fracture of welds or bolts.

Using a maximum axial elongation of 5/8 inch for shear connections, Equation 2.16 gives θ_u values from 0.12 to 0.06 radians for spans from 15 to 45 feet with a value of 0.10 radians for a 20- feet span. This value is consistent with the results of full-scale tests of frames with shear connections, presented in Chapters 3 and 5 where the beam span was 20 feet and the rotation at the ultimate load prior to fracture of the connection elements was about 0.11 radians.

With the value of θ_u established and given by Equation 2.16, the maximum load carrying capacity, P_u, of the span in Figure 2.6 is calculated from:

$$P_u = 2\theta_u T_u \tag{2.17}$$

Where, T_u is the LRFD capacity for the failure mode that governs in the connections or in the member when subjected to axial tension. To have a robust and stable structure, it is preferred to have yielding of the connection or the member as the governing failure mode rather than the

fracture failure modes such as fracture of the net area, block shear failure, edge distance failure or fracture of the welds and bolts. If yielding of the connection governs, a value of $\Delta_{u\text{-}conn}$ equal to 5/8 inch can be used in Equation 2.16 to obtain the value of θ_u to be used in Equation 2.17. Otherwise, an appropriate value of θ_u needs to be established for the angle of rotation at the time of reaching the governing failure mode.

2.3. NUMERICAL EXAMPLE:

Consider the two span- frame shown in Figure 2.7 where the middle column on line C has been suddenly removed.

a. Calculate the progressive collapse resistance of the 2-span beam shown in Figure 2.7 where the beams are W18x35, A912 Gr. 50 and the end connections are shear tabs shown in the figure.

b. Suggest improvements for connection detail to increase the progressive collapse capacity such that the service load P = 12 kips (DL) + 10 kips (LL) can be supported on this two-span frame after removal of the column.

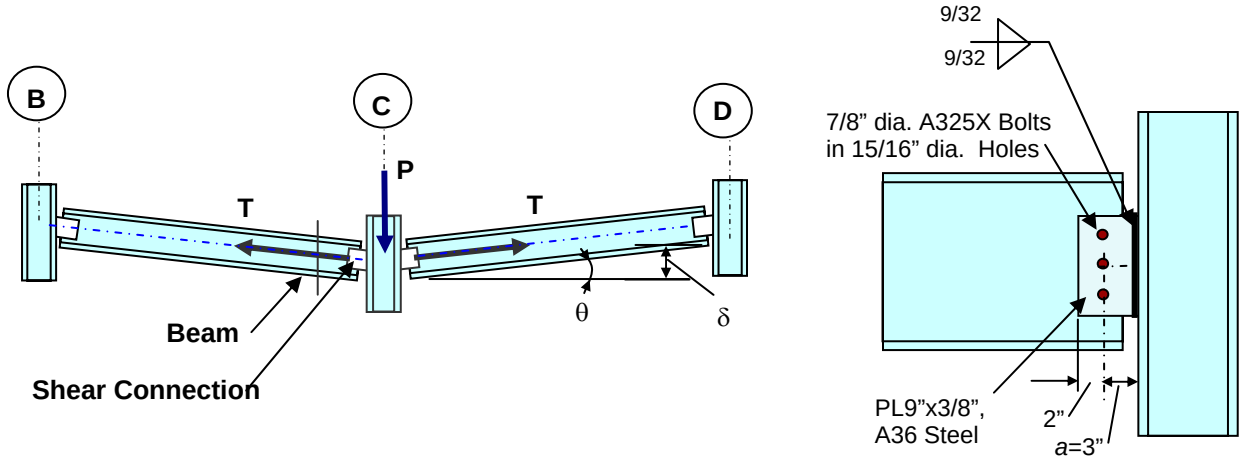

Figure 2. 7. Frame and Connection Details for Numerical Example

Solution for Part a:

Since a shear tab has a smaller area than the member does, the failure modes of the shear tab needs to be checked using LRFD equations but with a ϕ factor of 1.0 as prescribed by GSA (2003) and using a value of 1.0 for acceptable *DCR* (Demand-to-Capacity Ratios) instead of the values greater than one given in Table 5.1 of GSA (2003) for various structural components. The reason for using a *DCR* value of one is that the GSA (2003) values for *DCR* are to be used with "linear" analysis. The analysis presented earlier, following the Timoshenko, equations is not linear.

Check Yielding of Gross Area:

$\phi R_n = \phi_t F_y A_g$ =1.0x36ksi ×9x(3/8")=<u>121 kips</u>

$T_{u1} = DCR\ (\phi R_n)$= 1.0x 121= 121 kips

Check Fracture of Effective Net Area:

$\phi R_n = \phi_t F_u A_e$

$A_e = U A_n$

$U = 1$

$A_n = A_g - 2N(d_h + 1/16")(t) + \sum(s^2/4g)(t)$

$A_e = A_n = 9x0.375 - 3x(15/16 + 1/16)(0.375") = 2.25 \text{ in}^2$

$\phi R_n = \phi_t F_y A_g = 1.0 \times 58\text{ksi} \times 2.25 = \underline{130}\text{k}$

$T_{u2} = DCR\ (\phi R_n) = 1.0x\ 130 = 130$ kips

Check Block Shear Failure of Plate (t=0.375, A36 steel):

$\phi R_n = \phi R_n = 1.0x0.6F_y A_{gv}$

$A_{gv} = (2x3)(0.375)(2" - 1.0"/2) = 3.4 \text{ in}^2$

$\phi R_n = (1.0)(0.6)(36)(3.4) = 73$ kips

$T_{u3} = DCR\ (\phi R_n) = 1.0x\ 73 = 73$ kips

Check Block Shear Failure of Beam Web (t=0.3, Gr. 50 steel):

$\phi R_n = \phi R_n = 1.0x0.6F_y A_{gv}$

$A_{gv} = (2x3)(0.3)(2" - 1.0"/2) = 2.7 \text{ in}^2$

$\phi R_n = (1.0)(0.6)(50)(2.7) = 81$ kips

$T_{u4} = DCR\ (\phi R_n) = 1.0x\ 81 = 81$ kips

Check Bolt Failure:

$\phi R_n = \phi F_{bv} A_b = 1.0(3)(60\text{ ksi})(0.601) = \underline{108\text{ kips}}$

$T_{u5} = DCR\ (\phi R_n) = 1.0x\ 108 = 108$ kips

The bolt bearing failure mode is not checked here since any bearing failure short of causing an edge distance fracture will be helpful in hole elongation, adding to the elongation of the beam, and increasing the value of θ_u as well as increasing P_u. The edge distance failure is prevented by checking the block shear failure and providing ample edge distance.

Check welds:

$\phi R_n = \phi F_w A_w = (1.0)(9)(2)(9/32)(0.707)(0.6)(70) = \underline{150\text{kips}}$

$T_{u6} = DCR\ (\phi R_n) = 1.0x\ 150 = 150$ kips

The governing failure mode is block shear of the shear tab plate by bolts moving in horizontal direction with an LRFD (ϕ=1.0) capacity of T_{u3}=73 kips axial load.
Since yielding was not the governing failure mode, the maximum elongation capacity of 5/8 inch as suggested earlier for the shear connection with yielding cannot be used as the governing failure mode. Instead, due to slippage of the connections, the elongation of the members is used. Assuming a value of 1/8 inch for the slippage at each connection at the time of reaching the maximum load of 73 kips, the elastic equations given by Timoshenko (1955) to establish the value of angle θ_u is used when the block shear failure occurs, in this case while the beam is still elastic. The equations governing the elastic behavior were given earlier in this chapter and are used here to establish θ_u .

$\varepsilon_u = \Delta/L$=2(1/8")/(19ftx12in/ft)=0.0011 in/in
$\theta_u = (2\varepsilon_u)^{0.5}$= [2(0.0011)]$^{0.5}$=0.047 radians
The capacity P_u, under static load application, is then:
$P_u = 2T_u\ \theta_u$ = 2x73 kips x 0.047= 6.8 kips.
Applying a reduction factor of 2.0 for the dynamic effects of the sudden removal of the column, as given in GSA (2003), can obtain the design value of strength of this system to resist the load P as:
$P_d = P_u/2.0$=6.8/2.0=3.4 kips.

Capacity P_d of "as is" system =3.4 kips

Solution for Part "b":

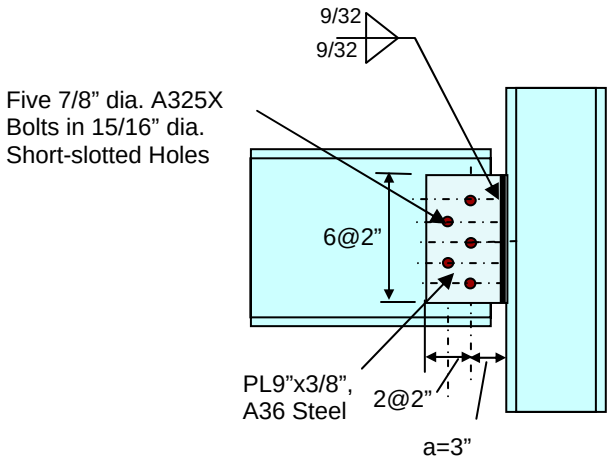

Figure 2.8. Improved Connection for Progressive Collapse Prevention

The connection in Figure 2.8 is designed to carry the load given in Part b. The design is given as follows.

Establish Factored Loads:
According to GSA (2003) as well as DOD (2005), the factored combined load for progressive collapse analysis is:
$P_{LRFD} = 2(DL+0.25LL)$= 2(12+0.25x10)=29kips

Since the governing failure mode in Part a was the block shear failure of the shear tab connection, the capacity ended up being relatively small. Changing the shear tab dimensions to make the yielding of the gross area of the shear tab the governing failure mode of the connection, gives a larger angle of θ_u at failure and a larger capacity P_u. The shear tab is thus designed to have a yield capacity corresponding to the applied load of 29 kips, and the other failure modes are checked to ensure that their capacities in tension are larger than the tension force corresponding to 29 kips applied load. The LRFD methods with ϕ=1.0.are used.

Design of the Shear Tab to Make Yielding the Governing Failure Mode:
P_u=28 *kips*

$$\theta_u = \sqrt{\left(1+\frac{2\Delta_{u-conn}}{L}\right)^2 - 1}$$

θ_u = [(1+2x0.625"/228")^2-1]$^{0.5}$= 0.105 radians
$T_u = P_u/(2\theta_u)$ = 29kips/(2x0.105)= 138 kips
$A = T_u/F_y$= 138kips/36 ksi= 3.9 in^2 Try PL12"x3/8", A36 steel
Yield capacity of plate used = $T_y = AF_y = AF_y$= 12x0.375x36=162 kips

Check Fracture of Effective Net Area:
Five 7/8 inch diameter A325 bolts are used (Figure 2.8) instead of the three originally used (Fig. 2.7) $\phi R_n = \phi_t F_u A_e$
$A_e = U A_n$
U= 1
$A_n = A_g - 2N(d_h + 1/16")(t) + \sum(s^2/4g)(t)$
$A_e = A_n$=12x0.375-5(15/16+1/16)(0.375")+ (4x2^2/4x2)(0.375)= 5.25 in^2
$\phi R_n = \phi_t F_y A_g$= 1.0×58ksi × 5.25=<u>304 kips</u>
$T_{u2} = DCR\ (\phi R_n)$= 1.0x 304= 304 kips <u>> 162 kips O.K.</u>

Check Block Shear Failure of Plate (t=0.375", A36 steel):
Two rows of bolts 2 inches apart are used (Figure 2.8)
$\phi R_n = \phi R_n$ = 1.0x0.6F$_y$ A$_{gv}$
A_{gv}=(2x3)(0.375)(4"-1.25"/2)+(2x2)(0.375)(2"-1.25"/2)=9.7 in^2
ϕR_n = (1.0)(0.6)(36)(9.7) =<u>209 kips</u>
$T_{u3} = DCR\ (\phi R_n)$= 1.0x 239= 209kips <u>> 162 kips O.K.</u>

Check Block Shear Failure of Beam Web (t=0.3", Gr. 50 steel):
Two rows of bolts 2 inches apart are used (Figure 2.8).
$\phi R_n = \phi R_n$ = 1.0x0.6F$_y$ A$_{gv}$
A_{gv}=(2x3)(0.3)(4"-1.25"/2)+(2x2)(0.3)(2"-1.25"/2)=7.4 in^2
ϕR_n = (1.0)(0.6)(50)(7.4) =<u>222 kips</u>
$T_{u3} = DCR\ (\phi R_n)$= 1.0x 222= 222kips <u>> 162 kips O.K.</u>

Check Bolt Failure:
Use five 7/8 inch diameter A325X bolts instead of the three originally used (Figure 2.7)
$\phi R_n = \phi F_{bv} A_b$ =1.0(5)(60 ksi)(0.6)=<u>180 kips</u>
$T_{u4} = DCR\ (\phi R_n)$= 1.0x 180= 180 kips <u>> 162 kips O.K.</u>

Check welds:
Use ¾ of the plate thickness as the weld size following Astaneh-Asl, (2005). The weld size will be ¾ x 0.375 = 9/32" which is the same used in original design above
$\phi R_n = \phi F_w A_w$ =(1.0)(12)(2)(3/8)(0.707)(0.6)(70)=<u>267 kips</u>
$T_{u5} = DCR\ (\phi R_n)$= 1.0x 267= 267 kips <u>> 162 kips O.K.</u>
All failure modes have a capacity larger than the capacity due to the yielding of the gross area. Therefore the design is complete, and the connection in Figure 2.8 is capable of resisting the applied loads.

3. TESTS OF A STEEL FRAME WITH BOLTED SEAT AND WEB ANGLE SHEAR CONNCTIONS

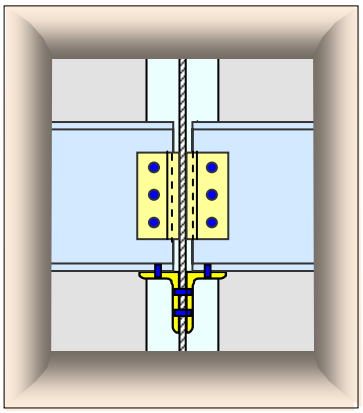

3.1. INTRODUCTION

This chapter presents a summary of the tests conducted at the University of California, Berkeley on a typical modern steel building structure with simple beam-to-column connections and a concrete slab steel deck floor.. The shear connections used in the tests summarized in this chapter were bolted bottom flange seat angles with an added bolted single angle on the web. The main objective was to establish the strength of the system to resist progressive collapse in the event of elimination of a column. An added objective was to use the test results to develop design- information on the potential of the existing typical steel structures with no prior provisions against progressive collapse actually to become systems that can resist progressive collapse. The tests reported in this chapter were primarily supported by the General Services Administration and in part by the American Institute of Steel Construction Inc. For more information on these tests, the reader is referred to the final report of the project by Astaneh-Asl et al. 2001b).

3.1.a. Test Specimen

The test specimen was a 60 foot by 20 foot one- story steel structure with a steel deck and concrete slab floor system and wide flange beams and columns. The test specimen was a full-size representation of a single floor of a typical modern steel frame building with simple connections. Figure 3.1 shows a plan view and elevation of the test specimen. The height of the columns in the specimen, for safety reasons, was equal to 6 feet, to limit the drop height of the floor in case the floor collapsed after removal of the middle column. The north side of the specimen, which had a similar steel frame, had catenary cable in it. The frame with steel cable on the north side was used first to test the catenary action of the cable. The results of these tests are summarized in Chapter 4 .

The beam-to-column shear connections of the “collapsing” frame of the test specimen were bolted seat angles plus a single bolted angle on the web of the beam. Figures 3.2 and 3.3 show views of the connections.

The tested structure had a simple (shear) beam-to-column connection that was not part of the lateral load resisting system of the building. The full-size specimen, Figure 3.1, had four bays in the longitudinal direction and one bay in the transverse direction. The north side, which

had cables in it, had longitudinal and transverse rebars placed into the floor slab above the longitudinal beams. However, the south side, the subject of the tests reported in this chapter, did not have any substantial rebar other than the standard 6x6 wwf wire mesh. Figures 3.4 and 3.5 show the beam-to-column connections in the longitudinal and transverse directions, respectively. Figure 3.6 shows the floor slab during construction. The beams, columns, angles, and shear tabs were specified as A36 steel. The concrete in the floor slab was specified as normal weight concrete with f'_c of 4000 psi. The slump of the concrete was 4 ½ inches.

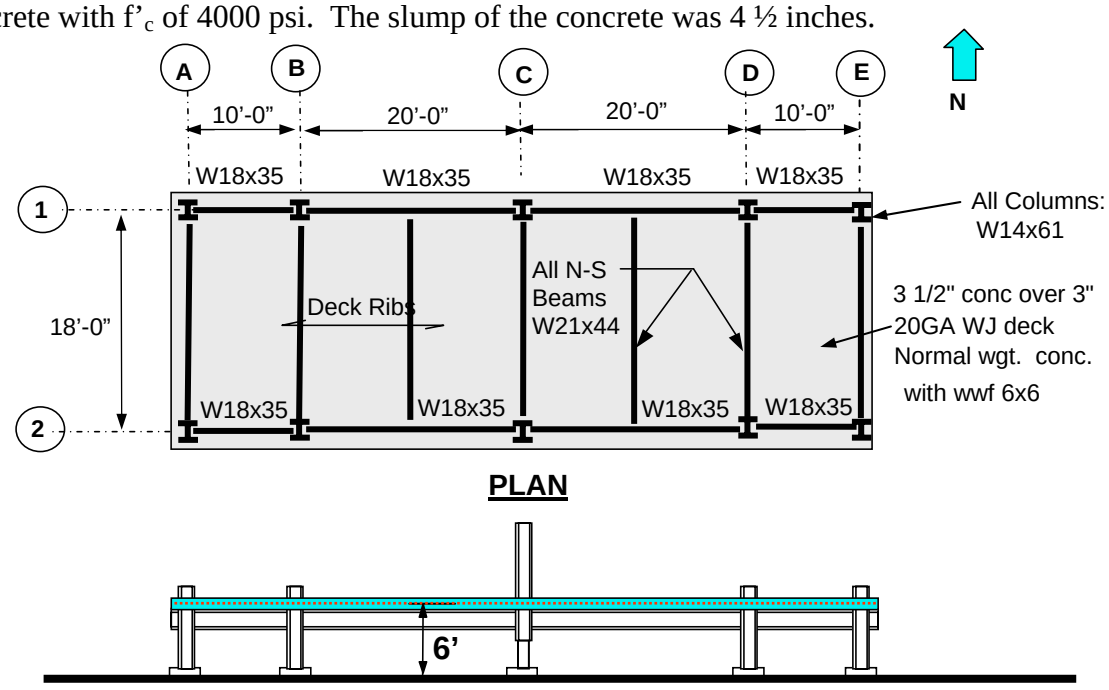

Figure 3.1 Test Specimen

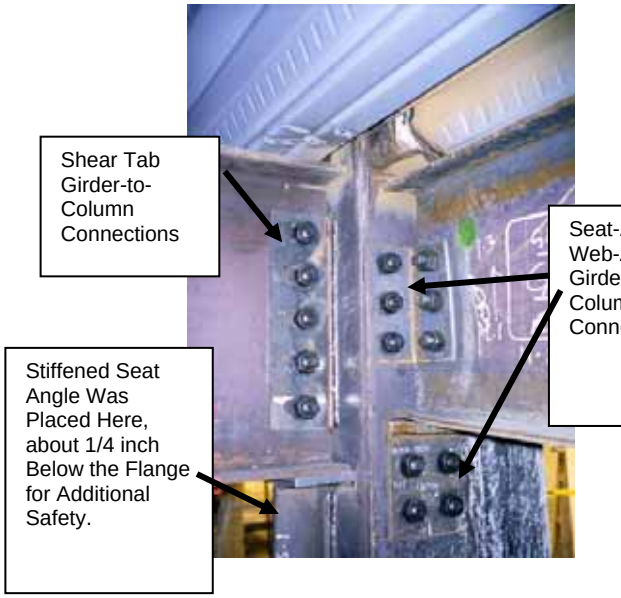

Figure 3.2. A View of the Beam-to-Column Connections

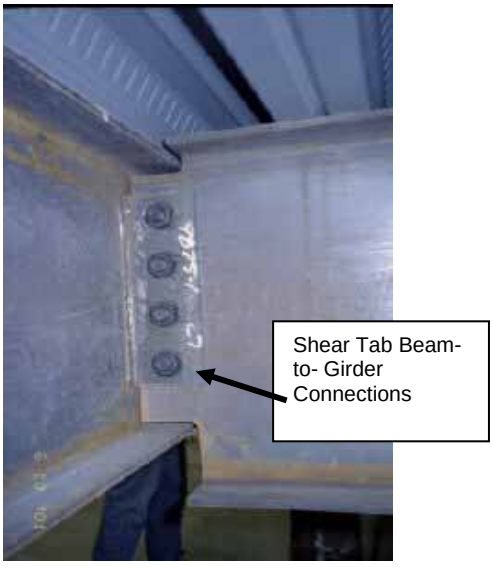

Figure 3.3. A View of the Beam-to-Girder Connections

All the bolts were A325X, 7/8-inch diameter. The lengths of the bolts were governed by the widths of the connecting material, with either 2 ¼- inch or 3-inch bolts providing the required length. All welds were performed in the shop by the Herrick Corporation. Verco Structural Steel Decking donated the Type W3 Formlok, Gauge 20 steel deck. The Nelson Studs supplied and installed the ¾ inch diameter, 4 ½ inch long shear studs used in the test structure free of charge. The shear studs were at 8-inch centers along the longitudinal beams and 1'-0 ¾" centers along the transverse beams. The wire mesh inside the floor slab was W1.4xW1.4 flat sheet reinforcement with 6 inch by 6-inch openings. More information on details of the test specimen is found in Astaneh-Asl et al (2001a, 2001b and 2001c).

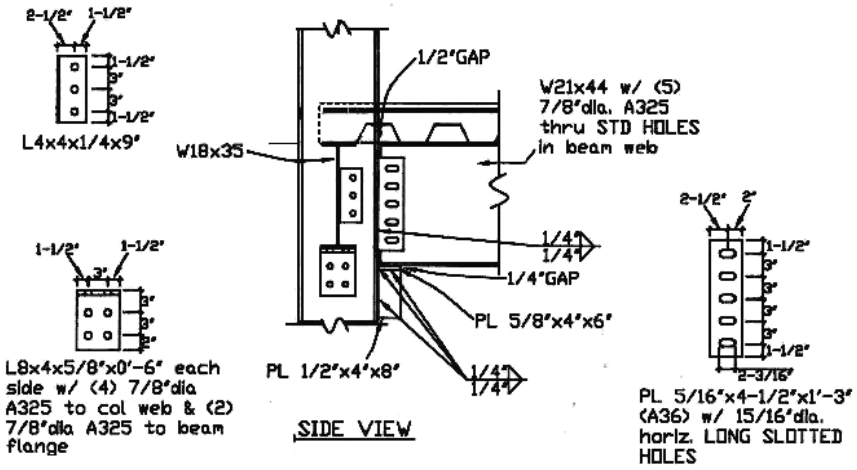

Figure 3.4. Beam-to-Column Connections in Longitudinal Direction
(Astaneh-Asl et al., 2001a)

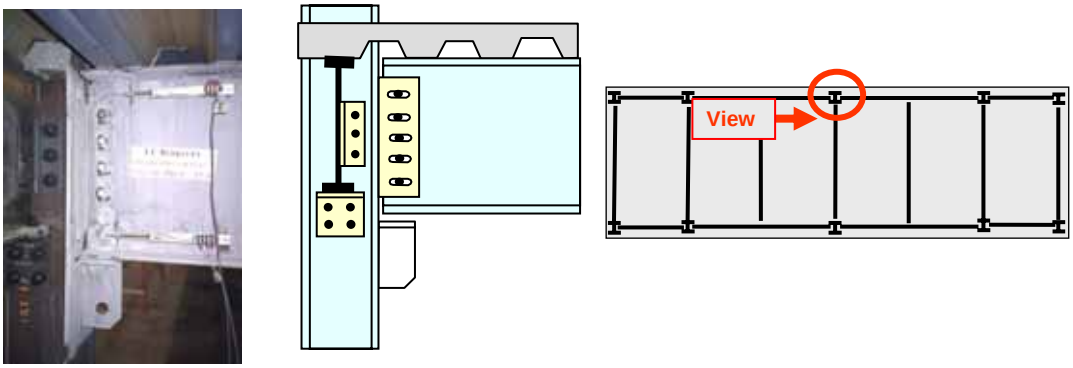

Figure 3.5. Details of the Beam-to-Column Connections

Figure 3.6.View of the specimen prior to and during placing concrete

3.1.b. Test Procedures

The research project investigated the capacity of the structure to resist progressive collapse in the event of an explosion removing one of the column supports in the building. For practical and safety reasons, no explosives were used to destroy the column supports. Instead, the specimen was designed, built, and tested to simulate the instantaneous loss of an exterior column. The center columns on each longitudinal frame of the specimen (columns C1 and C2 in Figure 3.1) were constructed to terminate 36 inches above the laboratory floor. With hydraulic actuators, each of these "drop columns" could be pushed downward as much as 36 inches. The hydraulic actuators imposed a downward force on the drop column to simulate the gravity load of the drop column. When they were not being tested, the drop columns were supported on 36-inch short stub columns. The research project described in this chapter specifically tested column C2, located on the south side of the specimen, Figure 3.1. This column, which was pushed down during the test, will be denoted here as the drop column.

When the drop column was pushed downward, the end of each adjacent W18x35 beam connected to the drop column also moved downward, resulting in rigid body rotation of the beams, Figure 3.7. As the displacement increased, the structure resisted progressive collapse by developing catenary action in its beams and the floor attached to the beams. In the original un-deformed configuration, the beams were oriented horizontally and their shear connections provided very low vertical stiffness to prevent downward movement of the drop column. However as the drop column moved downward, the adjacent beams rotated and the geometry of the beams formed a V shape as shown in Figure 3.7. The V shape of the beams resulted in large axial catenary forces developed in the beams shown as forces T on Figure 3.7. The vertical components of the axial catenary forces were the reactions to support the drop column and prevent its progressive collapse. The relationships among P,T, θ, and δ were given in Chapter 2.

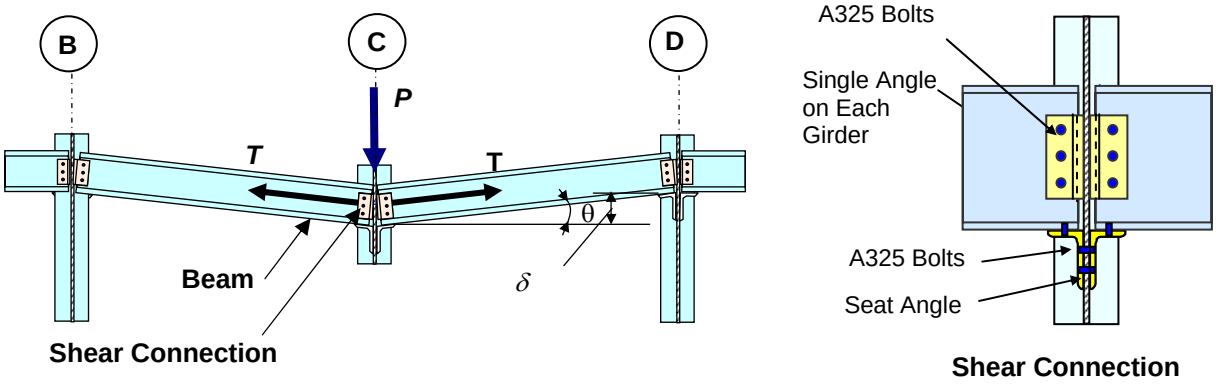

Figure 3.7. Example Subassembly of Simply Supported Frame

Three consecutive tests were performed on the specimen. Each test started with removing Column C2 in Figure 3.8 and, immediately after the removal, applying a concentrated vertical load to the column on top of the removed column. The concentrated load applied to the top of the column simulated the effects of both the dead load, due to nonstructural elements, and the live load, which were not present on the floor at the time of the tests. The column on the top of the removed column was pushed down at a rate of 0.25 inches/second to three different

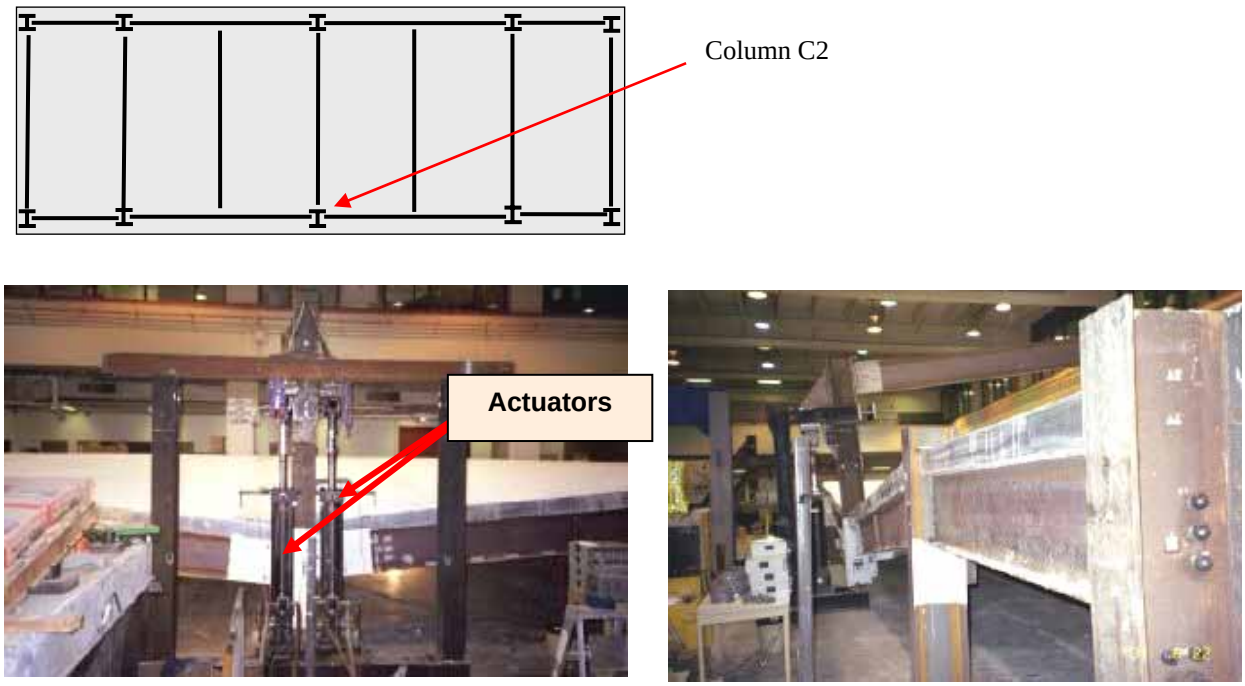

Figure 3.8. Actuators to Apply Additional Gravity Load to the Specimen

3.1. c. Test Results

The variations of force in the column that was collapsing (that is Column C2 in Figure 3.3) versus the vertical drop of the column are shown in Figure 3.9.

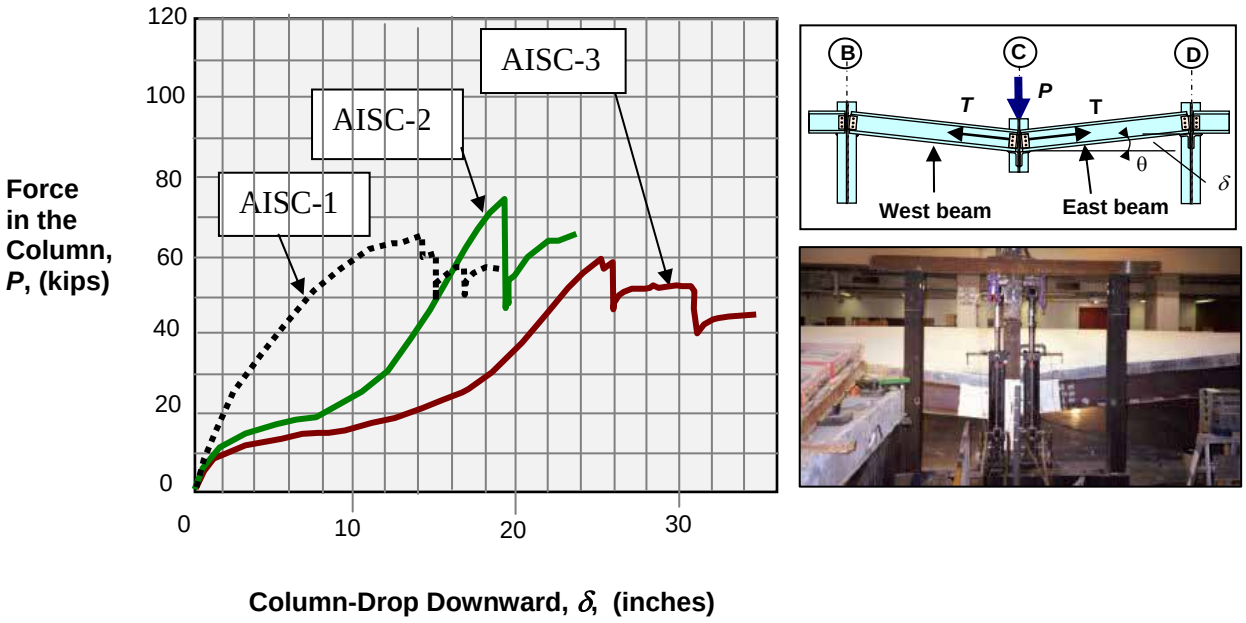

Figure 3.9. Load versus Downward Displacement of Column C2 for AISC Tests

3.1.d. Behavior of the Specimen during the Tests

Three tests were conducted on the specimens. The tests, denoted as AISC-1, AISC-2, and AISC-3, had column drop displacements of 19, 24, and 35 inches, respectively. In the following, behavior of the specimen during the tests is discussed.

Behavior of the Specimen during Test AISC-1 (19 inches Column Drop)

During the first test (Test AISC-1), as the column displacement downward exceeded 14 inches, the top two bolts on the vertical leg of the seat angle of the longitudinal beams fractured in tension combined with prying action; see Figure 3.10. The end of the bolts, including the nuts, shot violently through the air while the head of the bolts remained in place. A total of four bolts connected the seat angle to the column web. After fracture of the two bolts on the upper row, the remaining two bolts in the lower row continued to resist tension combined with prying action. Following the fracture of the two upper bolts, the seat angle experienced local yielding and large inelastic deformations, Figure 3.10. Note that the dark area on the seat angle, where the whitewash paint is separated, indicates yielding of the angle leg.

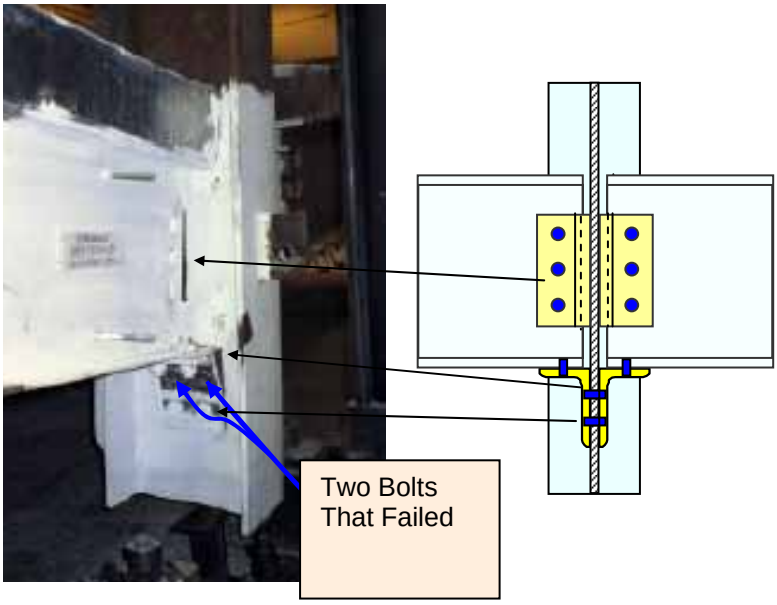

Figure 3.10. Failure of Two Bolts and Deformation of Seat Angle

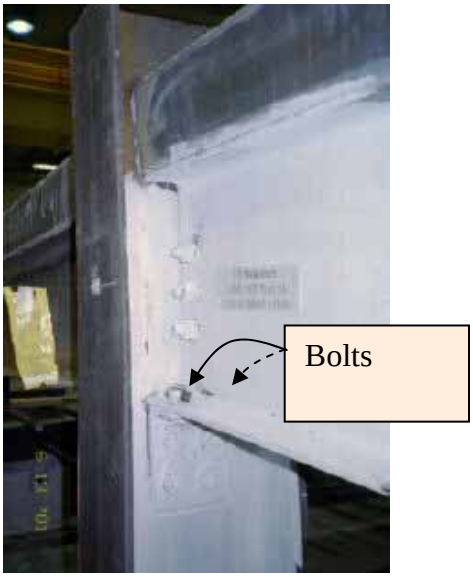

Figure 3.11. Failure of Bolts on Bottom Flange

As the displacement approached 15 inches, the two bolts that had secured the beam to the top of the seated angle at the other end of one of the longitudinal beams, west of the displaced column, failed in shear and popped; Figure 3.11. As the displacement approached 17 inches, slippage occurred at some point within the structure. Although the load- carrying capacity of the structure decreased abruptly at that point, the load gradually increased to the same value as before the spike. A fracture failure would have resulted in unrecoverable decreased capacity, whereas the slippage resulted only in a temporary decrease in the load- carrying capacity followed by recovery of the strength and stiffness.

The concrete slab separated from the columns as the displacement increased. At the final displacement of 19 inches, a gap of approximately 1 inch was visible between the floor slab and Column B2. After Column C2 reached a downward displacement of 19 inches, the displacement was held constant for approximately 1 minute before returning to a displacement of 17 inches. The total sustained force in the drop column, including the dead load, at the final displacement of 19 inches was 54.0 kips. Approximately 10 minutes later, the column was pushed up and returned to its original height, corresponding to zero displacement. Afterwards the two bolts that had failed on the seat angle, Figure 3.10, were replaced. Due to the seated angle deformation noted above, a ¼-inch gap remained along the shaft of the bolt after the nut was tightened.

Figure 3.12. Failure of Bolts Connecting the Beam Bottom Flange to the Seat Angle

During the tests the behavior of the steel deck was monitored by strain gauges. A maximum strain of 1450×10^{-6} was measured on the steel deck during the test. The specified yield stress of the deck was 33 ksi, corresponding to a yield strain that was calculated as 1140×10^{-6} by dividing the yield stress of 33 ksi by 29000 ksi, modulus of elasticity of steel. Since the measured strain in the deck (1450×10^{-6}) was larger than the yield strain, it indicated the possible yielding of the deck

Behavior of the Specimen during Test AISC-2 (24 inches Column Drop)

The second test (Test AISC-2) was conducted by dropping the upper column 24 inches. As the column reached a displacement of approximately 19 inches downward, which was the maximum displacement during the previous test, the two bolts that held the longitudinal beam east of the loaded column on the seated connection at column C2, failed. The dramatic drop in the load is evident as a spike in Figure 3.9. The local yielding of the seated connection was also observed. The cracking and tearing of the connecting angle between the loaded column and the longitudinal beam directly east of the connection had begun. After the column reached a displacement of 24 inches during this test, the displacement was held constant for approximately one and a half minutes before returning to a displacement of 20 inches. The total sustained

force, including dead load, at the maximum displacement of 24 inches was 62.8 kips. Approximately 10 minutes later, the column was returned to the original height, corresponding to zero displacement.

While attempting to replace the same top two bolts on the seat angle connection that had failed during Test AISC-1 and had been replaced after that test, we noticed that the bolts had not failed, but had undergone large deformations. Though the bolts were removed, we could not replace them with new ones due to the large deformations of the seat angles.

The force-displacement plot (Figure 3.9) shows a gradual stiffening of the structure once the displacement had passed 5 inches, which is due to the replacement of the two bolts in the seated connection at the drop column. The ¼-inch gap that had remained after the replacement affected the behavior of the structure. As the bolts adjusted to the gap and engaged themselves, the structure became stiffer.

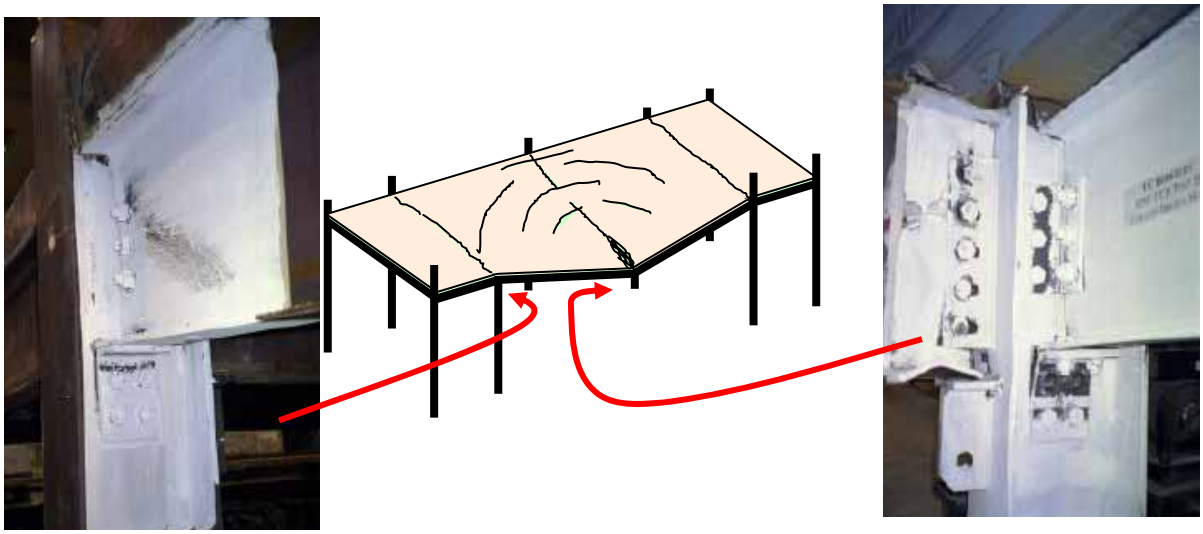

Connection B2 Connection C2

Figure 3.13. View of Two Connections at the End of Test AISC-2 (Column Drop of 24 Inches)

The steel deck suffered noticeable damage. Major deformations were noted along the column line of the displaced column, with concentrated damage occurring near the beam to column connections. The steel deck was ripped near columns B2 and D2, while bending was widespread. A maximum micro-strain of 1560 was measured during displacement. The corresponding maximum stress was calculated to be 45.2 ksi. The strains for the second subtest included any residual strains that existed within the gauges after the column had returned to a position of zero displacement.

Figure 3.13 shows the connection of the column of the test specimen after Test AISC-2 (maximum column drop of 24 inches). Figure 3.14 shows other views of the specimen after this test.

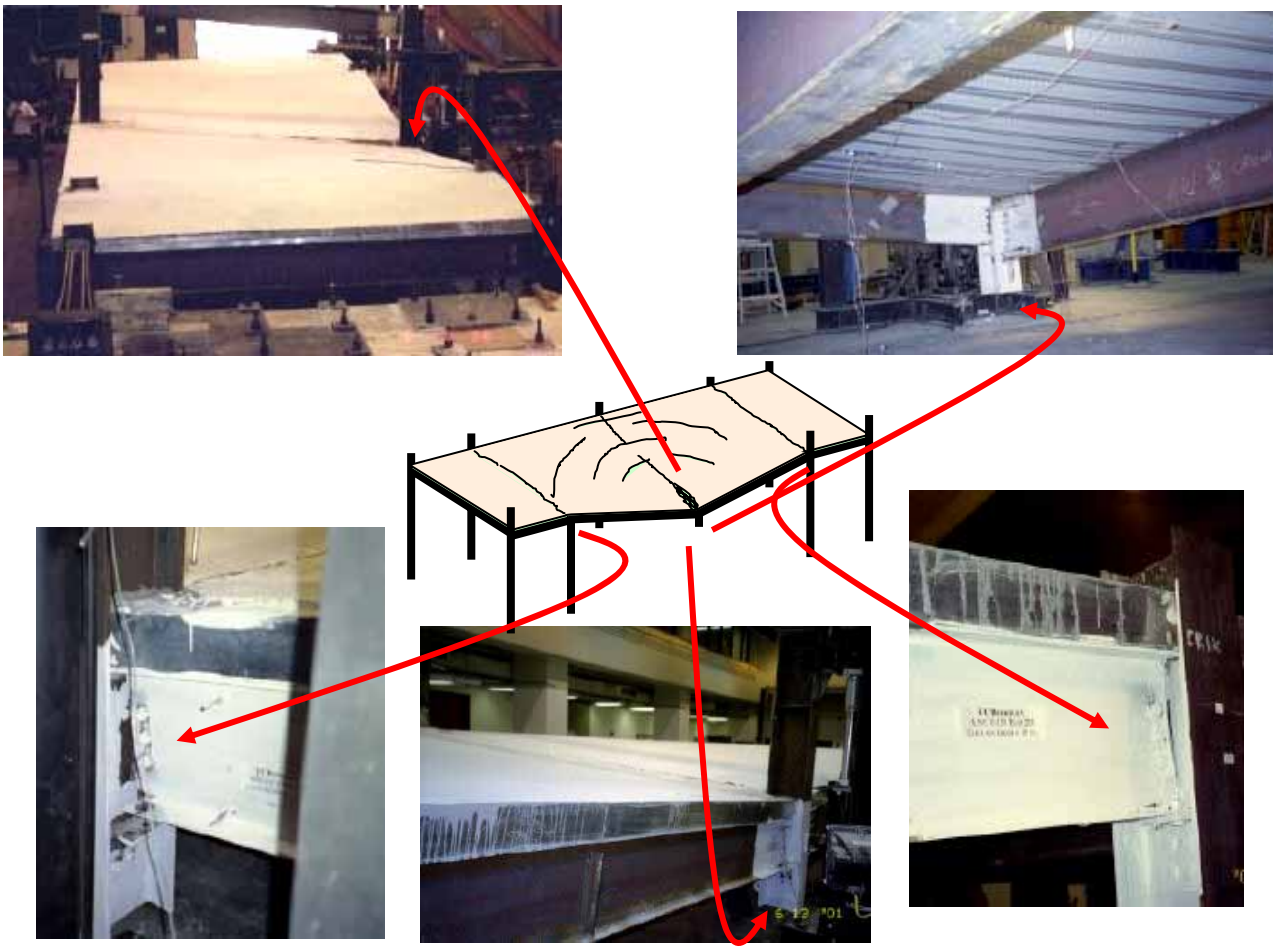

Figure 3.14. View of Specimen at the End of Test 2B (Column Drop of 35 inches)

Behavior of the Specimen during Test AISC-3 (35 Inch Column Drop)

The third test was conducted by pushing the column down 35 inches. The force displacement curve can be seen in Figure 3.9. In addition to the above noted behavior, as the column displacement approached 26 inches, complete failure occurred on the connecting angle between the drop column C2 and the longitudinal beam directly east. After the angle had failed, the concrete slab was the primary element transferring the applied force to the longitudinal beam directly east of the displacing column. Unable to maintain this force transfer, the slab failed in shear along the transverse beam connecting the two columns C1 and C2. Figure 3.15 shows hair cracks as well as major cracks on the top surface of the floor slab at the end of this test. Figure 3.16 shows views of the specimen at the end of Test AISC-3.

The concrete slab and steel deck suffered significant damage during the 35-inch displacement. The steel deck continued to tear, opening up gaps both within and between deck segments. The damage was concentrated along the column line of the drop column. There was a separation of at least 1 inch between deck segments along the transverse beam connecting the

two C1 and C2 columns. Near column D2, the deck tore, opening up a hole that measured more than 3 inches between the steel deck and concrete slab.

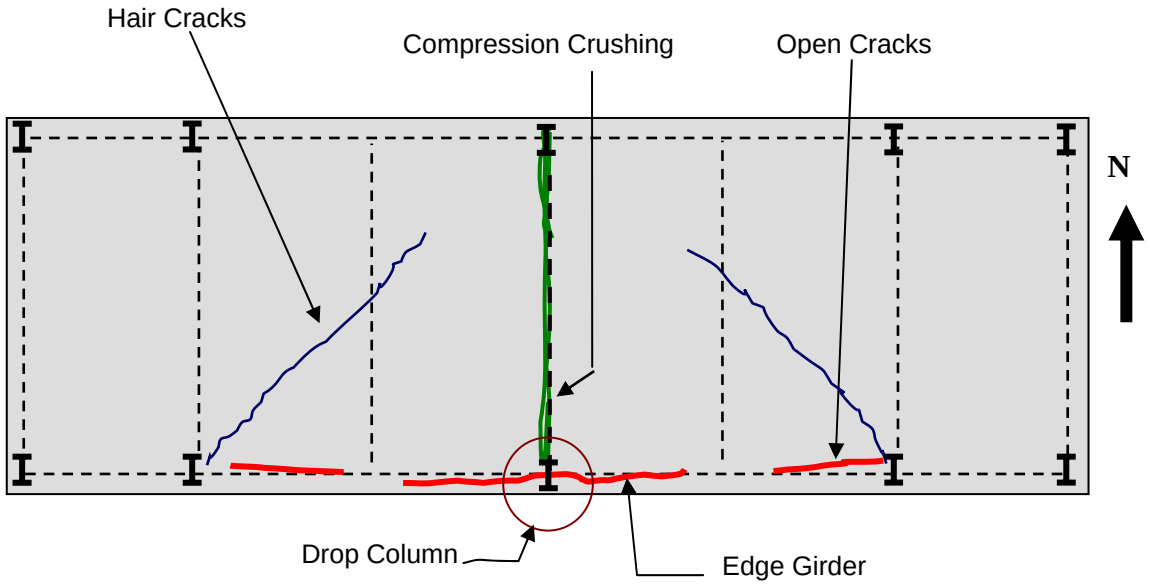

Figure 4.15. Crack Pattern on the Floor Slab at the End of Test AISC-3

After the column reached a displacement of 35 inches, the displacement was held constant for approximately 2 minutes before returning to a position of approximately zero applied force. The total sustained force, including dead load, at the final displacement of 35 inches was 44.5 kips. The structure remained in the position of zero applied force, corresponding to a displacement of approximately 27 inches for several days. While the structure was displaced 27 inches, the research team inspected and made notes of the relevant deformations. The following week, the column was returned to its original height, corresponding to zero displacement.

3.2. SUMMARY OF TEST OBSERVATIONS

The following conclusions were reached by observing the behavior of the test specimen and by studying the collected test data.

1. The ultimate capacity of the structure following the loss of a column was limited by the beam-to-column connection capacity to carry axial catenary forces. The catenary action of the beams and steel deck was adequate here to prevent progressive collapse. If connection bolts had not fractured in tension, it is expected that larger catenary forces could have been carried by the beam, resulting in its resisting the larger vertical load of the removed column.

2. The ribs in the steel deck of the test specimen were parallel to the edge girders. As a result, similar to the edge girders, the steel deck also developed catenary action and was effective in redistributing the vertical load, resulting from the lost column, to adjacent columns. Maximum stress readings during the tests were mostly between 5 and 15 ksi; however, localized small areas of the deck yielded. Failure of the steel deck through ripping or tearing was isolated and did not limit the strength of the deck system.

3. The combined catenary action of the floor steel deck and the simply supported edge girders was able to prevent collapse of the column with a load of about 63 kips in the column. This load corresponds to about 300 pounds per square feet of tributary area of the floor. Considering a reduction factor of 0.5 due to impact as prescribed by GSA (2003), the floor gravity load that was carried by catenary action could be established as about 150 pounds per square feet of tributary area.

4. This test only established the potential of a typical steel structure to resist progressive collapse in the event of sudden removal of a column. Further research is needed to establish the parameters that affect this resistance and to develop appropriate design guidelines to take advantage of this phenomenon in preventing progressive collapse of steel structures.

5. The bulk of the progressive collapse resistance of the tested structure was the result of the development of tension catenary force in the beams as well as the connections. Because steel as a material has almost equal tensile and compressive strength, the tensile catenary forces could be resisted by the beam, which was designed to carry only bending, and by the shear connections, which were designed to carry only shear. This ability of steel to resist stresses in directions that were not considered in design, as well as its very high ductility, seems to present a great potential for steel structures to resist progressive collapse even if they were not designed for such an abnormal loading. It appears that such a reserve capacity to resist progressive collapse by developing catenary forces may not exist in reinforced concrete structures, since concrete itself cannot resist any significant catenary force and the catenary action will come only from the steel longitudinal rebars in the beams. The amount of catenary force that can be developed in reinforced concrete beams will be the force that can be carried with the smallest amount of rebar throughout the length.

4. USING CATENARY CABLES TO PREVENT PROGRESSIVE COLLAPSE

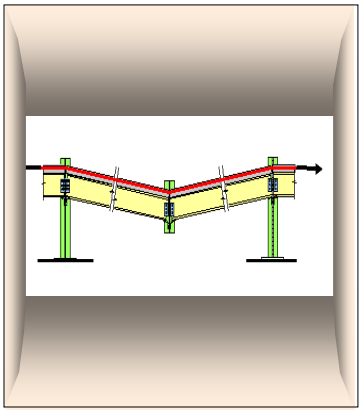

4.1. INTRODUCTION

This chapter summarizes the results of tests of a cable-based mechanism that can be applied to steel structures to prevent progressive collapse in the event of a blast attack or similar damaging factors and sudden elimination of one of the columns. For more detailed information, the reader is referred to the final report of the project (Astaneh et al., 2001a) available for free download from http://www.ce.berkeley.edu/~astaneh. The concept that my colleagues and I tested and verified was proposed by Magnusson, Klemencic, Associates ,(formerly Skilling, Ward, Magnusson, Barkshire), the structural and civil engineers, Seattle. The concept of using the catenary action of cables to prevent progressive collapse was suggested by Joseph Penzien (2001), Professor emeritus at UC Berkeley in the aftermath of the progressive collapse of the Murrah Building in Oklahoma City, which was the subject of a terrorist car- bomb attack in 1995. The concept consists of placing horizontal cables through the floors above the top flange of the girders along the exterior column line and using the catenary action of the cables to redistribute the load of the eliminated column to the rest of the structure. Following the discussion of the test results, I provide recommendations for the design. equations for this

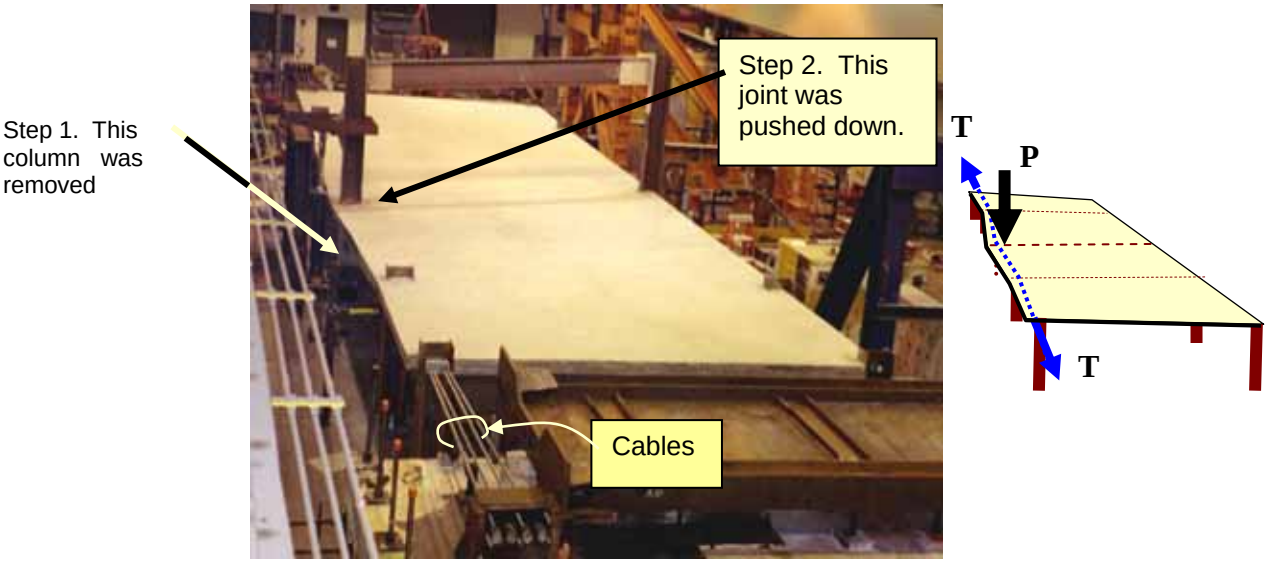

Figure 4.1. Test Structure and Development of Catenary Forces in the Cables after Removal of a Column

versatile progressive collapse prevention technology. Figure 4.1 shows a view of the full-size test structure in the UC Berkeley Davis Hall Laboratory and the location of the cable to prevent progressive collapse of the floor.

4.2. TESTS OF A CABLE-BASED MECHANISM FOR PROGRESSIVE COLLAPSE PREVENTION

The test specimen for these tests was the same specimen described in Chapter 3. The main objective of the tests was to establish that the catenary action of steel cables placed into the floors of steel building structures would prevent progressive collapse of the structures in the event of removal of one exterior column. The other objective was to use the test results to develop design recommendations for analysis and design of catenary cables and other details of the structures using this system. The tests clearly established that using a relatively small amount of steel cable can prevent the progressive collapse of steel building structures. The structural damage to the system during the tests was controlled, non-consequential and limited to deformations of the connections within the area tributary to the drop column. The floor's concrete slab also developed relatively minor tension cracks and compression crushing.

4.2.a. Test Specimen

The tests reported in this section were conducted on the north side of the full-scale specimen shown in Figure 4.2, which gives details of the specimen. The north side of the specimen had catenary cables placed into the floor slab.

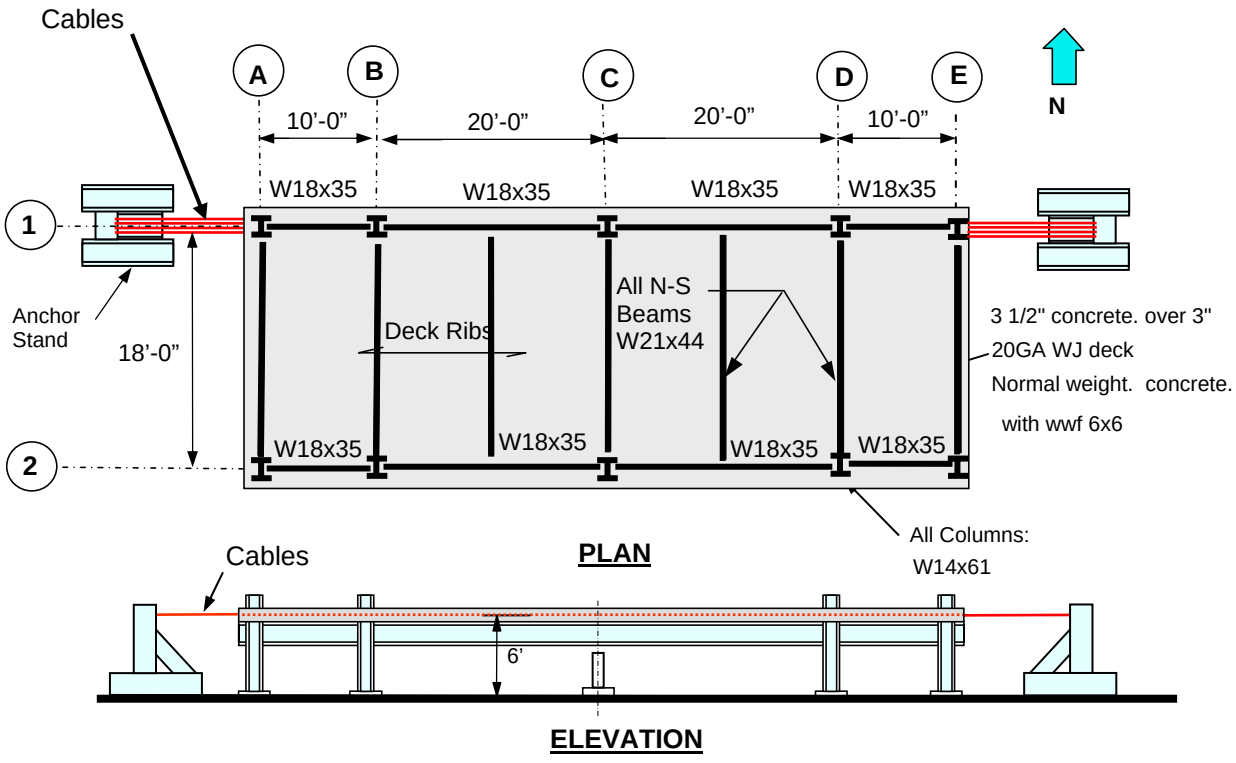

Figure 4.2. Test Specimen

The specimen was a full-scale representation of one floor of a typical modern steel building structure with its floor slab, steel deck, supporting beams, girders, and columns. The specimen was designed by MKA and the test protocol and setup was developed by the MKA and the author at UC Berkeley jointly. The size of the specimen was 18 feet x 60 feet x 6 feet. The test plans consisted of constructing the specimen at the civil engineering laboratory of UC Berkeley, adding the instrumentation to the specimen, removing a middle column (Column C1 in Figure 4.2), pushing the joint above the removed column down, and observing and collecting the data on performance of the structure after removal of the column.

4.2. b. Pretest Analytical Studies

Prior to performing the tests, analytical studies were conducted to predict the behavior and establish proper test protocol and instrumentation plans. The pretest analytical studies consisted of building a realistic model of the test structure and subjecting the model to two types of loading:

(a) The gravity load consisting of the weight of the specimen and the concrete blocks placed on top of the floor slab on the specimen. The weight of the specimen and the concrete blocks represented the total design dead load and live load present at the time of blast.

(b) The gravity load consisting of the weight of the specimen and a force applied by a hydraulic jack to the top joint of the removed column.

The main objective of the analytical studies was to compare the test results under conditions (a) and (b) and to establish the amount of the actuator load applied and its velocity that would create the same effects on the specimen as the concrete blocks placed on the floor slab would do. About thirty-three 6 foot x 2 foot x 2 foot concrete blocks, each weighing 3.4 kips, would have to be placed on the floor and dropped freely when the column was removed. To perform the tests in a realistic manner, but to maintain a safe environment, my colleagues and I decided to apply the gravity effects using hydraulic actuators instead of free fall of the concrete blocks

To ensure that the hydraulic actuator would produce the same effect on the system as the gravity load had created by the weight of the concrete blocks, I designed an analytical model of the specimen with assumptions and interpretations of the test results The model was analyzed by Dr. David McCallen and Charles Noble of the Lawrence Livermore National Laboratory (McCallen, Noble, and Astaneh-Asl 2001).

The analysis consisted of building a realistic nonlinear finite element model of the specimen shown in Figure 4.3. The steel members and the connections were modeled as realistically as possible. The reinforced concrete corrugated steel deck slab was modeled as an equivalent slab with properties similar to the actual floor. The analysis code NIKE-3D, a powerful analysis program developed at the Lawrence Livermore National Laboratory was used to conduct the nonlinear time history analyses. Cases (a) and (b) were analyzed.

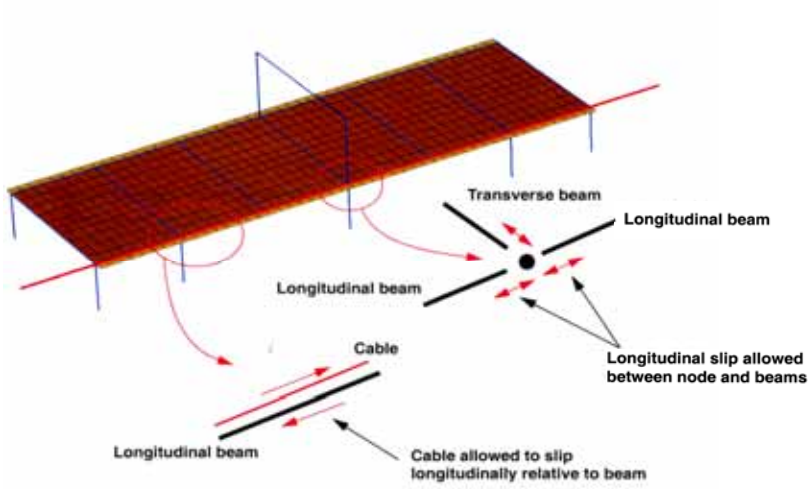

(a) Finite Element Model of the Test Structure Used in the Analyses

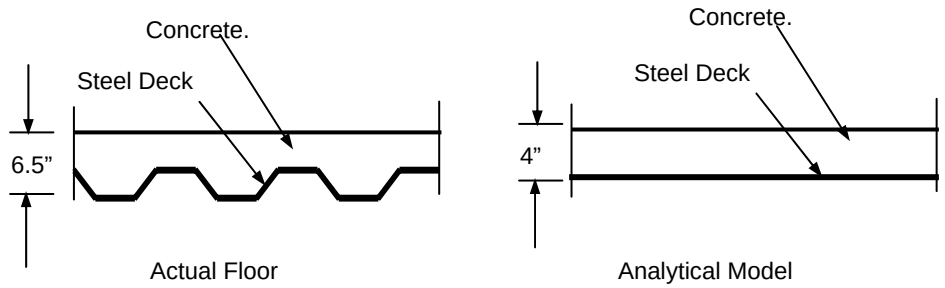

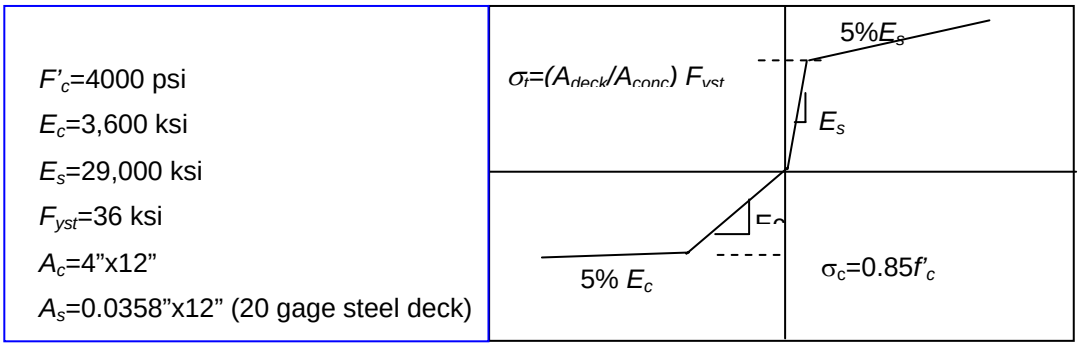

(b) Nonlinear Model of Steel Deck/Concrete. Slab Used in the Analyses

Figure 4.3. (a) Finite Element Model of the Deck and (b) Floor Deck/Slab Model

Figure 4.4 shows a comparison of the cable force developed using concrete blocks and using a hydraulic actuator with 80 kips maximum force applied with a rate of 5 kips per second. The analysis indicated that the cable force of about 66 kips was developed in both cases of either using concrete blocks or the hydraulic actuator. It should be mentioned that when the concrete blocks were used, the force in the column that was to be removed was about 66 kips. To generate the same effects, the actuator load had to be 80 kips.

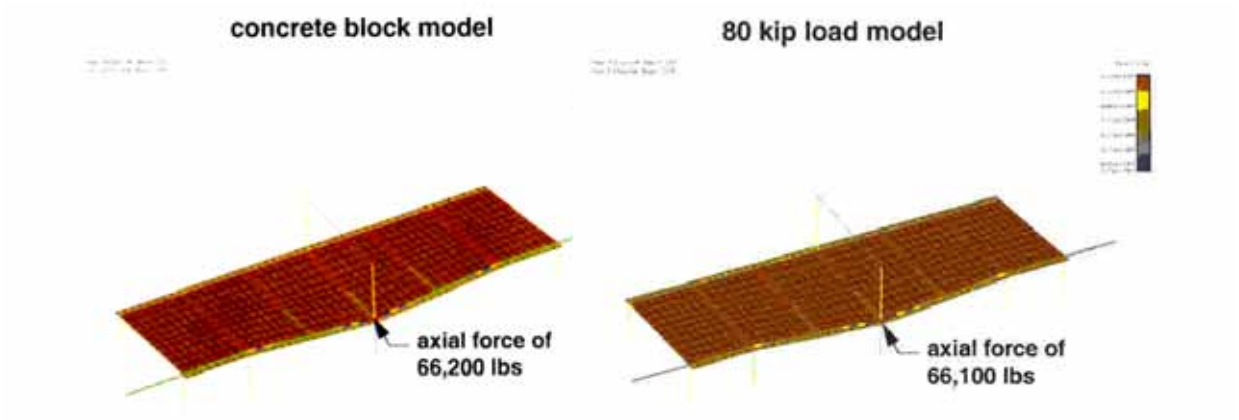

Figure 4.4. Comparison of Cable Force Using Concrete Blocks or Hydraulic Actuator (Axial force of 66.2 kips is for one cable. Total force for 4 cables is 4x66.2=264.8 kip)

Figure 4.5 shows a comparison of displacement (vertical drop) of the column joint after removal of the column. The vertical drop at about 21 inches is almost identical for two cases of either using concrete blocks or a hydraulic actuator with a maximum load of 80 kips applied with a rate of 5 kips per second. Figure 4.5 also shows vertical displacement contour lines for the entire slab with the red color representing about zero displacement, yellow,5, green 10, light blue 15, and dark blue 20 inches of vertical displacement of the floor slab. The deformed shape of the floor slab is almost identical in both cases.

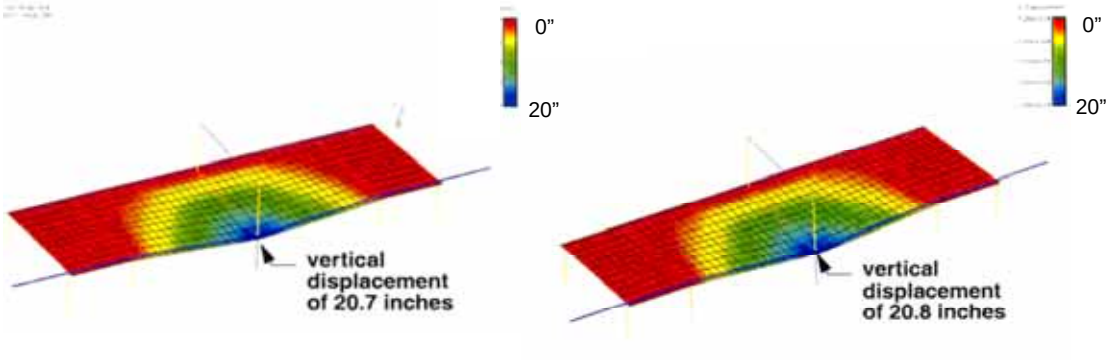

Figure 4.5. Comparison of Vertical Drop Using Concrete Blocks (left) or Hydraulic Jacks (right)

4.2.c. Instrumentation

Transducers and strain gages were used to measure relative local and absolute global displacements as well as local strains. The full data collected by the instruments is provided in the Astaneh-Asl et al, (2001a).

4.2.d. Loading History

The loading for the test consisted of applying 100 kips force to pull the column down. After the first test, since the specimen was able to support the load with the vertical displacement of the

drop column being about 19 inches and with minor damage, my colleagues and I decided to conduct more tests and pull the column further to observe the failure modes and inelastic behavior. The maximum vertical displacement of the column that could be utilized was 35 inches downward. Following the first test, denoted as GSA-1 test, we conducted three more tests, GSA-2, GSA-3, and GSA-4, with maximum column drop of 20, 24, and 35, inches respectively

4.3. SUMMARY OF TEST RESULTS

The final report of the project by Astaneh-Asl et al. (2001a) presents a complete result of the tests. Table 4.1 provides a brief summary of the highlights of the test results and the significant behavior during the tests. Figure 4.6 shows load versus displacement for Column C1 for the four tests.

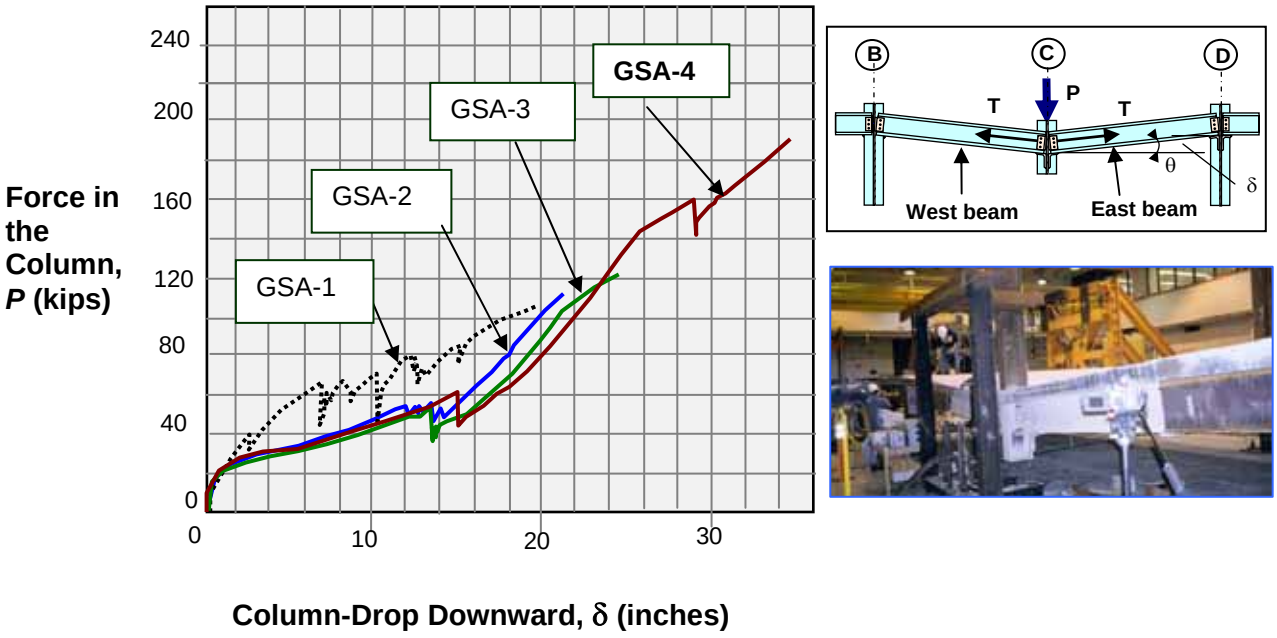

Figure 4.6. Load versus Downward Displacement of Column C1 for GSA Tests

Figure 4.7. Displacement of Drop Column, Test GSA-1

Figure 4.7 shows a typical view of the specimen at the end of Tests GSA-1, 2, 3, and 4 when the vertical displacement of the drop column was 20, 21, 24, and 35 inches respectively. Table 4.1 summarizes the behavior of the specimen in all four tests.

Table 4.1. Summary of Test Observations

Test Number (and Date)	**Maximum Drop of Column (inches)**	**Load in the Column at Maximum Drop Point (kips)**	**Major Event during the Test**
Test GSA-1	20	110	Hair cracks occurred on girder lines B, C, and D and diagonal cracks in the panels BC and CD. Four bolts broke. The broken bolts were two tension bolts in the seat angles of column C2 and two bottom flange bolts, one in each of the columns B1 and D1. The web angle at connection C1 had opened up showing hair cracks at the bottom half of the east web angle. The bolts in slotted holes had moved to the near end of the slot. The web of girders B1-C1 and C1-D1 buckled locally at the location of columns B1 and D1, respectively
Test GSA-2	21	140	The column was raised to its original level and dropped again. A few more hair cracks occurred on the girder lines B, C, and D and diagonal cracks in the panels BC and CD. The broken bolts were replaced, two of them with 1/2 inch bolts. All four bolts broke again. Horizontal shear bolt connecting girder C1-D1 to the seat angle failed. The seat angles at connection C1 had further pulled away from the column. The web angle at connection C1 had further opened up and showed a visible crack at the bottom half of the east web angle. The bolts in the slotted holes had moved to the end of the slot.
Test GSA-3	24	150	The column was raised to its original level and dropped again. More hair cracks occurred on the girder lines B, C, and D as well as diagonal cracks in the panels BC and CD. The seat angles at connection C1 had pulled further away from the column. The web angle at connection C1 had extended its opening showing a visible crack along almost the entire length. The bolts in the slotted holes had moved to the end of the slot and pushed into the shear tab edge distance ,bending the edge distance.
Test GSA-4	35	190	The web single angle completely fractured through its fillet zone. All four bolts on the vertical leg of the seat angles fractured, and the seat angles on both sides of the column web separated from the column. The shear tab on the transverse beam, located on line C, underwent large deformations around the bottom bolts. At B1, the beam web buckling became more pronounced during this test, and the bottom flange also showed more pronounced local buckling. The concrete slab during this test continued to develop more cracks but nothing serious. Heavy compressive crushing of the concrete was seen stemming from Column C1 towards Column C2.

Figure 4.8 shows the pattern of cracks on the floor slab observed at the end of Test GSA-4 when column C1, the drop column, had dropped 35 inches. The cracks of the slab where generally hair cracks sometimes difficult to notice with the naked eye. There were three clearly visible cracks clearly visible which are highlighted in Figure 4.8 by using thick red lines. Figure 4.9 shows the specimen before and after the tests.

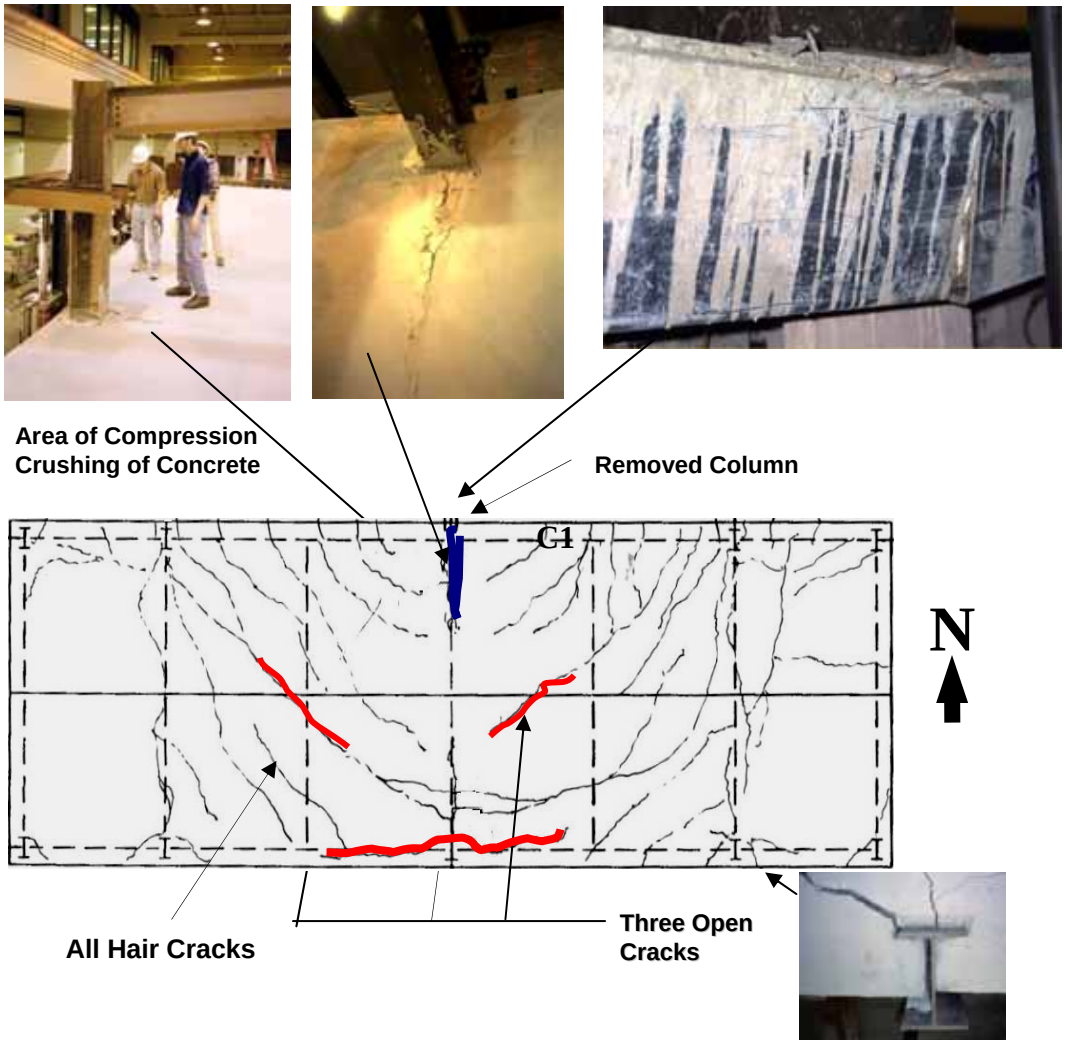

Figure 4.8. Crack Pattern on the Slab after Completion of Tests

Figure 4.9. Specimen before and after the Test

Behavior of the Specimen during Test GSA- 1 20 inch Column Drop)

This test was the first test of the specimen after its construction. The test started with removing the stub column that was temporarily supporting the drop column at location C1 see Figure 4.2. Initial warm-up tests were conducted ,during which a very small amount of drop (0.07 inches) was applied to check the equipment, instrumentation ,and data- acquisition systems. When all members of the research team were at a safe distance from the specimen, the Chief electrical engineer began to lower the actuators at the speed of approximately 1 inch per second. The test column dropped a total of 19.8 inches, and the test was terminated when the actuator load neared 100 kips, exceeding the design displacement. The specimen was held at the maximum load briefly before being released down to zero loads in the actuator. Displacement at load zero was 15 inches. The entire test took approximately 30 seconds from start to finish.

The drop column for this test was column C1, Figure 4.2. No noticeable damage or deformations to the structure was observed during the test with the exception of the damage of the transverse beam on axis C as well as the two beams on axis 1, all three beams connected to the drop column. The connections of these beams also sustained damage during the test. No deformation was noticed in the column itself, though the areas behind the angles, where the bolts attached, were not visible and the potential for yielding was much more likely there. Figure 4.10 shows a view of the connection at location C1. Clearly the transverse beams on the left has rotated freely by bolts moving inside the long slots intentionally designed to allow a rotation of about 0.15 radians at the end of the transverse beam. At the connection to the transverse beam, the bolts had slid along the slots in the shear tab. The shear tab itself had undergone slight deformations, if any, while the transverse beam had buckled slightly around the beam seat. The web of the transverse beam also showed some yielding near the base of the shear tab. This yielding was not as noticeable on the other side of the girder. The horizontal edge distance of the shear tab showed signs of deformation and initiation of failure, as can be seen in Figure 4.10.

Figure 4.10. Loss of Two Bolts on the Seat Angle, Deformation of a Single Angle on the Web, and Free Rotation of the Beam in Slotted Holes

The single angle bolted to the web of the beams in the east- west direction and bolted to the web of drop column C1 underwent large inelastic deformations as shown in Figure 4.10. The center of the angle was very shiny. That area was previously ground down for strain gauging,

which was now exposed as it yielded and the whitewash flaked off. Yielding was also clear at the base of the angle and on the longitudinal beam it was attached to. The bottom seat angles attaching the E-W beams to the drop column had deformed away from the column. The angle attached to the web also had pulled away from C1, as the bare face of the column web was exposed from behind it in Figure 4.10. The beam seat had managed to stay connected to the longitudinal beam through its two vertical bolts; however, of the four horizontal bolts connecting the longitudinal beam seats to the column, the top two bolts had failed as shown in Figure 4.10. The end connection of the east longitudinal beam at the location of column B2 showed a crescent- shaped buckling of the web as shown in Figure 4.11. The buckling of the web was related to the rotational restraint provided to the end of the beam by bolts connecting the bottom flange of the beam to the horizontal leg of the seat angle.

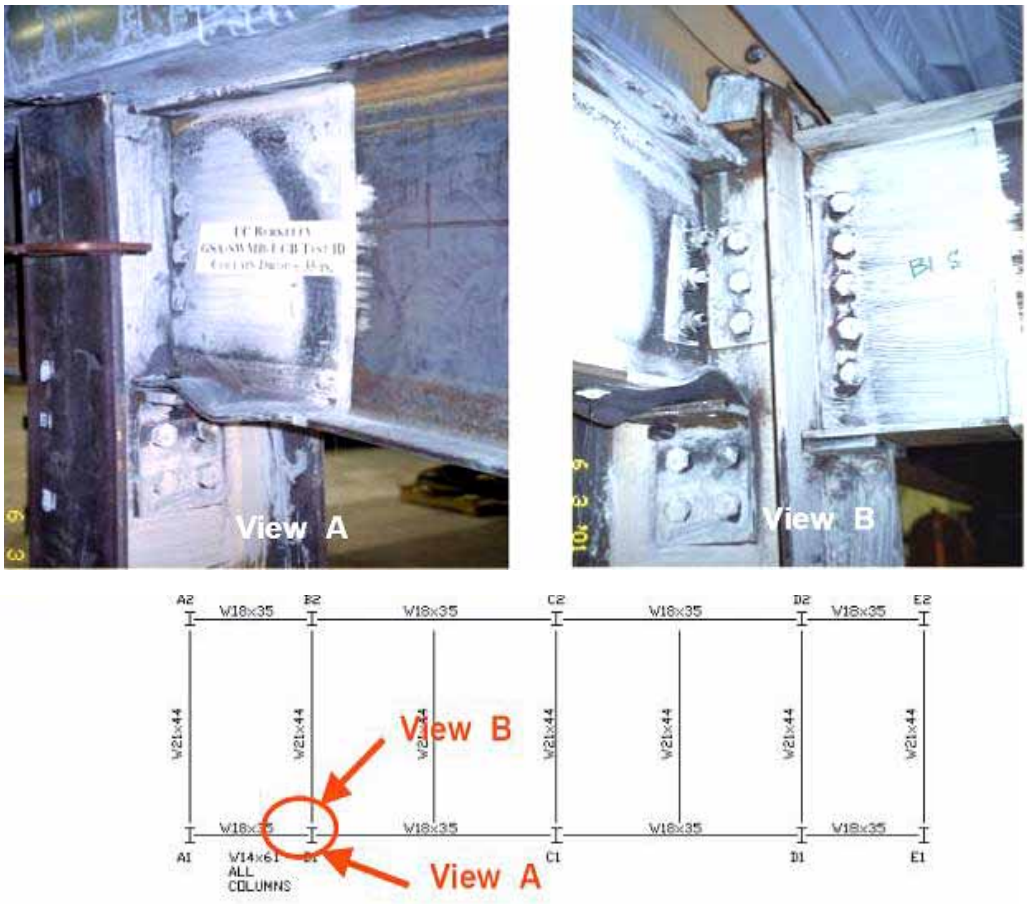

Figure 4.11. Buckling of the Web of Longitudinal Beam at Location B1

As expected, the concrete on the composite deck cracked in tension areas as the drop column went down and bent the deck. In addition, a compressive crushing failure was also observed on the deck along the line 1-2, above the transverse beam as shown on Figure 4.8 . Tension cracks occurred in a semicircular pattern around the test column, often framing from sides B1 and D1 and flaring out towards C2. These cracks are shown in Figure 4.8. All cracks occurring during Test GSA-1 were marked with blue. The concrete separated away from column C2 and cracked at least 1 inch deep for several feet on either side. Over columns D1and B1,

Figure 4.11, the concrete appeared to crack off the top of the saddle boxes, which were welded to the top of the girder for cables to pass through. The deck also split and bowed out away from the structure at C1 as the concrete crushed slightly. Despite the high level of cracking observed, the deck appeared to have retained a good degree of structural capability. Little damage, virtually no cracking, was found in either of the end bays between columns A and B and between columns D and E.

Behavior of the Specimen during Test GSA-2 (21 inch Column Drop)

Prior to conducting this test, the drop column C1 had been restored to zero displacement following the collection of data from Test GSA-1. Again the specimen was raised slightly, and the jack was removed from beneath the specimen and the test commenced.

As we lowered the structure, there were again a series of loud bangs and pops from the structure. These could possibly be attributed to separation between the concrete slab and the metal decking, cracking of the concrete, and bending of the entire slab. Test GSA-2 achieved 21 inches of maximum displacement at about 100 kips, approximately the same force in the actuator as in Test GSA-1. This is not too surprising since the specimen had already been deflected 19.8 inches during the previous test. Damage to the structure during the 21-inch test was minimal. There were slight extensions of the yielding that occurred during Test GSA-19, but the steel frame did not experience any other notable deformations. The concrete deck experienced more cracking. Most of the cracks were extensions of cracks already created and a few new hairline cracks, but again, there was no significant damage. Following the test, the specimen was left at its position of zero load while data were gathered, then returned to the point of zero displacement and the test stopped.

Behavior of the Specimen during Test GSA-3 (24 inches Column Drop)

The specimen was damaged more during Test GSA-3 than it had during Test GSA-2. Columns A1, A2, B2, D2, E1, and E2 and the members framing into them still experienced little if any noticeable yielding. However, the yielding that began at locations B1, C1, C2, and D2 continued further and caused tearing in one of the angles connecting to Column C1.

As before, yielding occurred to a great degree in the angles and the beam seats bolted to the drop column. However, due to the additional rotation and force applied by the 24 inches displacement of the test column, the single angle on the web of the beam on the east side of the column fractured almost half the way up the fillet area of the angle as shown in Figures 4.12. Excessive yielding had occurred in the angle in Test GSA-1 well before this test, as shown in Figure 4.10. As the figures show there is also definite yielding on both the longitudinal beam and the column. A light series of striations can be seen on the column underneath the angle. Heavier yielding is also noticeable just to the right of the bottom set of bolts on the beam seat. Note also that practically no whitewash remains on the beam seat at this point. It is also important that the vertical bolts on the seat remained intact on the east side depicted. This clearly helped to deform the angle to failure by allowing the beam to take more load in catenary action. The vertical bolts on the west side failed during the test. The angle went through extreme deformation; however, no tearing or separation of the steel was visible.

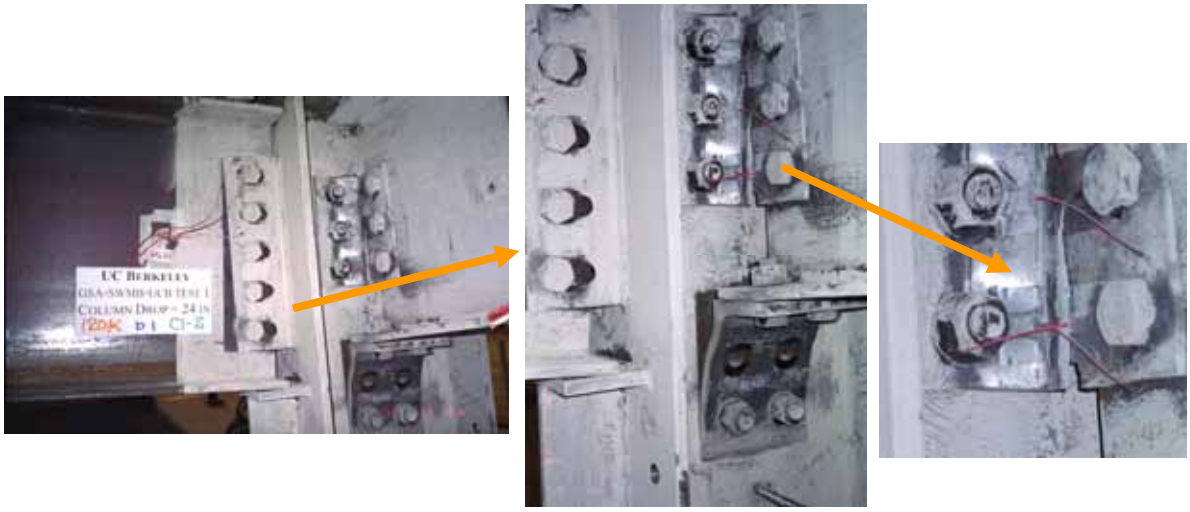

Figure 4.12. Further Damage to the Joint under the Drop Column during Test GSA-3

The transverse beam also underwent slight deformations. The most noticeable yielding occurred in the shear tab, where the bottom bolt created a semicircular deformation at the edge of the tab and yielded the steel in between. A larger quantity of un-whitewashed steel was exposed from underneath the shear tab in Test GSA-3 than during previous tests. This points out also that since the level of deformation was very low in both the shear tab and the transverse beam, the slotted connection was very effective in allowing rotation and transmitting the gravity shear force to the support without restraining the rotation of the transverse beam.

The area around column C2 also underwent some deformations. With the extra 3 inches of displacement downwards in this test compared to the previous test, the bottom flange on the transverse beam between C1 and C2 yielded around the beam seat attached to C2. The web also yielded at the base of the shear tab. Further deformations were noticeable in the shear tab itself. The transverse beam pulling heavily on the top bolt stretched the shear tab around the bolt.

The deck experienced further cracking during this test; and the existing cracks expanded further, and more new tension cracks formed.. Compressive crushing was quite advanced along both the north and south sides of drop column C1. The north side can be seen in Figure 4.8. Here the steel decking had bowed outwards and split (this happened in Test GSA-1, but not as extreme), and the concrete was broken loose and crushed. The slab had pulled farther away, also, from Column C2 than previously and the gap spread longitudinally along the top of the slab.

Behavior of the Specimen during Test GSA-4 (35 inch Column Drop)

The main objective of this test was to push the drop column down to the maximum possible and observe ultimate failure modes. As mentioned in Chapter 3, the floor was constructed 6 feet above the laboratory floor and the bottom of the drop column was 3 feet above the floor. This was done intentionally for safety reasons if floor collapsed during the tests, the drop height would be relatively low. Therefore, the maximum vertical drop for the drop column was set at 35 inches with a 1 inch space to the floor at this maximum displacement. In order to meet this displacement and the relatively large column axial forces it was clear some changes in testing

were necessary. Since during Test GSA-3, we had already utilized the maximum capacity of the actuator (120 kips), it was decided to use two actuators for this test with a maximum of 240 kips capacity. Several alterations were also made to the instrumentation, and the lost strain gages were reinstalled.

While several of the connecting elements around the test column did fail during this test, the structure itself did not fail and remained able to bear the load. The structure did reach a displacement of 35 inches and an actuator tensile force of 190 kips, as shown in Figure 4.5. In the following, the important observations made during this last test are summarized. For more detailed information, the reader is referred to Astaneh-Asl et al (2001a).

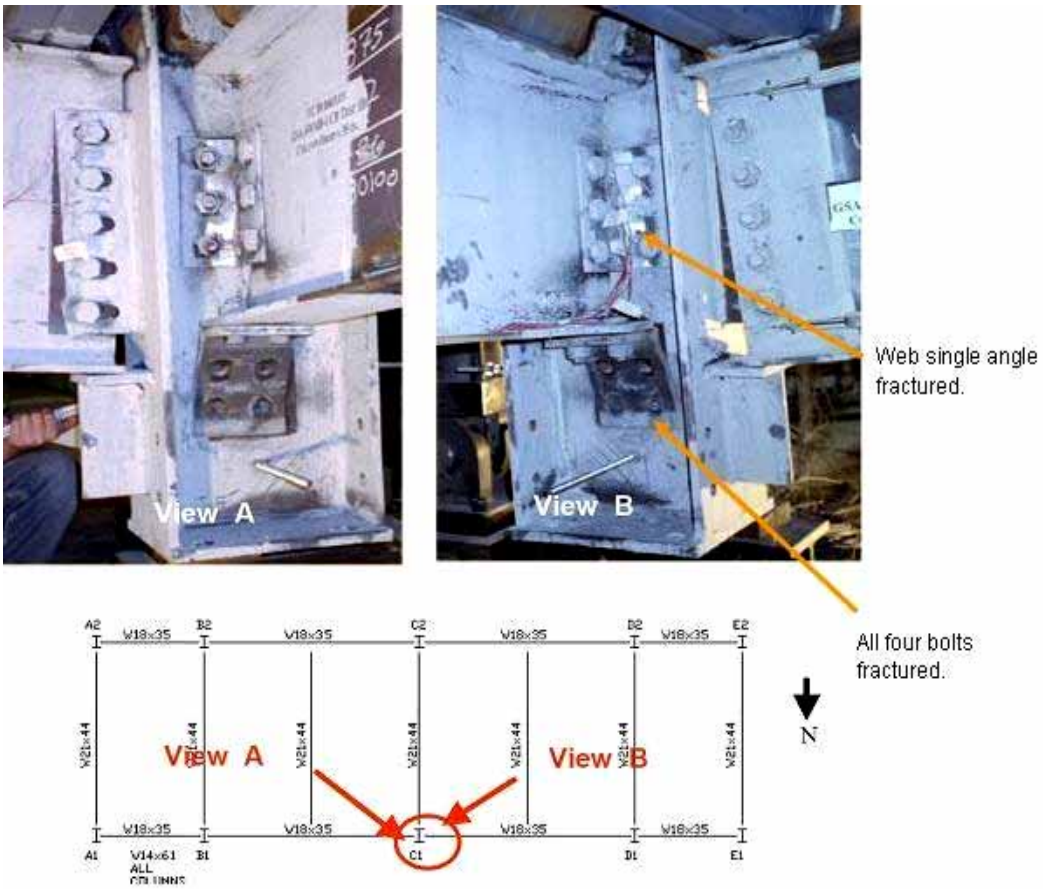

Figure 4.13. Fracture of Web Single Angle and Bolts on the Seat Angle during Test GSA-4

The connection of drop column to beams at the conclusion of this test is show in Figure 4.13. As discussed earlier, in Test GSA-3, the angle connecting the east longitudinal beam to the test column tore halfway. Test GSA-4 completed this task and separated each steel web angle connection from the test column, leaving the east beam connected only through the deck. Heavy yielding had clearly occurred from the bottom right corner of the angle on the web, and also at both the top and bottom of the angle on the column web. During the test both sets of horizontal bolts on the vertical leg of seat angles fractured, and the seat angles on both side of the column web separated from the column. At this point, with, fracture of web angle and the seat angle,

both longitudinal beams were totally separated from the drop column C1. The floor was not supported any more on the girders but was instead suspended from the catenary cables placed inside it.

The shear tab on the transverse beam, located on line C, underwent large deformations around the bottom bolt, as seen on the left in Figure 4.13. The area all around the bolt yielded and pulled outward, extending the slot even farther.

At B1, the beam web buckling became more pronounced during this test, and the bottom flange also showed more pronounced local buckling as seen in Figure 4.14. After further deformations of the bottom flange, the two bolts connecting the bottom flange to the seat sheared off. Heavy bending of the beam flange and yielding of the web were evident. Yielding was observed not just on the beam seat but also on the web all around the beam seat at this location. The influence of the angle upon the web deformation was also much better illustrated here.

The concrete slab during this test continued to develop more cracks but nothing serious. Heavy compressive crushing of the concrete was seen stemming from column C1 towards column C2 as shown in Figure 4.8. The crushing extended for approximately 4 to 5 feet from C1. Crushing was also very heavy on the overhang of the structure. The area of concrete between columns B1, C1, and D1 and the edge of the steel deck experienced extensive crushing. The vertical northern edge of the steel deck bowed outwards separating completely from the concrete for at least a quarter of a span in both directions at each column. The concrete was heavily damaged and spalled loose from the rebar. Another crack spanning orthogonally to the compressive area at C1 ran longitudinally along the slab. This crack was unique because it was not in line with any tension or compression line, but actually it was just over 3 feet from the edge of the slab, the approximate distance where the top reinforcement in the slab ended. This indicated that the reinforcement most likely carried quite a bit of force, and that cracking and spalling would have been much greater had it not been for the rebar.

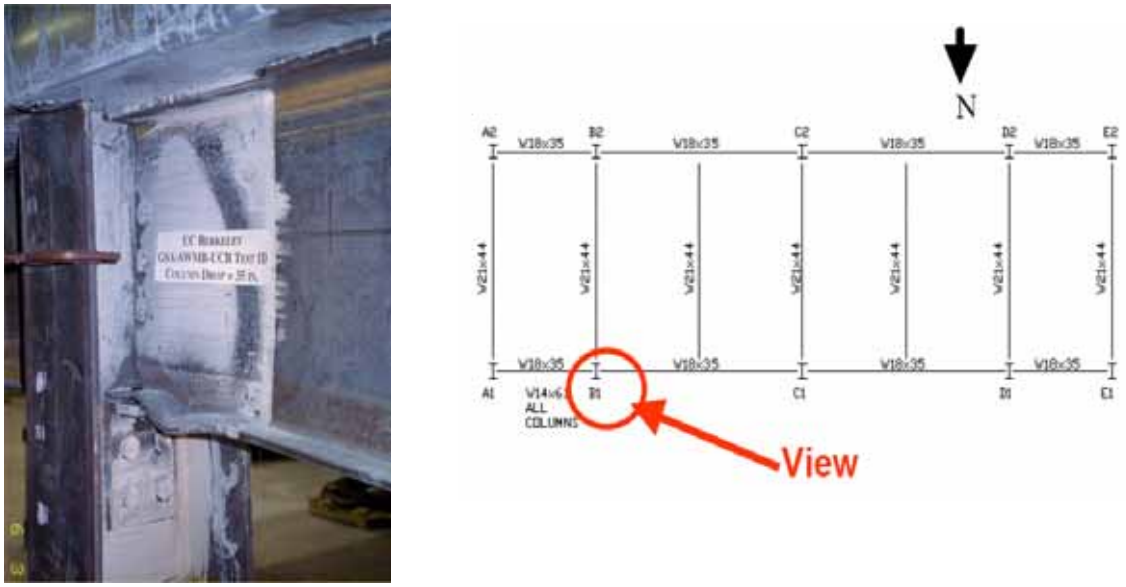

Figure 4.14. More Buckling of Web and Bottom Flange Occurred during Test GSA-4

4.4. SUMMARY OF OBSERVATIONS

The tests reported were conducted on the north side frame of the specimen where four 1 1/4 inch cables were placed in the slab. For more details of structure, the reader is referred to the final report of the project by Astaneh-Asl et al. Following is a summary of observations on the tests.

1. The analyses indicated that hydraulic jacks could be used to simulate the effect of gravity on the floor. The total load applied to the column statically(acceleration = 0.0) by the hydraulic jacks and the weight of the floor should be about 1.45 times the actual gravity load supported by the column that would be dynamically dropped in the event of removal of the column. The impact factor of 1.45 (or approximated in design by 1.50) can be used in the design of the cable-supported system. The dynamic effect of the free fall of the floor with the acceleration of gravity is compared to the results of tests when the floor was pushed down with a constant velocity (zero acceleration). The impact factor of 1.4 in this case is evident. Figure 4.15 shows a comparison envelope of test results and the same envelope divided by 1.45 to include dynamic effects.

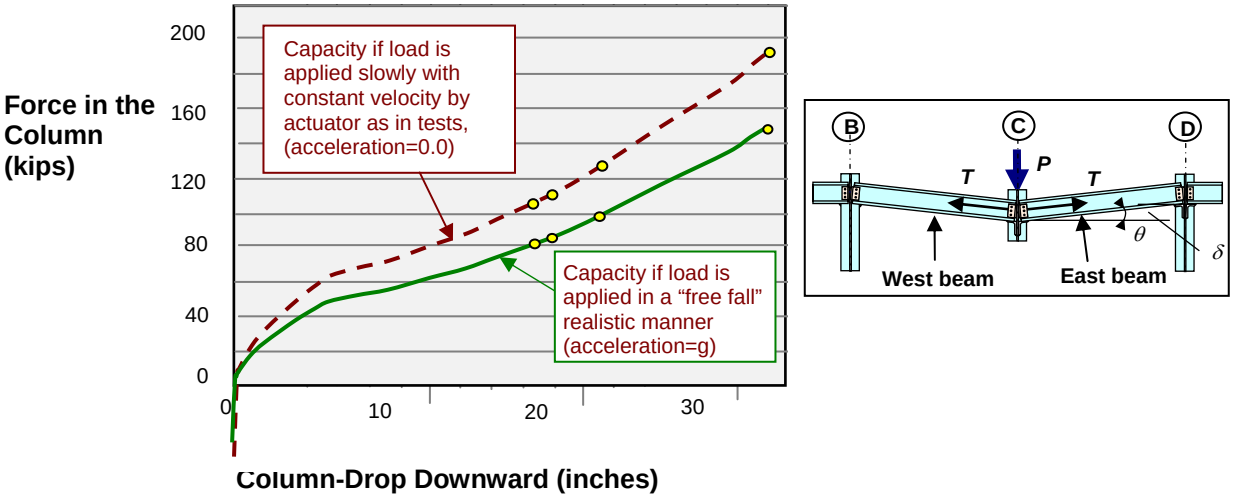

Figure 4.15. Dynamic Expected Behavior and Static Curves for Tests

2. Figure 4.16 shows the envelope of the load-displacement curves for the north frame, which had the catenary cables, and the south side frame, which did not. The steel frames on the north and south side of the specimen were identical except for the steel cables and the reinforcement of the floor slab around the cables, which were present in the north side frame only. The testing of the south side frame and its behavior were discussed in Chapter 2. Figure 4.17 shows the contribution of the cables and the structure to the overall strength and stiffness of the system. Initially, up to a column load of about 60 kips corresponding to a drop of about 10 inches, the resistance to the column drop primarily was provided by the structure itself. Beyond this point, when the top two bolts of the seat angle supports fractured, some of the resistance to the column load came from the cables as well. As the column load increased, the contribution of the structure

decreased, and the cable carried most of the load. Beyond about 27 inches of column drop, the cable was carrying more than half of the column load, as seen in Figure 4.16.

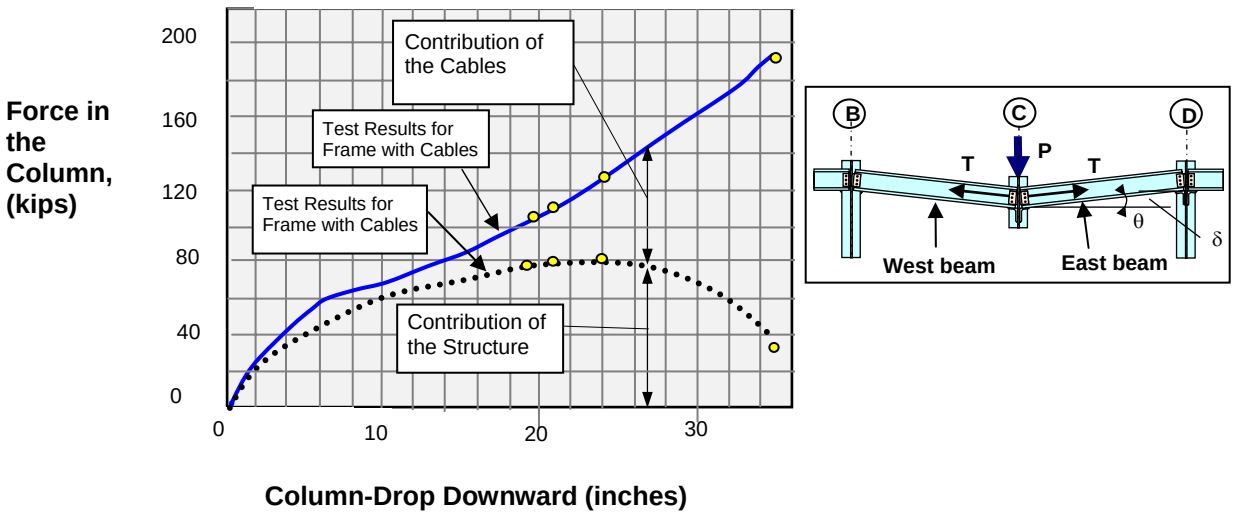

Figure 4.16. Total Load for the Frames with and without Cables

3. The system with catenary cables performed well, and damage was limited to the fracture of two out of four bolts connecting the vertical legs of the seat angles to the middle column and the relatively minor cracks in the slab and local buckling of the beam webs.

4. The bolted seat angles performed as expected. During the first test the two bolts (on the top row) on the vertical leg of the angle fractured and, as the load in the column increased, the two bottom row bolts also fractured. This of course left the web single angles as the only elements to carry shear in the connection. The web single angles fractured through the fillet during the final test (35-inch drop).

5. The long-slotted shear tab connections on the transverse beams (north-south beams) performed well, and as intended. The bolts traveled the length of the slotted holes on the shear tab, and the end of the beam was allowed to rotate more than 0.14 radians without serious damage to the connection that would have caused it to need a repair or would have affected its future performance.

6. When the transverse beam rotated large amounts, the bottom flange of the beam was bearing on the stiffened "safety" seats. These safety seats were placed under the transverse beams, with a ¼ inch gap, to prevent the beam from collapsing in case the shear tab connections failed. The excellent performance of the shear tabs indicated that these safety seats might not be needed.

7. Other than during the very early stages of the first test (virgin specimen), it appeared that there was not any significant bound between the steel cables and the concrete floor slab. In other words, almost all the tension force in the cable was transferred to the end

anchors without any significant amount being transferred to the floor slab and deck.

8. The connection of the cables to the columns and tops of the beams performed well and there was no sign of any distress or cracking of concrete in these areas.

9. About a 2 feet wide strip on the north edge of the slab (where the cables also were placed) had reinforcement. This area performed well, with only hair cracks visible on the slab on this strip.

10. The steel deck performed well with only small permanent deformation visible.

11. It was clear that, after removal of the middle column, initially the beams and bolted seat angles were supporting some of the floor load by developing catenary action. However, after reaching a column load of about 60 kips, when the bolts on the seat angle fractured, the cables were the primary elements supporting the load. The second phase of the project (Astaneh-Asl et al 2001a), conducted on the south side of the specimen (which did not have the cables), indicated that indeed the steel structure alone could support about 60 kips in the column before the bolts on the seat angle fractured. The latter project is summarized in Chapter 3.

12. The cables were connected to two anchors outside the test specimen. The anchors performed well and indicated that, in actual structures, attention should be paid to the design of mechanisms that can transfer the catenary tension of the cables. The cables can be anchored to braced bays or to the last column, which in effect transfers the tension in the cable to the floor diaphragm and then to the braced bays.

5. USING CATENARY CABLES TO RETROFIT EXISTING STEEL STRUCTURES

5.1. INTRODUCTION

This chapter discusses the research project conducted to investigate the possibility of using catenary cables to retrofit existing structures to prevent their progressive collapse. The project was funded in part by the National Science Foundation and conducted at the University of California, Berkeley and involved testing a one- story, full-size specimen, Figure 5.1, before and after the retrofit. The following sections provide a summary of the tests followed by design recommendations and applications. For more information on the experimental research, the reader is referred to the final report of the project by Tan and Astaneh-Asl (2003) available for free download at the web site of the National Science Foundation, www.nsf.gov ,or from www.ce.berkeley.edu/~astaneh.

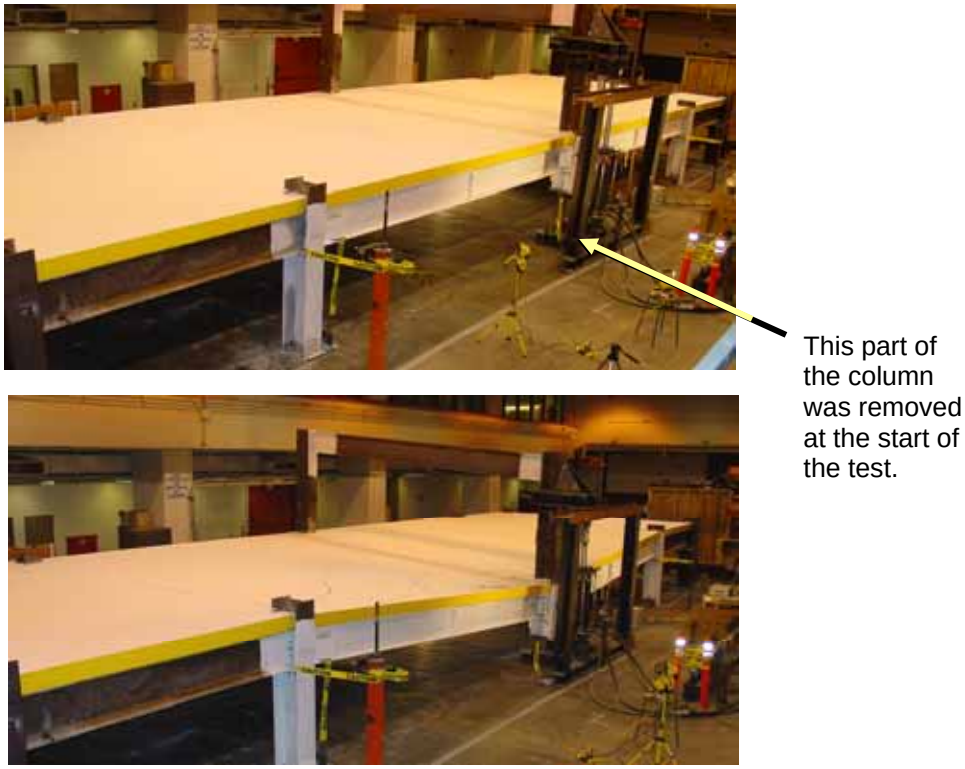

Figure 5.1. Views of the Specimen without Retrofit before (Top) and during the Test (Bottom)

5.2. TEST PROGRAM

The test program consisted of testing a full-scale specimen that represented typical existing modern steel structure with simple shear tab connections and establishing its performance after removal of an exterior column. The main objectives of the study were (a) to gain better understanding of progressive collapse of frames with shear tab connections, (b) to develop a cable-based retrofit system that would prevent progressive collapse of the structure after removing one column, and (c) to elaborate the construction techniques and procedures of the system applicable to existing building structures. The cable retrofit system was designed to increase the capacity of the structure with a construction procedure that would have the least disturbing effect on ongoing functionality of the existing building during retrofit.

We performed three column-drop tests on the existing and retrofitted test structure. The tests are referred to as tests NSF-1, NSF-2, and NSF-3. The specimen for Test NSF-1 did not have cable retrofit. The objective of this test was to investigate whether a steel structure with single-plate shear tab connections could resist progressive collapse by developing catenary forces in the beams and the floor. The specimen for Test NSF-2 was the same specimen as for Test NSF-1 but retrofitted using cables. The first objective of Test NSF-2 was to develop a cable retrofit technique to increase the resistance of the existing steel structures against progressive collapse. The second objective was to investigate the specifics of performance and resistance of a cable- retrofitted steel structure against progressive collapse through catenary action of its beams, floor slab, and retrofit cables. The specimen for Test NSF-3 was also the retrofitted specimen, and the objective of the test was to displace the drop column as much as the limitations of the test setup would permit and to observe the behavior of the test specimen under very large displacements.

5.2. a. Test Specimen

The test specimen was a single-story steel structure with a steel deck and concrete slab floor system acting as a composite element with the steel beams. The specimen was the same one tested in previous phases of the project and is described in detail in Chapter 3. A plan view and elevation of the specimen are shown in Figure 5.2. The floor slab in the specimen measured approximately 20 feet by 60 feet in plan. The beam-to-column connections were all shear connections. Columns, beams, and steel shear tab plate connections were specified as *ASTM* A36 steel (F_y = 36 ksi). The floor slab concrete was specified to have $f'c$ = 4000 psi. Bolts at the shear tab connections were 7/8-inch diameter grade ASTM A325X. Welding was performed using E70xx (70 ksi) electrodes. More information on construction of the specimen can be found in Chapter 3 and in Astaneh-Asl et al. (2001a).

5.2.b. Retrofit System

The specimen was retrofitted by placing two horizontal high- strength steel cables within the web of the exterior girders on the south façade as shown in Figure 5.4. The cables were ¾-inch diameter ASTM A586 zinc-coated helical steel wire structural strands. The helical cables had a minimum breaking stress, F_{pu} = 220 ksi, and elastic modulus, E = 24,000 ksi . Each cable was approximately 61 feet -3 inches long. The cables had zinc-poured sockets, or end fittings, at both

ends, which secured the ends of the wires and provided a bearing surface for the end anchorage, Figures 5.3 and 5.4. Four-inch diameter holes were cut into the column webs to allow the cable end fittings (3 5/8 inches in diameter) to pass through the columns. Doubler plates were welded back later onto the column webs to reinforce the web area around the 4-inch holes. First the cables were passed through the columns then were attached to the W18x35 beams every 10 feet with L2x2 angles, Figure 5.5. Finally, the cables were anchored and tightened against the end columns (Columns A2 and E2, Figure 5.2) with E- shaped finger plates and tightened with screws to remove the slack in the cable, Figures 5.3 and 5.4.

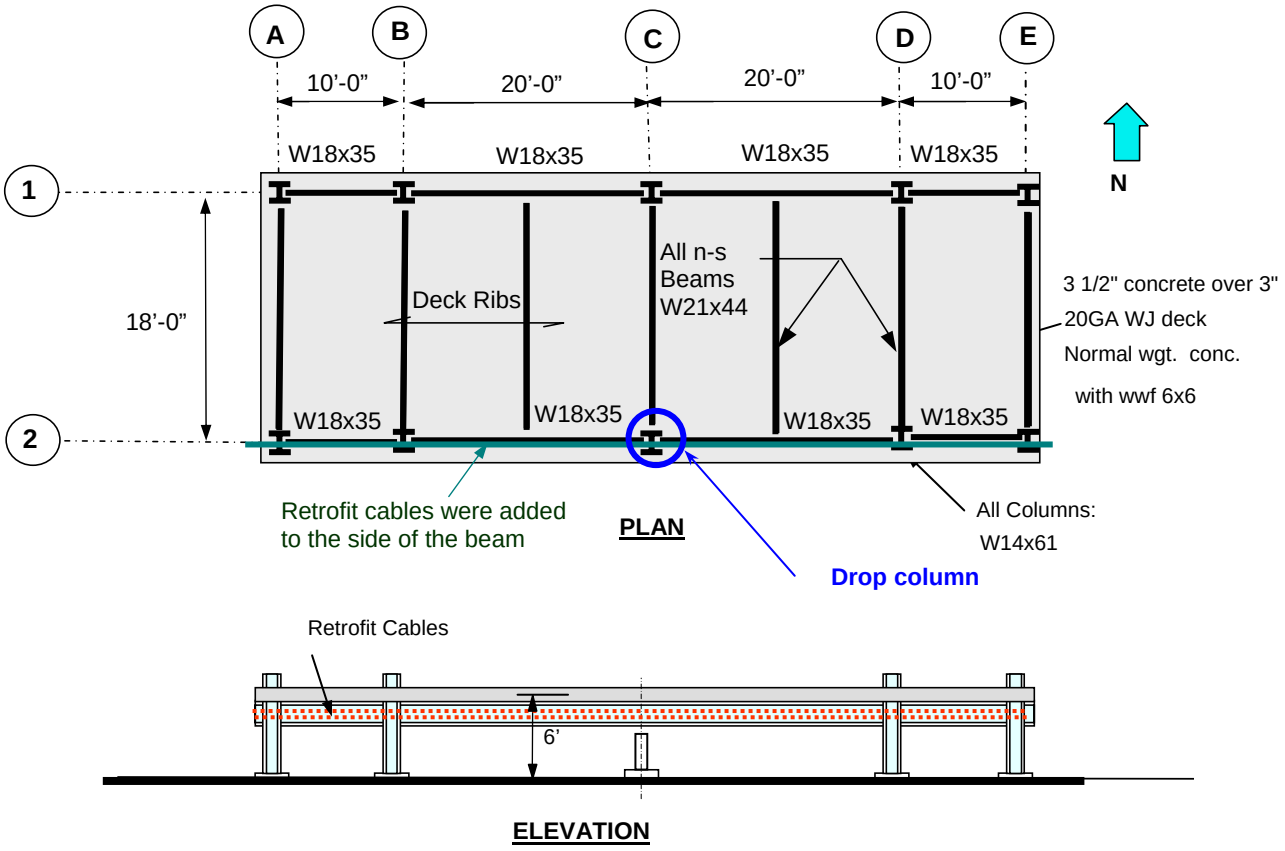

Figure 5.2 Test Specimen

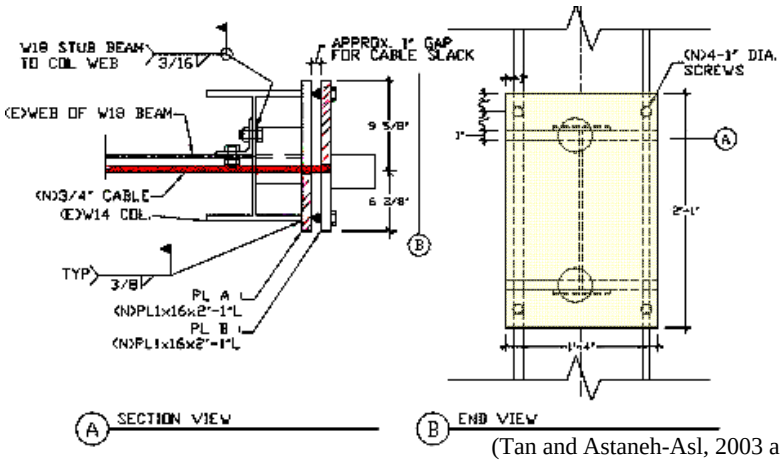

(Tan and Astaneh-Asl, 2003 a and 2003 b)

Figure 5.3. End Column Detail for Cable Retrofit

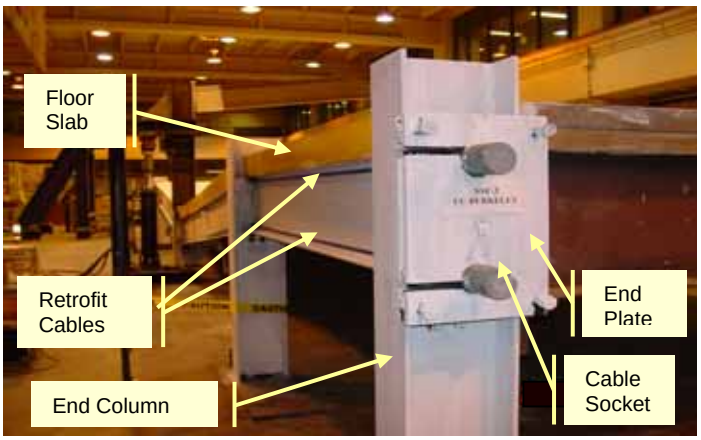

Figure 5.4. A View of the Specimen and the Retrofit Cable End Anchorage.

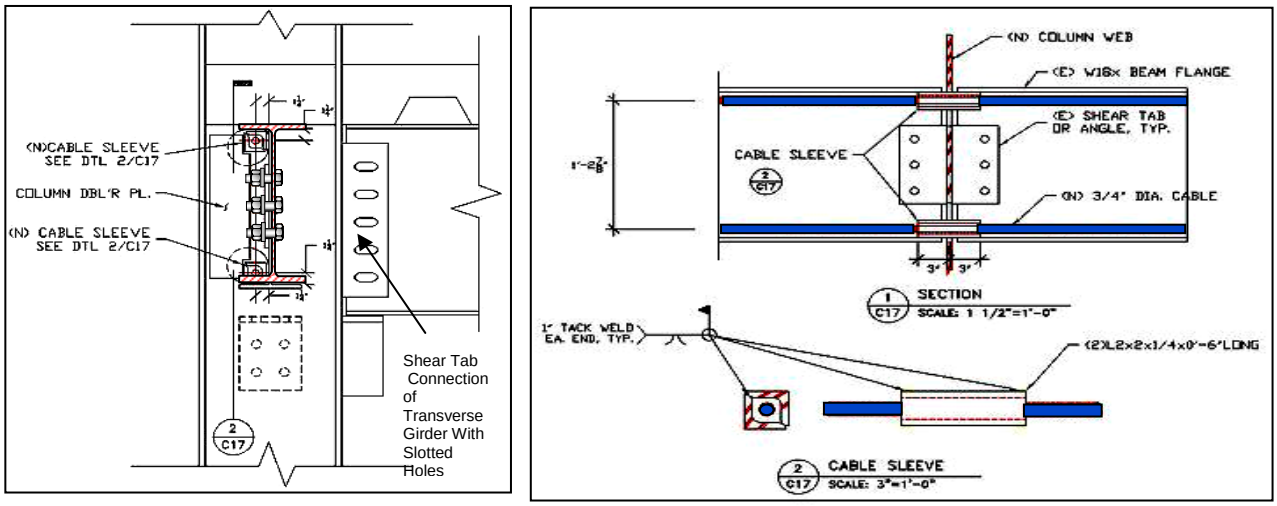

(Tan and Astaneh-Asl, 2003 a and 2003 b)

Figure 5.5. Cable Sleeves at Drop Column

The cables were protected from damage in areas where they were in contact with sharp steel edges that is in the holes cut in the column web. As the drop column displaced downward, the web of the drop column would bear down on the cables. The cables would in turn develop catenary forces and transfer the load to adjacent columns and the rest of the structure. However, the "knife-edge" of the hole in the column web could damage the cables under the large column loads. To prevent such damage, 6-inch long cable sleeves (consisting of L2x2 angles) were installed around the cables to protect them as they passed through the column webs (Figure 5.5). Angle sleeves were also used on the beams to indirectly connect the retrofit cables to the longitudinal beams on frame line 2 (south façade in Figure 5.2). Figure 5.6 shows a view of the cable sleeves on the beams.

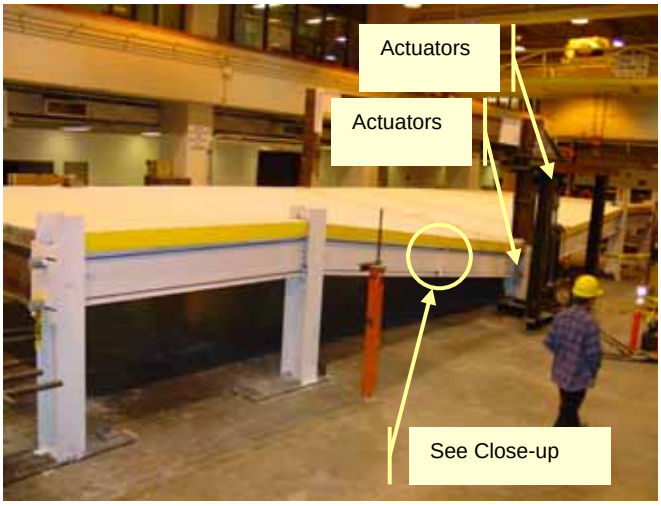

Close-Up of Sleeves on the Beams

Figure 5.6. Cable Sleeves on the Beams

5.2.c. Test Procedures

During the tests, the dead load of the slab and steel framing were already present. To apply the remainder of the design dead load and live load, my colleagues and I attached two 120 kips capacity hydraulic actuators to the top of the drop column as shown in Figure 5.6. The actuators pushed the drop column downward to simulate the weight of the floor (dead and live load) supported by the drop column. The loading sequence was displacement-based, and the actuators imposed downward displacements with a constant velocity of ¼-inch per second. Data was collected from instrumentation at a time increment of 0.067 seconds. Three tests were conducted on the specimen. A summary of the main properties of each test is given in Table 5.1. During tests NSF-1 and NSF-2, the drop column was pushed down 22 inches while during test NSF-3, which was the final test, the drop column was pushed down a maximum displacement of 32 inches.

Each test started with the floor beams at their initial horizontal position, then the stub column supporting the drop column was removed, and immediately afterwards the drop column was pushed downward by the actuators. The downward push of the drop column continued until it reached a maximum displacement predicted by pretest analyses. After reaching the pre-

assigned maximum displacement, the drop column was partially unloaded by pushing it up by about 2 inches. This unloading allowed the actuator forces to drop to a level at which it was safe to enter the area below the collapsed floor for close- up observations and note taking. After observations were complete, the drop column was completely unloaded by pushing it up until the beams reached their initial horizontal position. A total of 23 displacement transducers and 24 strain gauges were used to measure the displacements and strains, respectively, at critical points on the specimen.

Table 5.1. Summary of Tests NSF-1, NSF-2, and NSF-3

Test	**Beam to Column Connections**	**Retrofit Cables[2]**	**Maximum drop column displacement inches**
NSF-1	Shear tabs[1]	None	22
NSF-2	Shear tabs[1]	Two cables	22
NSF-3	Shear tabs[1]	Two cables	32

[1] Shear tabs were installed at grid locations B2, C2, and D2.
[2] Retrofit cables installed along the south side of the specimen frame line 2.

5.2 d. Test Observations and Results

Figure 5.7 shows the overall response of the test specimen in terms of load versus vertical displacement of the drop column. Table 5.2 provides a summary of the main data on performance of the specimen during the three tests NSF-1, NSF-2, and NSF-3.

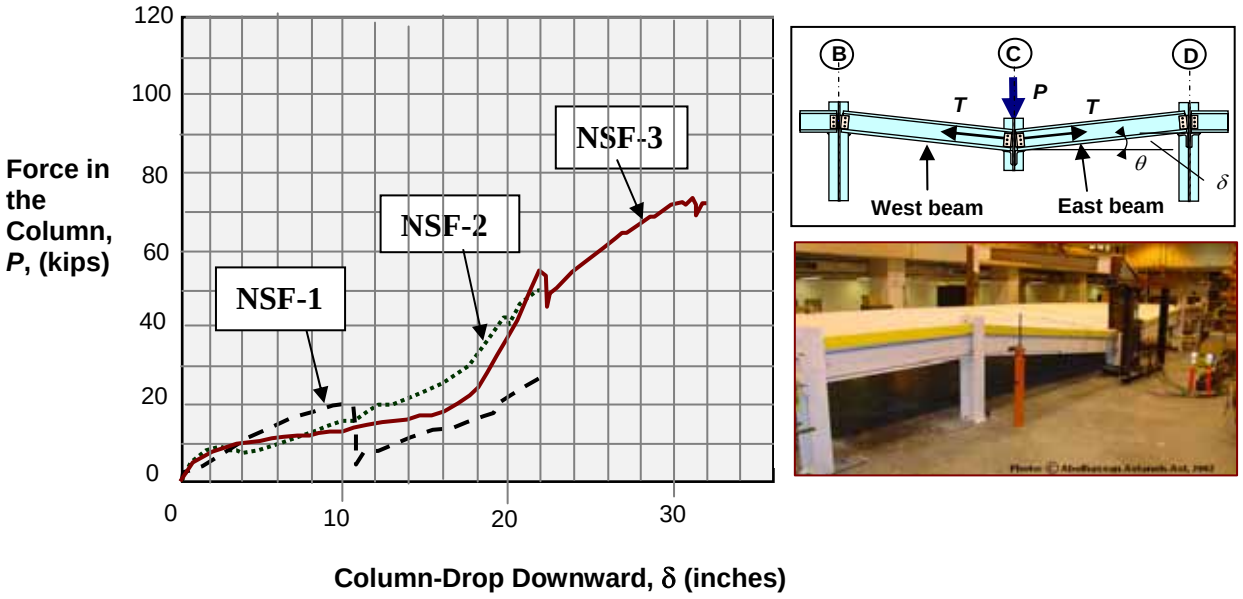

Figure 5.7. Load versus Downward Displacement of Column C2 for NSF Tests

Table 5.2. Summary of Forces, Deformations, and Strains

Parameter	Maximum Values		
	Test NSF-1, No Cables	**Test NSF-2, with Cables**	**Test NSF-3, with Cables**
Maximum Displacement of Drop Column (inches)	22	22	32
Maximum Axial Force in Drop Column, (kips)	27.8	53.2	76.3
Maximum Axial Force in W18x35 East Beam (kips)	73	89	91
Axial Force in Lower ¾-Inch Diameter Cable (kips)	N.A.	14	30
End-Rotation for East Beam (radians)	0.107	0.076	0.110
End-Rotation for West Beam (radians)	0.076	0.104	0.130
Rotation at South End of Transverse Beam (radians)	0.088	0.083	0.127
Rotation at North End of Transverse Beam (radians)	0.100	0.104	0.144
Deck Strain Measured at SG2 (x 10^6) (see Note)	400	-470	-650
Deck Strain Measured at SG5 (x 10^6) (see Note)	N810	N760	N1070

Note: A negative strain reading denotes compressive strain. Positive strain readings denote tensile strain.

Behavior of A Specimen during Test NSF-1 (with No Retrofit)

During Test NSF-1, as the drop column displacement approached 11 inches, there was a loud "boom" and the east beam fell 3 inches down to the catcher angle. Later inspection indicated that the weld on the east beam shear tab had fractured. I attributed the fracture to less than perfect quality of the field fillet welds connecting the shear tab to the drop column. The reason for field welds on the shear tabs was that, as mentioned earlier, we had already used this specimen to test progressive collapse while connections were seat and web angles (Chapter 3), therefore, for the tests summarized in this chapter I took the bolted seat and web angles out and welded shear tabs to the columns. The welding had to be done as field welds since the floors, beams and columns were already in place. In addition, during the previous test (presented in Chapter 3) the column was slightly out of alignment and as a result the drop column was pushed to the east about ½ inch, closing the gap between the beam and the face of the column. Consequently the details of the shear tab connection for the west and east side beams were as shown in Details A and B of Figure 5.8, respectively. Notice that the welds on the shear tab in Detail B are not two fillet welds, typical of shear tab connections. The atypical welding of the shear tab in Detail B, used on the east beam, might have contributed to the failure of this weld. The welds on the west beam, which were also field fillet welds, but according to Detail A, performed well throughout all tests without any sign of distress.

Even though the field welds on the shear tab of the east beam were done according to atypical Detail B in Figure 5.8 and did not have as good a quality as those of the actual buildings, still the welds were able to tolerate a combination of shear and axial catenary forces up to a rotation of about 0.07 radians prior to fracture of the welds.

After the fracture of the shear tab weld, we continued testing until the vertical displacement of the drop column reached the prescribed value of 22 inches for this test; see Table 5.1. During this phase of Test NSF-1 and after failure of the welds in the shear tab, as shown in Figure 5.7, the specimen continued showing almost the same stiffness as the stiffness exhibited prior to failure of the shear tab welds. However, the strength of the system, measured in terms of axial force in the drop column, was about one third of the strength prior to failure of the shear tab.

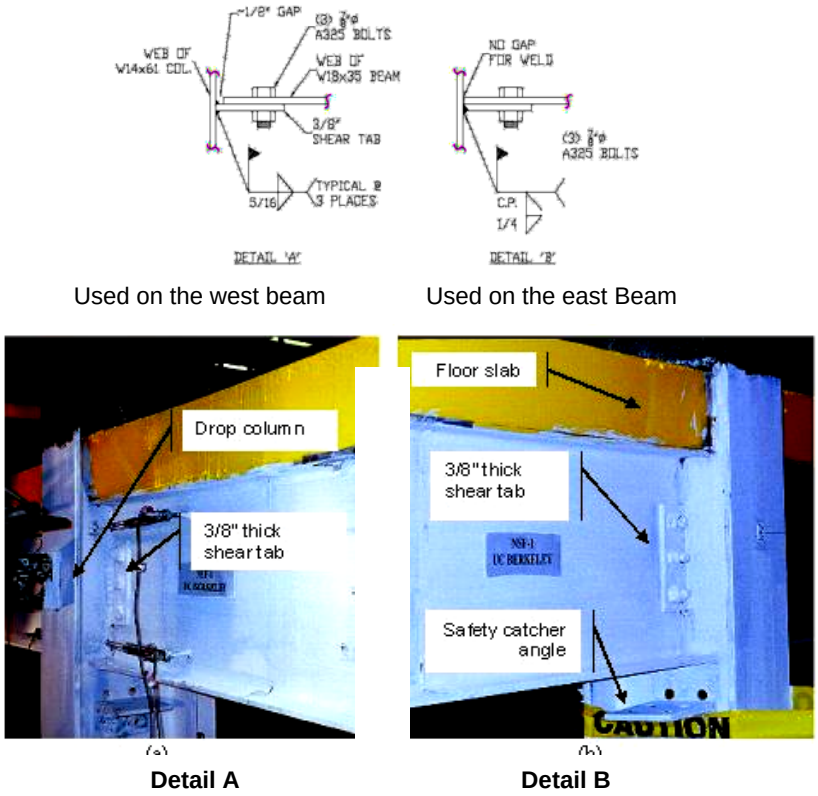

Figure 5.8. Two Details Used in Shear Tabs and views of Actual Shear Tabs (Tan and Astaneh-Asl 2003a and 2003b)

Obviously, fracture of the shear the tab on the east beam totally eliminated catenary forces developed within the beams in the areas adjacent to the drop column. By observing pre- and post failure behavior, I could conclude that the 1/3 strength that the system showed after fracture of the shear tab must have been due to catenary force developed in the steel deck above the beams providing some measure of continuity between the east and west beams and enabling the system to develop catenary force through this continuous load path. Strains at two points on the bottom surface of the steel deck are given in Table 5.2, and indicate participation of the steel deck in developing and resisting catenary forces, which in turn resulted in providing some resistance to the progressive downward collapse of the drop column. Notice that the yield strength of the deck was specified by the manufacturer as 33 ksi, which results in a yield strain of 33 ksi/29,000 = 1137×10^{-6}. During Test NSF-1, the strain gauge measurements did not exceed this value of yield strain, indicating that there was no widespread yielding of the deck. However, local yielding and local buckling of the steel deck were observed in the areas near the top flange support. Figure 5.9 shows local buckling of the steel deck adjacent to the top flange of the transverse beam.

After repairing the fractured weld on the shear tab, the testing continued with no significant event. At prescribed vertical displacement of 22 inches Test NSF-1.was stopped. Figure 5.10 shows the sequence of the drop of the column during the test, and Figure 5.11 shows the yielding and deformations in the connections. Figure 5.12 shows top and side views of the specimen at the end of Test NSF-1.

Figure 5.9. Local damage to Steel Deck Above the Top Flange

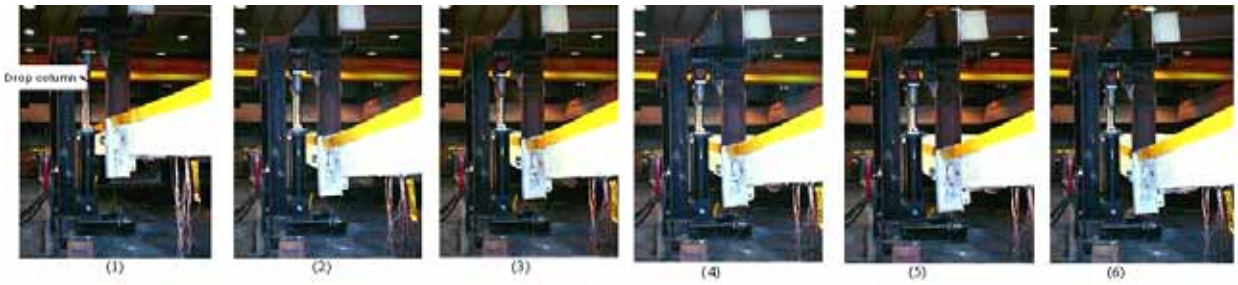

Figure 5.10. Sequence of the Drop Column in Test NSF-1 Moving Down

Behavior of the Specimen during Test NSF-2 (with Retrofit)

The main parameters of Test NSF-2 are given in Tables 5.1 and 5.2. For Test NSF-2, the damaged shear tab was replaced and re-welded, and the specimen was retrofitted with two ¾-inch diameter high-strength steel cables. The cables were attached to the beams and columns on the south elevation of the specimen. In Test NSF- 2, similar to Test NSF-1, the drop column was pushed down to a maximum displacement of 22 inches. At this point, the axial load in the drop column was approximately 53 kips. During Test NSF-2, the most significant damage to the

Figure 5.11. Yielding and Deformations without Fracture in the Connections, Test NSF-1

specimen was the onset of the edge distance fracture on the shear tab bolt holes. Large displacements of the drop column resulted in beam end rotations of up to 0.104 radians on the west beam. As the drop column displacement approached 9.5 inches, the bottom bolt of the west beam shear tab initiated edge distance fracture. At a drop column displacement of 20 inches, a complete edge distance fracture of the bottom bolt hole was observed, Figure 5.13.

Figure 5.12. Specimen at the End of Test NSF-1

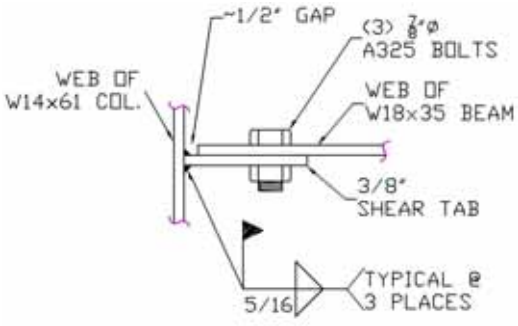

Shear Tab Detail

Figure 5.13. Edge Distance Failure Mode

Behavior of the Specimen during Test NSF-3 (with Retrofit, Pushed Down 32 Inches)
After completion of Test NSF-2, the drop column was pushed up 22 inches until the floor became flat at its original position. Then the shear tabs that were damaged during Test NSF-2 were replaced by new ones and the specimen became ready for Test NSF-3. In Test NSF-3, the drop column was pushed down to a maximum of 32 inches. Figure 5.14(a) shows the test specimen at the end of this test. At this displacement, the axial load in the drop column was 76 kips.

During Test NSF-3, the most significant damage of the specimen was edge distance fracture of the shear tab bolt holes. Edge distance fracture occurred on the shear tabs of the west beam and the south end of the transverse beam. At a drop column displacement of 22 inches, the bottom bolt hole on the west beam shear tab completely fractured through its edge distance. As the drop column displacement approached 28.5 inches, the bottom two bolt holes of the transverse beam shear tab and the middle bolt hole of the west beam shear tab suffered edge

distance fracture. At a drop column displacement of 31 inches, the last remaining bolt hole at the top of the west beam shear tab fractured, Figure 5.14(b) and (c). At this point, the shear tab connection lost all gravity load carrying capacity and the beam lurched upward in response to the column drop.

Figure 5.15 shows the variation in the axial force of the east beam during the three tests. These axial forces were computed as a product of the average longitudinal (catenary) strain of the beam multiplied by the elastic modulus of steel (29,000 ksi) and the area of the steel beam. As the drop column displacement increased, the axial forces of the beam, due to catenary action, also increased. At the time of fracture of the edge distances of the shear tabs, the axial load in the beam was about 91 kips see Figure 5.15.

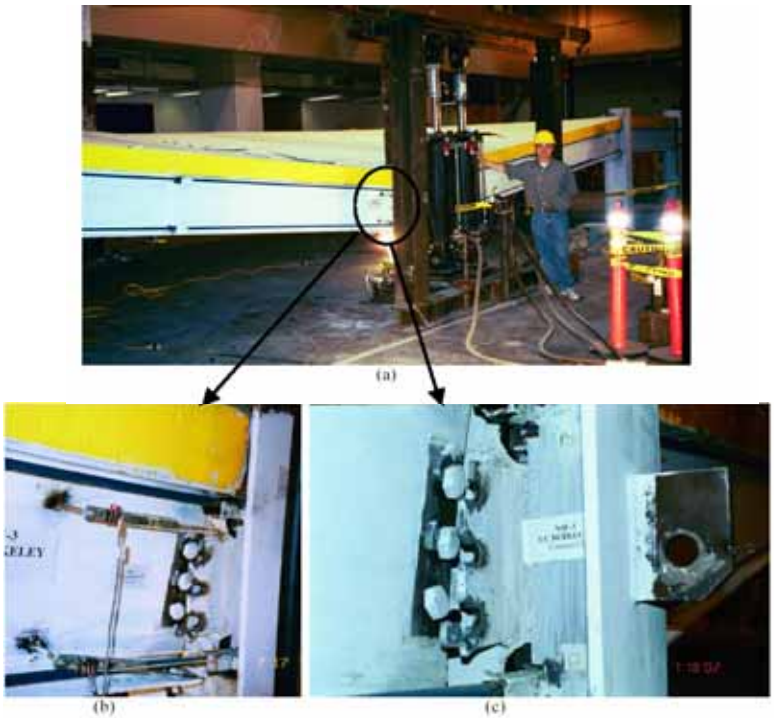

Figure 5.14. After Test NSF- 3: (a) Overall View of the Drop Column Specimen, (b) Shear Tab Block Shear Fracture through the Bolt Hole Edge Distance at W18x35 West of C2 (West beam and (c) Detail of the Shear Tab fracture at the West Beam.

In Test NSF-1, the axial force of the beam had reached a maximum of 73 kips. At this point the bolts on the shear tab and the edge distance had slightly deformed. During Test NSF-1, the specimen did not have cables; therefore, no cable forces are plotted on Figure 5.15. In Test NSF-2, the maximum axial force was 89 kips in the beam and 14 kips in the cable. In Test NSF-3, the maximum axial force of the beam was 91 kips and of the cable was 30 kips. When the axial load of the beam reached 91 kips, the three bolts on the shear tab completely came out of their holes by fracturing the edge distance in a "block shear" failure mode, as shown in Figure 5.15. The calculated capacity of the shear tab for this failure mode was 85 kips.

Assuming that shear connections are pin connections, the end rotations can be calculated by dividing vertical displacements of the drop column by the clear span of 19 feet for the beam.

Following this assumption, the calculated values of the end rotations of the tests were 0.096, 0.096, and 0.14 radians for Tests NSF-1, NSF-2, and NSF-3, respectively. The actual displacements were about 80 percent of these calculated values. The difference between the measured and calculated values can be attributed to the effect of the end moments that were developed due to semi rigidity of the end shear tab connections creating end moments in the beams.

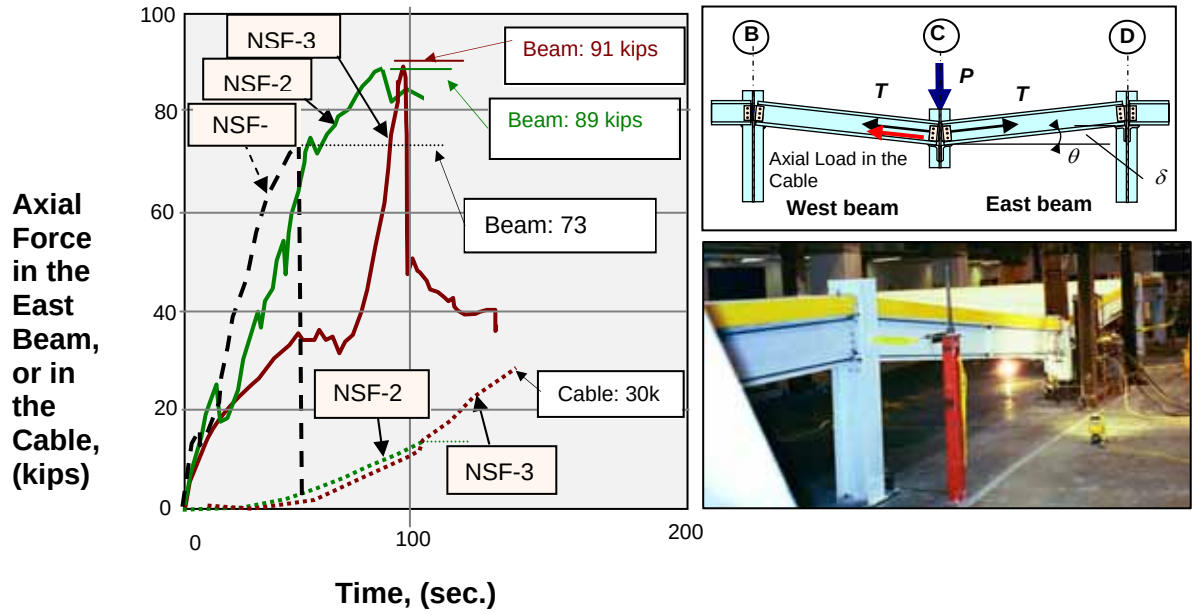

Note: During Test NSF-1, retrofit cables have not been added yet.

Figure 5.15. Axial Forces in the Beam and Lower Cable

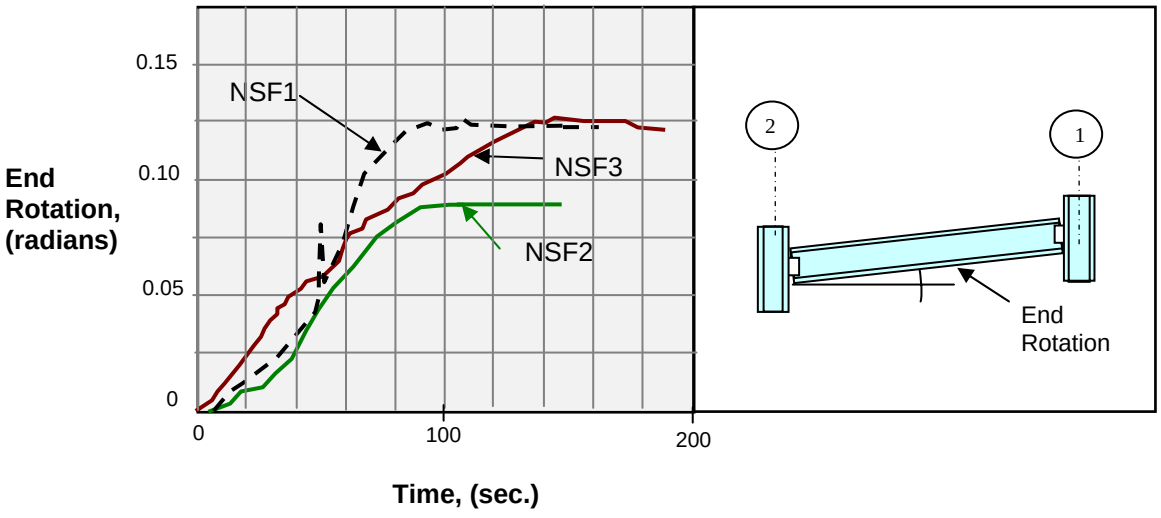

Figure 5.16. Rotation of the Transverse Beam at the South End

Figure 5.17 shows the south end rotation of the transverse beam framed into the drop column in north-south direction. The W21x44 transverse beam had shear tabs with long slotted

holes on both ends. These rotations were computed using data from the displacement transducers mounted on the beam and connected to the drop column. Beam end rotation was computed as the difference of the top and bottom transducer reading divided by the vertical distance between the transducers. The maximum relative rotations at the south end were approximately 0.09, 0.08, and 0.13 radians for Tests NSF-1, NSF-2, and NSF-3, respectively. The maximum relative rotations at the north end were approximately 0.10, 0.10, and 0.14 radians for the three tests, respectively. Assuming that the shear tabs act as perfectly pin connections, the calculated values for these rotations were, 0.11, 0.11 and 0.16 radians. The measured values are about 90% of the calculated values. The difference can be attributed to the contribution of the floor slab to the stiffness and bending strength of the end connections. Since the bolt holes on the shear tabs were long slotted, it appears that this may have caused more rotational flexibility in the end connections, making the measured values only about 10% different than the calculated values.

Figure 5.18 shows the crack patterns on the floor slab after completion of the three tests.

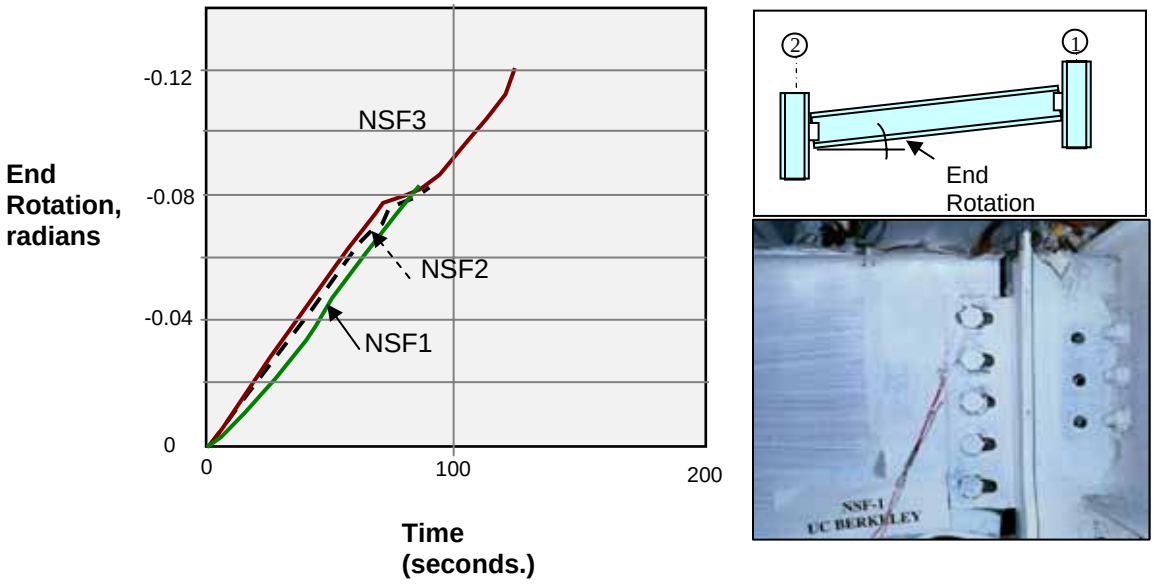

Figure 5.17. End Rotation of the Transverse Beam at the South End (End 2)

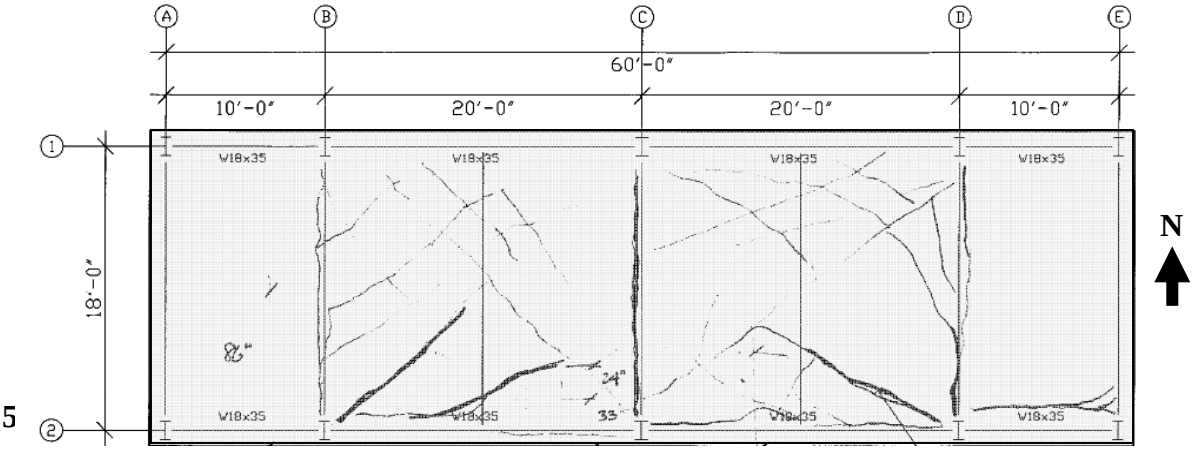

Figure 5.18. Crack Patterns on the Top Surface of the Concrete Slab after Test NSF-1 (Tan and Astaneh-Asl, 2003).

Conducting three tests on a specimen before and after its retrofit I made the following observations and deductions.

1. Steel frames with shear tab beam-to-column connections have considerable capacity to resist progressive collapse in the event of removal of a column. In Test NSF-1, the load *P* of the drop column in Figure 5.19 was equal to 27.8 kips. The maximum vertical displacement ,δ, of the drop column at this point was 22 inches. The load *P* equal to 27.8 kips was considered the maximum capacity, since at this point the signs of the edge distance failure were visible on the shear tabs. If, considering the sudden removal of the column, a dynamic factor of two, as given by GSA (2003), is applied, the factored load capacity will be 27.8/2 = 13.9 kips, which corresponds to a tributary area of about 120 square feet supported by the drop column., The side spans of the test specimens were 20 feet and the transverse span was 18 feet. The mechanism supporting the drop column was primarily the catenary force *T* developed in the beam and the steel deck adjacent to it. When the drop column load was at its maximum value of 27.8, catenary force *T* of the beams was measured as 73 kips. The beam end rotations for the east and west beams at the maximum load point were about 0.10 and 0.07, respectively.

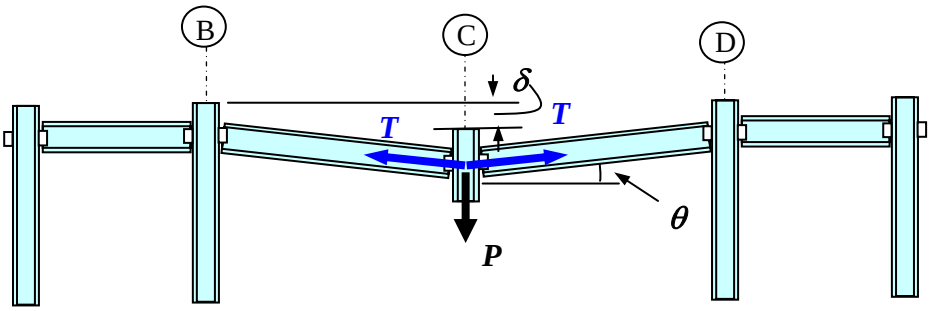

Figure 5.19. Forces and Displacements of the Specimen

The failure mode observed was the fracture of the horizontal edge distance of the shear tab, Figure 5.14 The shear tabs were subjected to a combination of a constant shear force made of increasing axial catenary force and a decreasing small moment. Behavior and design of shear tabs subjected to a combination of shear and axial force were discussed in another Steel Technical Information and Product Services (TIPS) report by the author (Astaneh-Asl 2005a and 2005b).

3. In the tests, one shear tab connection experienced weld fracture. The fractured weld line was a field weld of low quality and therefore not a good representative of the welding. The welded shear tab, as well as all the other shear tabs, did not show any sign of distress. The fracture of the weld had also occurred after the shear tab had undergone a rotation of about 0.07 radians during the test. Shear tabs were designed according to the current design procedures of the AISC Manual (AISC, 2005a), which are based on the methodology recommended by Astaneh-Asl et al (1989), and currently form the shear tab design tables of the AISC Manual (AISC 2005a). According to these provisions, the governing failure mode in the design of shear tab is yielding of the shear tab, which is a ductile failure mode. The other, less ductile failure modes, such as the failure mode of the

weld fracture, bolt fracture, or net area fracture, have larger capacity than the yield failure mode. For more information on the design of shear tabs for shear and combined shear and axial load, see the Steel TIPS report by Astaneh-Asl (2005a).

4. I recommend the use of A36 steel for shear tabs, since it would facilitate hole elongation and rotation of the shear connections as the column moves downward and rotates the end connections. The test specimens had reached a maximum rotation of about 0.13 radian. To facilitate rotation, slotted holes may be used.

5. The floor slab/steel deck provided some tensile catenary capacity in resisting progressive collapse and added about 30% to the resistance provided by the catenary action of the beams. Since there was only minimal shrinkage reinforcement in the concrete slab, the resistance of the floor slab to progressive collapse was primarily attributed to the steel deck. Strain gauge measurements affirmed that tensile stresses approaching yield stress had developed in the steel deck. The deck with ribs parallel to the steel collapsing girders was actively developing large catenary forces, which would not have been possible if the ribs had been perpendicular to the girders. To develop catenary action independent of the direction of the deck ribs, the use of a cellular deck, those with a flat plate at the bottom, are recommended.

6. The high- strength steel cables provided additional strength, stiffness, and toughness to the structure to resist progressive collapse. The high- strength cables noticeably increased the stiffness of the specimen at drop column displacements by approximately 16 inches. They had also provided an adequate alternative load path for the drop column load and tie forces. The cables resisted their proportionate catenary forces without failure. The end columns supported additional load that was shed from the drop column with a maximum of ½ inch inward displacement.

7. The floor slab/steel deck was able to tolerate the in-plane compression forces due to tension in the catenary cables.

REFERENCES

1. AISC (2005a) *Specifications for Structural Steel Buildings.* Chicago, IL*:* American Institute of Steel Construction (free download at www.aisc.org).

2. AISC (2005b). *Manual of Steel Construction,* the 13 ed. Chicago, IL*:* American Institute of Steel Construction (can be purchased at www.aisc.org).

3. AISC (2005c). *Seismic Provisions for Structural Steel Buildings, Chicago, IL*: American Institute of Steel Construction. (Free download at www.aisc.org).

4. ASCE (1996). "The Oklahoma City Bombing: Improving Building Performance through Multi-Hazard Mitigation." *FEMA 277*. Reston, VA: Federal Emergency Management Agency Mitigation Directorate
5. "
6. ASCE (2005) "Minimum Design Loads for Buildings and Other Structures "Reston, VA: *ASCE Standard Number ASCE/SEI 7-05.*

7. Astaneh-Asl, A., E.A Madsen, , C Noble,., R. Jung, R., D McCallen, , M.S., Hoehler, W Li, and R.Hwa,." Use of Catenary Cables to Prevent Progressive Collapse of Floors"; Report Number UCB/CE-Steel-01/02 Department of Civil and Environmental Engineering, University of California, Berkeley September (www.ce.berkeley.edu/~astaneh).

8. Astaneh-Asl, A, D. McCallen, E. Madsen, and C. Noble (2001b) " Experimental and Analytical Studies of Floor Catenary Action to Prevent Progressive Collapse," Report Number UCB/CE-Steel-01/03*,* Department of Civil and Environmental Engineering, University of California, Berkeley, December (www.ce.berkeley.edu/~astaneh).

9. Astaneh-Asl, A., B Jones,., Y. Zhao,. and R. Hwa,. (2001c). "Progressive Collapse Resistance of Steel Building Floors", Report Number UCB/CEE-Steel-2001/03**,** Department of Civil and Environmental Engineering, University of California, Berkeley, September (www.ce.berkeley.edu/~astaneh).

10. Astaneh-Asl, A. (2002). Protection of Buildings against Terrorist Attacks and Lessons Learned from the Collapse of the World Trade Center" Proceeding*s,* a presentation at the American Association for the Advancement of Science Annual Meeting, "Science as a Way of Life," Denver Colorado, February 13 to 18.

11. Astaneh-Asl, A., C Heydari, and Q. Zhao,. (2003). "Vanadium Micro-alloyed Steel Case Study: Applications in Blast-Resistance of Building,", Technical Report. The Advanced Technology Institute, October (www.ce.berkeley.edu/~astaneh).

12. Astaneh-Asl, A. (2002). "*Proceedings World Trade Center,"* The Fire Resistance Determination and Performance Prediction Research Needs Workshop, NIST, Gaithersburg, MD, February.19-20.

13. Astaneh-Asl, A., and Q. Zhao,. (2002). Cyclic Behavior of Steel Shear Wall Systems , Proceedings, Annual Stability Conference, Structural Stability Research Council, Seattle, April 25 to 27.

14. Astaneh-Asl, A. (2002). "Field Investigation and Analysis of the Collapse of the World Trade Center," Proceedings (Keynote Speech,) Steel Structures ISSS'02, Seoul, South Korea, November 21 to 22.

15. Astaneh-Asl, A., C. Heydari,. and Q. Zhao,. (2003). "Analysis of Car-bomb Effects on Buildings using MSC-Dytran Software and Protective Measures," *Proceedings*, The MSC Software Virtual Product Development Conference, October 13-15, Dearborn, Michigan.

16. Astaneh-Asl, A. (2003). "Progressive Collapse Prevention in New and Existing Buildings," Proceedings , The 9th Arab Structural Engineering Conference., November. 29 to December. 1, 2003, Abu Dhabi, UAE.

17. Astaneh-Asl, A. (2003). "World Trade Center Collapse, Field Investigation and Analysis," Proceedings (Invited Key-note Speech,), The 9th Arab Structural Engineering Conference., November 29 to December 1, 2003, Abu Dhabi, UAE.

18. Astaneh-Asl, A., Q. Zhao,., C. Heydari,. and V. Tunga, (2005). "Performance of R/C and Composite Walls of Buildings under Blast Loads," Proceedings, The 76th Shock and Vibration Symposium (SAVIAC), October 30 to November 3, Destin, FL.

19. Astaneh-Asl, A. (2005). "Design of Shear Tab Connections for Gravity and Seismic Loads", Steel Technical Information and Product Services (Steel TIPS) Report, Structural Steel Educational Council (SSEC), Moraga , California, July.

20. Astaneh-Asl, A., J. Son, and M. Rutner,(2005) "Blast Resistance of Steel and Composite Bridge Piers and Decks," Proceedings, The 76th Shock and Vibration Symposium (SAVIAC), October 30 to Nov.3, Destin, FL.

21. Baker, J.F. D. Lax, and E.L. Williams, (1948). "The Civil Engineer at War." *The Institution of Civil Engineers.* London, England.

22. Baldridge, S. M. (2003) "Steel Protection" *Modern Steel Construction*. American Institute of Steel Construction.

23. CSI (2007) "*SAP 2000 Nonlinear Analysis Software,*" Berkeley, CA: Computers and Structures

24. De Stefano, M. and A. Astaneh-Asl, (1991). "Axial Force Displacement Behavior of Steel Double Angles," *Journal of Construct. Steel Research*, 20, pp.161 to 181.

25. DOAN&AF (1990). "Structures to Resist the Effects of Accidental Explosions," Army TM 5-1300, Navy, NAVFAC P-397, Air Force AFR 88-22, Departments of the Army, Navy, and Air Force November.

26. DOD (2001), "*Interim Antiterrorism/Force Protection Construction Standards, Guidance on Structural Requirements*, "Department of Defense. March.

27. DOD (2002): "Minimum Antiterrorism Standoff Distances for Buildings," Unified Facilities Criteria (UFC) 4-010-10 Distribution authorized to U.S. Government agencies and their contractors for operational use. This document is not available on the Internet.

28. DOD (2003) "Minimum Antiterrorism Standards for the Buildings," Unified Facilities Criteria, UFC 4-010-01 Department of Defense, approved for public release. distribution unlimited, October (URL :http://www.hnd.usace.army.mil/techinfo/engpubs.htm).

29. DOD (2005a) "Design of Buildings to Resist Progressive Collapse," Unified Facilities Criteria, UFC 4-023-03,Department of Defense approved for public release distribution unlimited, January(URL: http://www.hnd.usace.army.mil/techinfo/engpubs.htm).

30. DOD (2005b) "Security Engineering: Final Design," Unified Facilities Criteria, UFC 4-020-03 Department of Defense .

31. Ettouney, M., R Smilowitz,. and R Daddazio,.(1998). "Comparison between Design Requirements of Earthquake and Blast Events." Paper from Structural Engineers World Congress. T210-1, ISBN:0-08-042845-2. Elsevier Science Ltd.

32. FEMA (2003) "Primer for Design of Commercial Buildings to Mitigate Terrorist Attacks," FEMA 427 Federal Emergency Management Agency, June.

33. FEMA (2003) "Reference Manual to Mitigate Potential Terrorist Attacks Against Buildings," FEMA 426 Federal Emergency Management Agency, June.

34. GAO (1998). "Combating Terrorism: Threat and Risk Assessments Can Help Prioritize and Target Program Investments." *U.S.G.A.O. Report* to Congressional Requesters. GAO/NSIAD-98-74

35. GSA (2003). "Progressive Collapse Analysis and Design Guidelines for New Federal Office Buildings and Major Modernization Projects," General Services Administration, June.

36. Goodson, E., and A.Astaneh-Asl. (2004). "Use of MSC.Dytran in Developing Blast-Resistant Building Columns,*"* Proceedings, The MSC Software Virtual Product Development Conference, October 18 to 20, Huntington Beach, CA.

37. Hamburger, R. and A. Whittaker.(2004) "Design of Steel Structures for Blast-Related Progressive Collapse Resistance," presented at the 2003 AISC and Steel Institute of New York Steel Building Symposium: Blast and Progressive Collapse Resistance (symposium proceedings), American Institute of Steel Construction.

38. Ho, I., and A. Astaneh-Asl, (1993). "Behavior of Double Angle Connections Subjected to Shear and Axial Monotonic or Cyclic Loads" Report No. UCB/CE-Steel-93/17. Department of Civil Engineering, University of California, Berkeley.

39. Longinow, A and F. Alfawakhiri. (2003) "Blast Resistant Design with Structural Steel," Modern Steel Construction.

40. McCallen D., C. Noble and A.Astaneh-Asl, (2001). "Analysis of Performance of a Floor Catenary System," Analysis Report, UCB-LLNL Campus Laboratory Collaborative Research

(www.ce.berkeley.edu/~astaneh).

41. MSC/Dytran (2004) "MSC/Dytran Nonlinear Dynamic Analysis Software", MSC Software Corporation.

42. MSC/Patran (2004) "MSC/Patran/Dyran/Nastran Software," MSC Software Corporation, www.mscsoftware.com.

43. National Research Council (1995) "Protecting Buildings from Bomb Damage: Transfer of Blast-Effects Mitigation Technologies from Military to Civilian Applications," Commission on Engineering and Technical Systems, National Academy Press.

44. National Research Council (2000). "Blast Mitigation for Structures," 1999 Status Report on the DTRA/TSWG Program. National Academy Press. Washington, DC.

45. Penzien, J.,(2001). Personal Communication with the author ,A. Astaneh-Asl,, September
46. Rutner, M., A. Astaneh-Asl,. and J. Son, (2005). "Protection of Bridge Piers Against Blast" Proceedings, 6th Japanese-German Bridge Symposium, September 29 to October 1, Munich, Germany.

47. Shen, J. and A. Astaneh-Asl, (2000). "Hysteresis Model of Bolted Angle Connections," Journal of Constructional Steel Research, 54**,** pp. 317 to 343.

48. Son, J A. Astaneh-Asl,. and M. Rutner,. (2005). "Performance of Bridge Decks Subjected to Blast Loads," Proceedings 6th Japanese-German Bridge Symposium, September 29 to October 1, Munich, Germany.

49. Tan, S. and A. Astaneh-Asl,, (2003a). "Testing a Retrofit Concept to Prevent Progressive Collapse," Report Number UCB/CEE-Steel-2003/02, Department. of Civil and Environmental. Engineering., University of California, Berkeley.

50. Tan, S and A. Astaneh-Asl,. (2003b). "Use of Steel Cables to Prevent Progressive Collapse of Existing Buildings," Proceedings, Annual Meeting of the Los Angeles Tall Buildings Structural Design Council, Los Angeles, May 9.

51. Timoshenko, S.(1955). Strength of Materials New York: D. Van Nostrand Company.

52. Wearne, P..(2000). .Collapse: When Buildings Fall Down", Published by Channel 4 TV Books.

53. Wearne, P. (1999). Progressive Collapse, Progressive Security: Oklahoma City and Faulty Towers Published by Channel 4 TV Books.

About the Author:

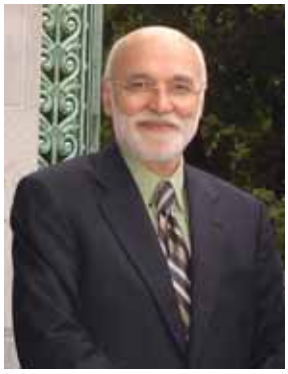

Abolhassan Astaneh-Asl, Ph.D., P.E., is a professor of structural engineering at the University of California, Berkeley. He is the winner of the 1998 T. R. Higgins Lectureship Award of the American Institute of Steel Construction. From 1968 to 1978 he was a structural engineer and construction manager in Iran designing and constructing buildings, bridges, water tanks, transmission towers, and other structures. During the period 1978–1982, he completed his M.S. and Ph.D. in structural engineering, both at the University of Michigan in Ann Arbor under the supervision of Professors Subhash C. Goel and Robert D. Hanson. Since 1982, he has been a faculty member of structural engineering involved in teaching, research, and design of both building and bridge structures, both in steel and composite, in the United States and abroad particularly with respect to the behavior and design of such structures under gravity combined with seismic effects. He has conducted several major projects on seismic design and retrofit of steel long span bridges and tall buildings. Since1995, he has also been studying the behavior of steel and composite structures, both buildings and bridges, subjected to blast and impact loads and has been involved in testing and further development of technologies and design concepts to reduce blast damage and to prevent progressive collapse of steel and composite building and bridge structures subjected to terrorist blast (car bombs) or impact (planes and rockets) attacks.

After the September 11, 2001, tragic terrorist attacks on the World Trade Center and the collapse of the towers, armed with a research grant from the National Science Foundation, he conducted a reconnaissance investigation of the collapse and collected perishable data. As an expert, he later testified before the Committee on Science of the House of Representative of the U.S. Congress on his findings regarding the collapse of the World Trade Center towers. His current research includes studies of blast effects on steel and composite long- span bridges and elevated freeways with the aim of developing technologies to prevent progressive collapse of these important transportation links.
Since 2004 he has been doing research on earthquake hazard reduction in the Middle East, particularly in developing low- cost steel frame buildings for rural areas of highly seismic countries in the Middle East.. His current projects include investigation of the April 30th collapse of the two spans of Mac Arthur Maze in Northern California due to fire funded by the National Science Foundation.

He can be reached at:
781 Davis Hall, University. of California
Berkeley, CA 94720-1710
Phone and Fax: (925) 946-0903
E-mail: Astaneh@ce.berkeley.edu
Web: http://www.astaneh.net and http://www.ce.berkeley.edu/~astaneh

Steel Technical Information and Product Services (Steel TIPS) reports available at http://www.steeltips.org

April 07: Progressive Collapse Prevention of Steel Frames with Shear Connections, by Abolhassan Astaneh-Asl.
Dec. 06: Seismic Detailing of Gusset Plates for Special Concentrically Braced Frames, by Abolhassan Astaneh-Asl, Michael L. Cochran, and Rafael Sabelli
Aug. 06: Alfred Zampa Memorial Steel Suspension Bridge, by Alfred Mangus and Sarah Picker
July 06: Buckling and Fracture of Concentric Braces Under Inelastic Loading, by B. Fell, A. Kanvinde, G. Deierlein, A. Myers, and X. Fu
Sept. 05: Notes on Design of Double-Angle and Tee Shear Connections for Gravity and Seismic Loads, by Abolhassan Astaneh-Asl
June 05: Design of Shear Tabs for Gravity and Seismic Loads, by Abolhassan Astaneh-Asl
Apr. 05: Limiting Net Section Fracture in Slotted Tube Braces, by Frances Yang and Stephen Mahin
July 04: Buckling Restrained Braced Frames, by Walterio A. Lopez and Rafael Sabelli.
May 04: Special Concentric Braced Frames, by Michael Cochran and William Honeck.
Dec. 03: Steel Construction in the New Millennium, by Patrick M. Hassett.
Aug 02: Cost Consideration for Steel Moment Frame Connections, by Patrick M. Hassett and James J. Putkey.
June 02: Use of Deep Columns in Special Steel Moment Frames, by Jay Shen, Abolhassan Astaneh-Asl, and David McCallen.
May 02: Seismic Behavior and Design of Composite Steel Plate Shear Walls, by Abolhassan Astaneh-Asl.
Sept. 01: Notes on Design of Steel Parking Structures Including Seismic Effects, by Lanny J. Flynn and Abolhassan Astaneh-Asl.
June 01: Metal Roof Construction on Large Warehouses or Distribution Centers, by John L. Mayo.
Mar. 0 1: Large Seismic Steel Beam-to-Column Connections, by Egor P. Popov and Shakhzod M.Takhirov.
Jan. 01: Seismic Behavior and Design of Steel Shear Walls, by Abolhassan Astaneh-Asl.
Oct. 99: Welded Moment Frame Connections with Minimal Residual Stress, by Alvaro L. Collin and James J. Putkey.
Aug. 99: Design of Reduced Beam Section (RBS) Moment Frame Connections, by Kevin S. Moore, James O. Malley, and Michael D. Engelhardt.
July 99: Practical Design and Detailing of Steel Column Base Plates, by William C. Honeck and Derek Westphal.
Dec. 98: Seismic Behavior and Design of Gusset Plates, by Abolhassan Astaneh-Asl.
Mar. 98: Compatibility of Mixed Weld Metal, by Alvaro L. Collin & James J. Putkey.
Aug. 97: Dynamic Tension Tests of Simulated Moment Resisting Frame Weld Joints, by Eric J. Kaufmann.
Apr. 97: Seismic Design of Steel Column-Tree Moment-Resisting Frames, by Abolhassan Astaneh-Asl.
Jan. 97: Reference Guide for Structural Steel Welding Practices.
Dec. 96: Seismic Design Practice for Eccentrically Braced Frames (Based on the 1994 UBC), by Roy Becker and Michael Ishler.
Nov. 95: Seismic Design of Special Concentrically Braced Steel Frames, by Roy Becker.
July 95: Seismic Design of Bolted Steel Moment-Resisting Frames, by Abolhassan Astaneh-Asl.
Apr. 95: Structural Details to Increase Ductility of Connections, by Omer W. Blodgett.
Dec. 94: Use of Steel in the Seismic Retrofit of Historic Oakland City Hall, by William Honeck and Mason Walters.
Dec 93: Common Steel Erection Problems and Suggested Solutions, by James J. Putkey.
Oct. 93: Heavy Structural Shapes in Tension Applications.
Mar. 93: Structural Steel Construction in the ’90s, by F. Robert Preece and Alvaro L. Collin.
Aug. 92: Value Engineering and Steel Economy, by David T. Ricker.
Oct. 92: Economical Use of Cambered Steel Beams.
July 92: Slotted Bolted Connection Energy Dissipaters, by Carl E. Grigorian, Tzong-Shuoh Yang and Egor P. Popov.
June 92: What Design Engineers Can Do to Reduce Fabrication Costs, by Bill Dyker and John D. Smith.
Apr. 92: Designing for Cost Efficient Fabrication, by W. A. Thornton.
Jan. 92: Steel Deck Construction.
Sept. 91: Design Practice to Prevent Floor Vibrations, by Farzad Naeim.
Mar. 91: LRFD-Composite Beam Design with Metal Deck, by Ron Vogel.
Dec. 90: Design of Single Plate Shear Connections, by Abolhassan Astaneh-Asl, Steven M. Call and Kurt M. McMullin.
Nov.90: Design of Small Base Plates for Wide Flange Columns, by W. A. Thornton.
May 89: The Economies of LRFD in Composite Floor Beams, by Mark C. Zahn.
Jan. 87: Composite Beam Design with Metal Deck.
Feb. 86: UN Fire Protected Exposed Steel Parking Structures.
Sept. 85: Fireproofing Open-Web Joists and Girders.
Nov. 76: Steel High-Rise Building Fire.

STRUCTURAL STEEL EDUCATIONAL COUNCIL

Funding provided by the California Field Iron Workers Administrative Trust
A Union Trust Fund

P.O. Box 6190
Moraga, CA 94570
Tel. (925) 631-1313
Fax. (925) 631-1112
Fred Boettler, Administrator

Steel TIPS may be viewed and downloaded at www.steeltips.org

Participating Members of SSEC

ABOLHASSAN ASTANEH-ASL, Ph.D., P.E.; UNIVERSITY OF CALIFORNIA, BERKELEY
FRED BREISMEISTER, P.E.; STROCAL, INC.
MICHAEL COCHRAN, S.E.; BRIAN L. COCHRAN ASSOCIATES
RICH DENIO; KPFF CONSULTING ENGINEERS
JEFFREY EANDI, P.E.; EANDI METAL WORKS, INC.
PATRICK M. HASSETT, S.E.; HASSETT ENGINEERING, INC.
JOHN KONECHNE, P.E.; CALIFORNIA ERECTORS, INC.
WALTERIO LOPEZ, S.E.; RUTHERFORD/CHEKENE
BRETT MANNING, S.E.
LARRY MCLEAN; MCLEAN STEEL, INC.
KEVIN MOORE; CETUS CONSULTING INC.
JAY MURPHY; MURPHY PACIFIC CORPORATION
RICHARD PERSONS; U.S. STEEL
JAMES J. PUTKEY, P.E.; CONSULTING CIVIL ENGINEER
STEVE THOMPSON; SME STEEL CONTRACTORS